INT 152/88 November 1988

RF MEASUREMENTS ON TCA

A.A. Howling

"But Alan, the vacuum loading isn't flat!"
TCA Team, 1988

CONTENTS

INTRODUCTION

This report analyses the circuit used to match the rf power to the antennae of TCA. The contents page describes the approach used in an attempt to measure the plasma loading and rf power as a function of AFCO frequency.

Previous reports are A. Lietti INT 121/85, G. Collins' GC1, G Besson INT 128/87 and A Lietti and G Besson (J. Phys. E: Sci. Instrum. 19 557 (1986)). The present report aims to demonstrate the measurement accuracy which can be reasonably expected and the validity of the circuit theory for the real antanna system. Several different methods are used to check the consistency of each measurement, and the conventional measurements are compared with measurements made directly on the antennae.

IMPORTANT NOTE FOR READERS:

FOR AN OVERVIEW (Lazy readers) Turn to pages 6, 15, 16/17, 24, 28, 31-33, 38, 39, 42,43, 46, 48-52.

FOR A QUICK SUMMARY (Very Lazy Readers) Turn to pages 6, 17, 42, 43, 49-52

PART 1 CIRCUIT ANALYSIS

SECTION 1 BASIC MATCHING CIRCUIT, R_{ant} and Z_{magic}.

The present matching circuit was designed for fixed frequency operation. Tuning capacitors, placed at a distance from the vessel, cancel out the largely inductive antenna load. The circuit Q is necessarily high because dissipative losses are kept to a minimum for high-power heating. The description below shows the simplification of the circuit, introducing the method of calculating R_{ant}, I_{ant}, P_{rf} and the definition of Z_{magic}. V_{gen} I_{gen} and ϕ_{gen} are the measurements made at the input of the matching circuit. Parasitic elements are ignored here, the cables are assumed to be ideal and the resistive losses are all included in R_{ant}. <u>All circuits shown below are equivalent:</u>

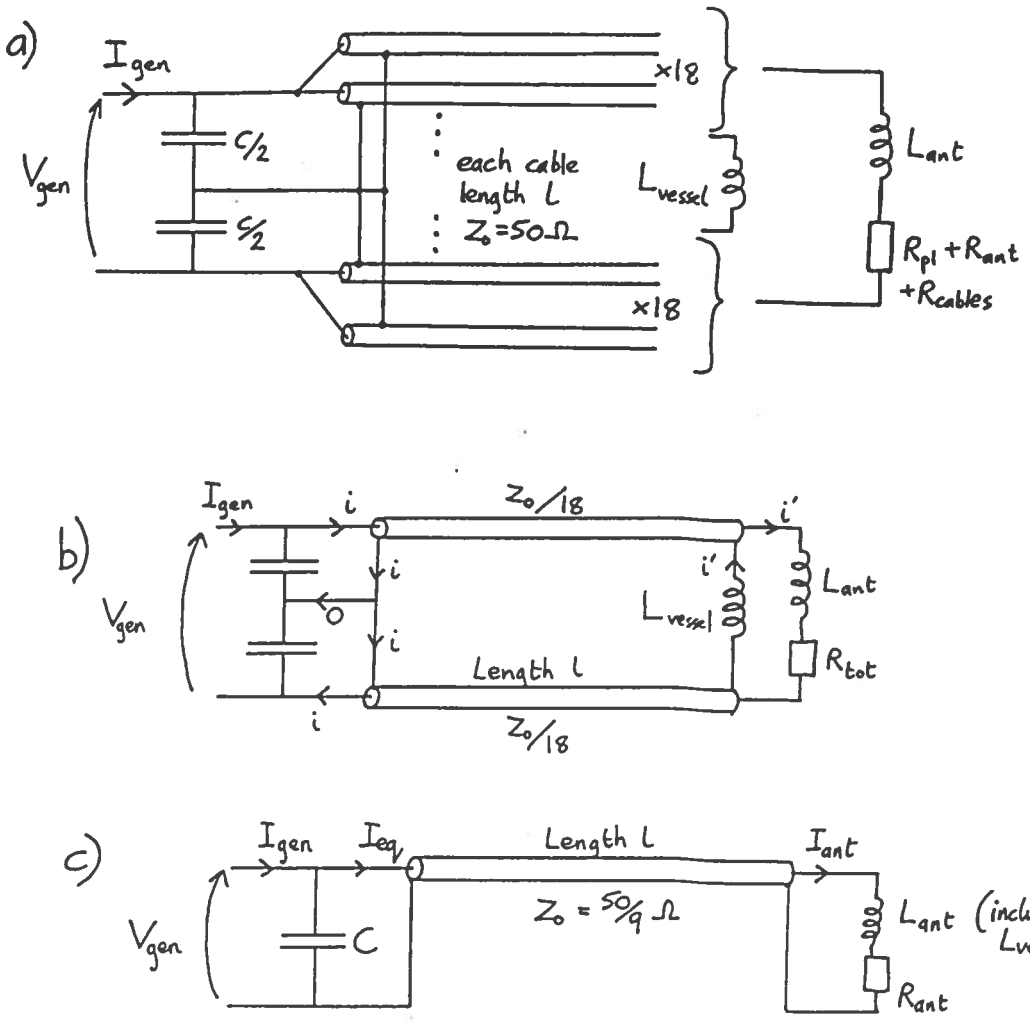

Note: $R_{ant} = R_{ant} + R_{plasma} + R_{cables}$ everywhere in Section 1.

Note: I_{eq} is not equal to I_{ant} because the cable is not terminated by its characteristic impedance.

d)

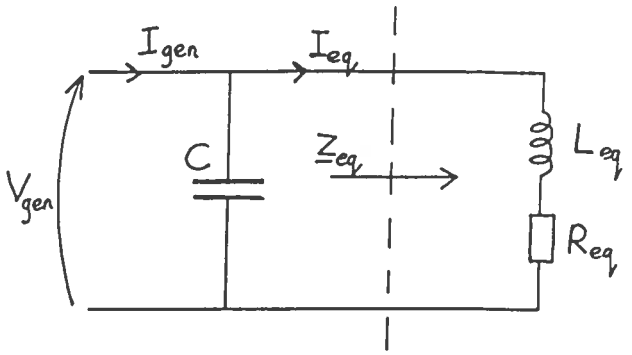

Where $\underline{Z}_{eq} = R_{eq} + j\omega L_{eq}$ and is the cable-transformed $\underline{Z}_{ant}$:

$$\underline{Z}_{eq} = (\underline{Z}_{ant} + Z_o' \tanh(\gamma l)) / (1 + Z_{ant} \tanh(\gamma l) / Z_o), \quad \gamma l = j\omega l/v$$

and $\tanh(\gamma l) = j \tan \text{mod}(\gamma l) = j\delta$ (say) where the cable is assumed to be ideal: cable losses have been transferred into R_{ant}.
Since $\underline{Z}_{ant} = R_{ant} + j\omega L_{ant}$ and $\underline{Z}_{eq} = R_{eq} + j\omega L_{eq}$, we have:

$$R_{eq} = R_{ant} (1 + \delta^2) / (1 - \omega L_{ant}\delta/Z_o)^2, \qquad \omega L_{eq} = (\omega L_{ant} + \delta Z_o) / (1 - \omega L_{ant}\delta/Z_o)$$

e)

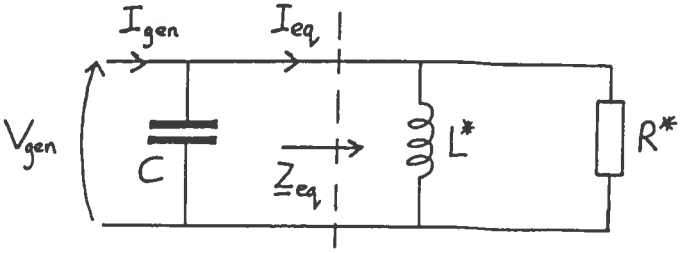

Equate admittance $\underline{Y}_{eq} = 1/\underline{Z}_{eq}$ for circuits d) and e):

$$\underline{Y}_{eq} = 1/j\omega L^* + 1/R^* = (R_{eq} + j\omega L_{eq})^{-1} = R_{eq}/\omega^2 L_{eq}^2 - j / \omega L_{eq} \quad (\text{for } R_{eq}^2 << \omega^2 L_{eq}^2)$$

therefore $L_{eq} = L^*$ and $1/R^* = R_{eq}/\omega^2 L_{eq}^2$

Now consider the admittance $\underline{Y}$ of the whole circuit e):

$\underline{Y} = j\omega C + 1/j\omega L^* + 1/R^*$. We measure I_{gen}, ϕ_{gen} and V_{gen}:

$$I_{gen} \cos\phi_{gen} / V_{gen} = \text{Re}(\underline{Y}) = 1/R^* = R_{eq}/\omega^2 L_{eq}^2 = R_{ant} (1 + \delta^2) / (\omega L_{ant} + \delta Z_o)^2$$

We can now define all the parameters of interest:

$R_{ant} = Z_{magic}^2 . I_{gen} \cos\phi_{gen} / V_{gen}$ where $Z_{magic}^2 = (\omega L_{ant} + \delta Z_o)^2 / (1 + \delta^2)$
for all frequencies (provided that $R_{ant}^2 << \omega^2 L_{ant}^2$).

To find I_{ant}, look at conservation of energy in circuits c) and d):

$I_{ant} R_{ant}^2 = I_{eq} R_{eq}^2$, and $I_{eq} = V_{gen} / Z_{eq} = V_{gen} / \omega L_{eq}$ approx.(for $R_{ant}^2 << \omega^2 L_{ant}^2$)

Therefore $I_{ant} = V_{gen} / Z_{magic}$ for all frequencies (provided that $R_{ant}^2 << \omega^2 L_{ant}^2$).

and Rf power $= V_{gen} I_{gen} \cos\phi_{gen} = I_{ant}^2 R_{ant}$, (independent of Z_{magic}).

For the circuit parameters:
Length of cables, $l = 5.25$m
$L_{ant} = 151$nH
$Z_o = 50/9\Omega = 5.556\Omega$
Velocity in cable $= 0.711c$,

we obtain the following curve for Z_{magic} (fig. 1.1) which agrees well with the straight line fit used by G Collins for the region f=2-3 MHz.

Note All calculations above are valid for all frequencies (provided that $R_{ant} << \omega L_{ant}$), and not just the resonant fequency.

PROBLEM The load and phase curve below (fig.1.2), using the mélangeurs, shows that the deduced vacuum loading appears to increase with frequency, both for shots at different fixed frequencies and for frequency sweeps. From the skin effect (proportional to $f^{0.5}$), we would expect an increase of only 5% for this frequency range.

CONCLUSION We must:
1) Locate any parasitic elements in the circuit,
2) Calibrate all circuit elements,
3) Modify the theory above in order to recover R_{ant} correctly.

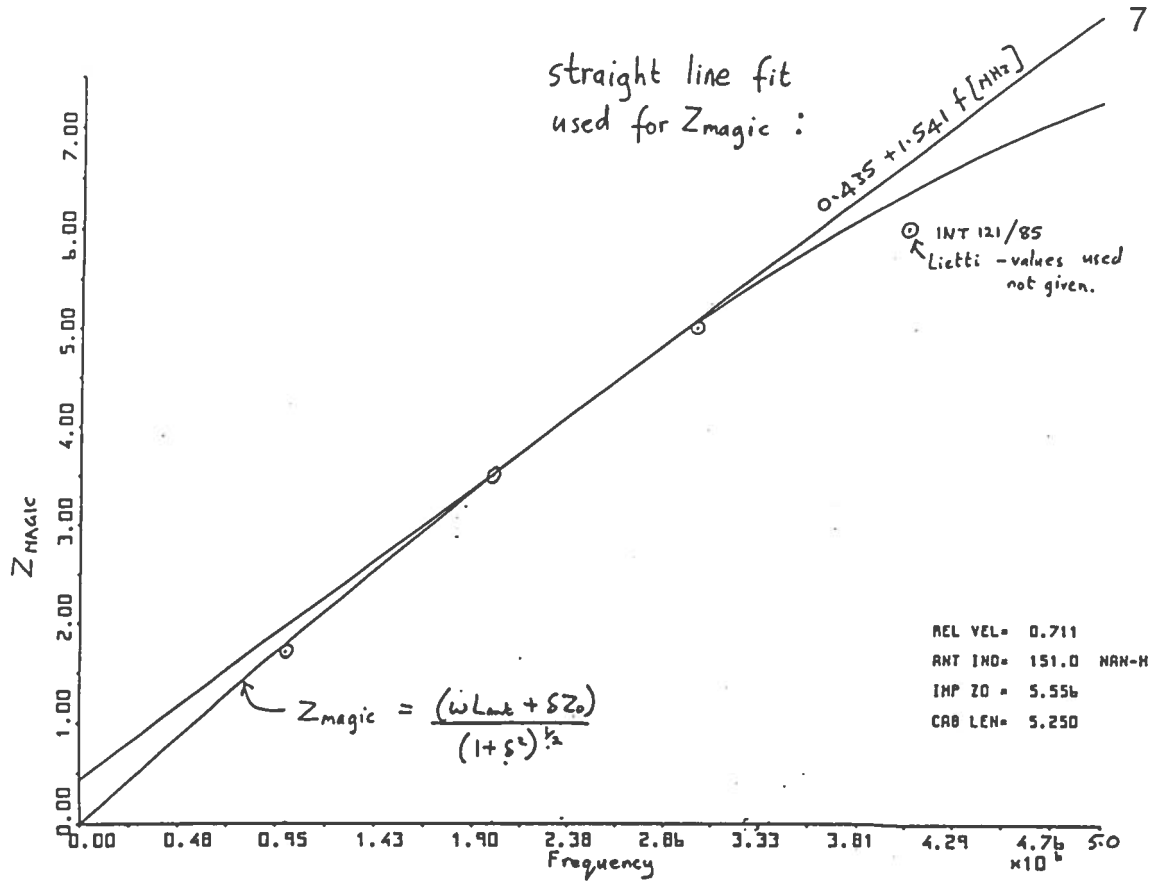

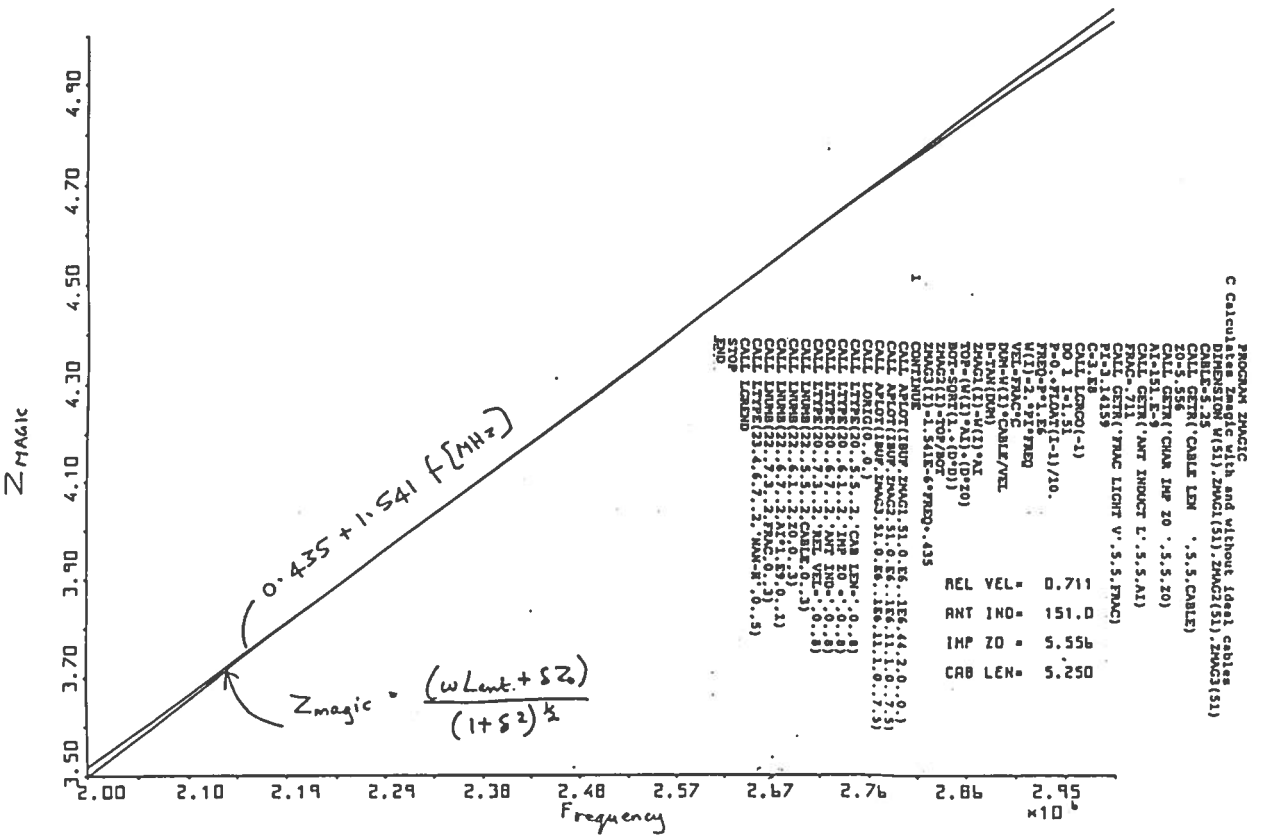

Figure 1.1 Straight-line fit approximation for Z_{magic}.

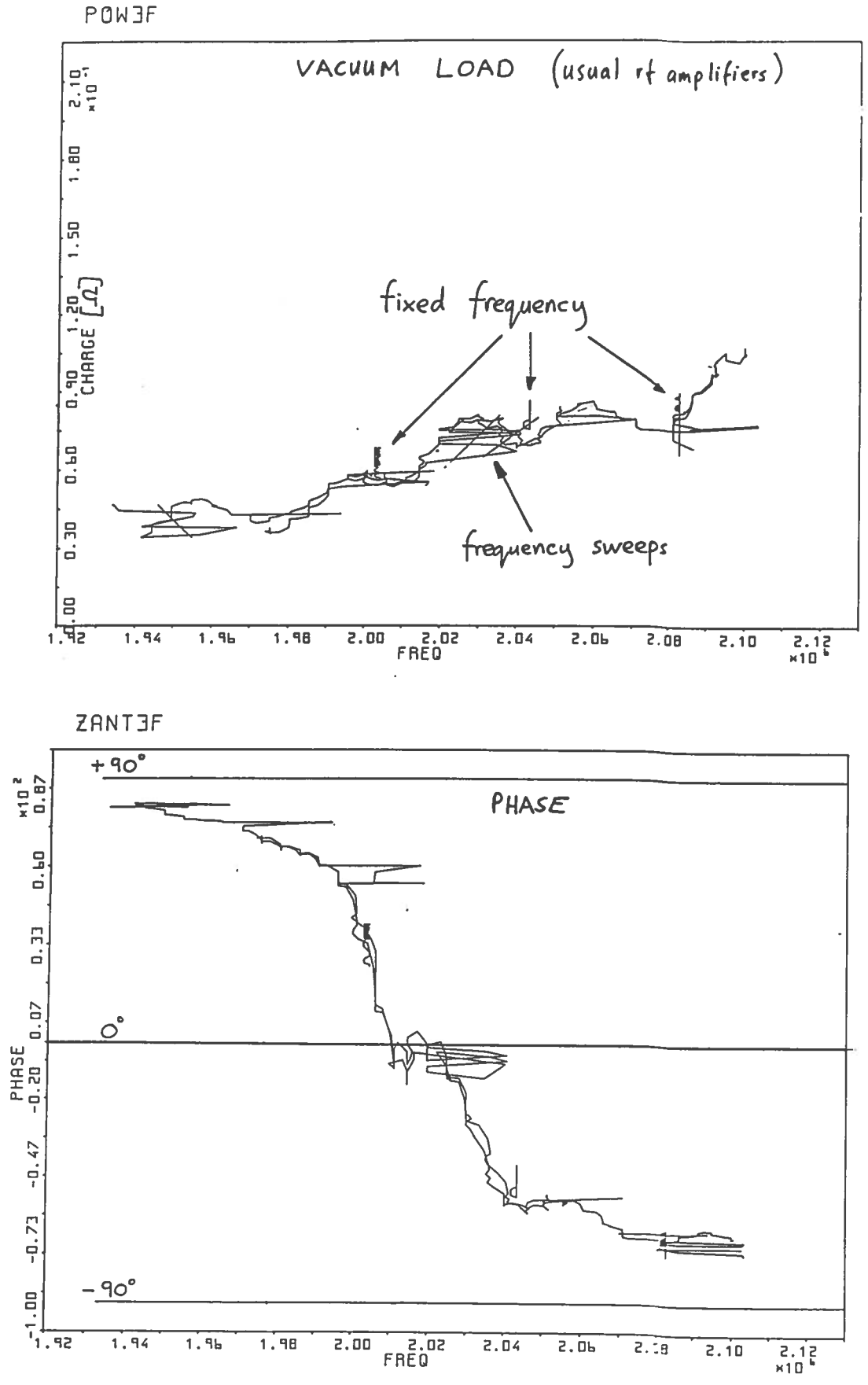

Figure 1.2 Vacuum load and phase using mélangeurs for 3 fixed- frequency shots and 2 frequency sweeps.

SECTION 2 PROBE SERIES INDUCTANCE L_{ser}

The H-P vector impedance meter replaces the TCA rf probes for these measurements. All measurements in this section refer to antenna 1.

* With the antenna cables removed from the capacitor plates, in the limit of low frequency, C = 15.66 nF. (Check: For the complete circuit, when f_{res} = 2.5 MHz, C = 10.5 nF (G Collins). At f_{res} = 2.03 MHz, C = 15.66 nF. Since the cable/antenna inductance is unaltered, we expect f_{res}^2.C = constant, which is correct to 4%.)

* A series resonance of the probe/capacitor (with all antenna cables disconnected) was found whose frequency depended on the H-P probe connection length. The zero-voltage frequency of G Besson's probe was 3.2+/-.03 MHz indicating a series inductance associated with the TCA probe/capacitor arrangement L_{ser} = 158+/-3 nH.

* By varying the H-P probe connection length, we estimate that approximately 30 nH and 10 mΩ are due to the capacitors themselves.

We now have the following modified circuit (fig 2.1):

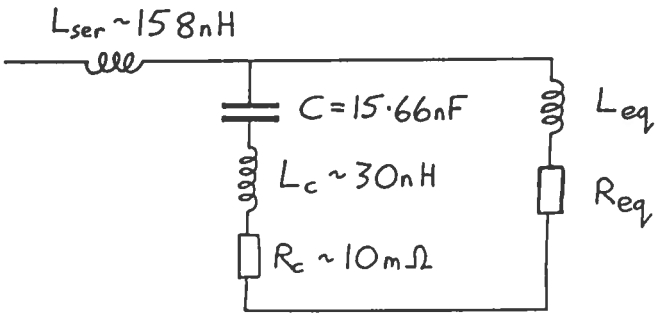

Figure 2.1 Parasitic components associated with matching box capacitor C and probe series inductance L_{ser}.

* For the complete circuit above, two resonances were identified, the first at f'_{res} = 2.033 MHz (parallel resonance of capacitor and cable-transformed antenna) and the second at f''_{res} = 3.8 +/-.2 MHz (series resonance of L_{ser} with the matching circuit) for G Besson's probe system, where:

$$\omega'^2_{res} = C\,(L_{eq} + L_c)^{-1} \quad \text{and} \quad \omega''^2_{res} = \omega'^2_{res}\,(1 + L_{eq}/L_{ser}).$$

A knowledge of f'_{res}, f''_{res} and C thus gives us an alternative approximate estimate of L_{ser} = 157+/-30 nH. A correction to the Alfvèn measurements for this parasitic component, taken to be L_{ser} = 158 nH, is presented in Section 5.

SECTION 3 ESTIMATION OF ANTENNA INDUCTANCE L_{ant}

The antenna inductance must be known before Z_{magic}, R_{ant} and I_{ant} can be calculated (see Section 1). Several methods are described, some of which test the theory of Section 1, and the different values obtained are reconciled in the summary.

Method 1 From Section 1, from the expression for L_{eq} we have:

$$\omega L_{ant} = (\omega L_{eq} - \delta Z_o) / (1 + \omega L_{eq}\delta/Z_o).$$

At the first resonance, $\omega_{res}^2 = C(L_{eq} + L_c)^{-1}$, which enables us to determine L_{eq}. Since f_{res} = 2.03 MHz, C = 15.66 nF and L_c = 30 nH, we have L_{eq} = 363 nH, also δ = $\tan(\omega l/v)$ = 0.325, Z_o = 5.556 ohm.
Therefore $L_{ant}(1)$ = 174+/-20 nH, assuming the simple theory of Section 1.

Method 2 Using a calibrated Rogowski (see Section 9.3) and antenna voltage probe, the impedance of the antenna can be directly measured. We find Z_{ant} = 1.25Ω with ϕ = 87 degrees. Since $Z_{ant} = j\omega L_{ant} + R_{ant}$, we find $L_{ant}(2)$ = 98+/-10 nH

Method 3 Three resistances were adapted to bolt across the antenna terminals, adding R_{cal} in parallel across the antenna as shown in fig.3.1. (Since the three resistances R are in parallel, $R_{cal} = R/3$).

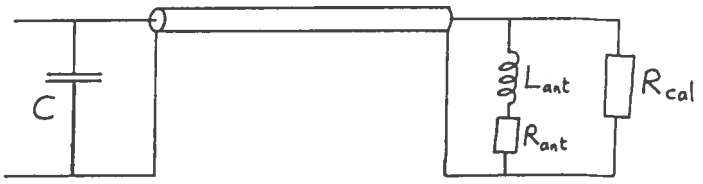

Figure 3.1

The effect of R_{cal} is to change R_{ant} to $R_{ant} + (\omega L_{ant})^2/Rcal$ but L_{ant} is unchanged (for $R_{cal} >> \omega L_{ant}$). By measuring the change in R_{ant} we can thus estimate L_{ant}. From Section 1:

$$R_{ant} = Z_{magic}^2 I_{gen} \cos\phi_{gen} / V_{gen} = Z_{magic}^2 / Z_{ant} \quad \text{at resonance,}$$

which we compare with $R_{ant} + (\omega L_{ant})^2 / R_{cal}$ ie:

$(\omega L_{ant} / Z_{magic})^2 = R_{cal} (Z_{ant}^{-1} - (Z_{ant})_o^{-1})$ at resonance,

where $(Z_{ant})_o$ is the impedance of the circuit measured by the H-P probe at the matching box for no resistors connected. The following Table 3.1 was drawn up:

TABLE 3.1

f_{res}(MHz)	$Z_{ant}(\Omega)$	$R_{cal}(\Omega)$	$R_{cal}\,(1/Z_{ant} - (1/Z_{ant})_o)$
2.034	135.0 (=$(Z_{ant})_o$)	None	-
2.035	123.1	188	0.135
2.035	116.1	118	0.142
2.037	81.7	29	0.142

Note that the resonant frequency is changed only very slightly, showing that the resistances do not change the inductance of the system. The fact that the right-hand column values are (approximately) constant is a confirmation of the theory used to calculate the antenna loading, and gives an estimation of $\omega L_{ant}/Z_{magic}$. Since Z_{magic} is a function of L_{ant} and the known values δ and Z_o, we can calculate L_{ant} independently of any further assumptions. This gives a value $L_{ant}(3a) = 79$ nH. If, however, we take $Z_{magic} = 3.57\Omega$ from Section 1 (at 2.03 MHz), we obtain the antenna inductance $L_{ant}(3) = 105 \pm 10$ nH. (See bottom of Table 3.3 for an explanation of the difference between $L_{ant}(3a)$ and $L_{ant}(3)$).

Method 4 A direct resonance measurement was made on one pair of antenna bars (one antenna comprises six bars) as described in fig. 3.2.

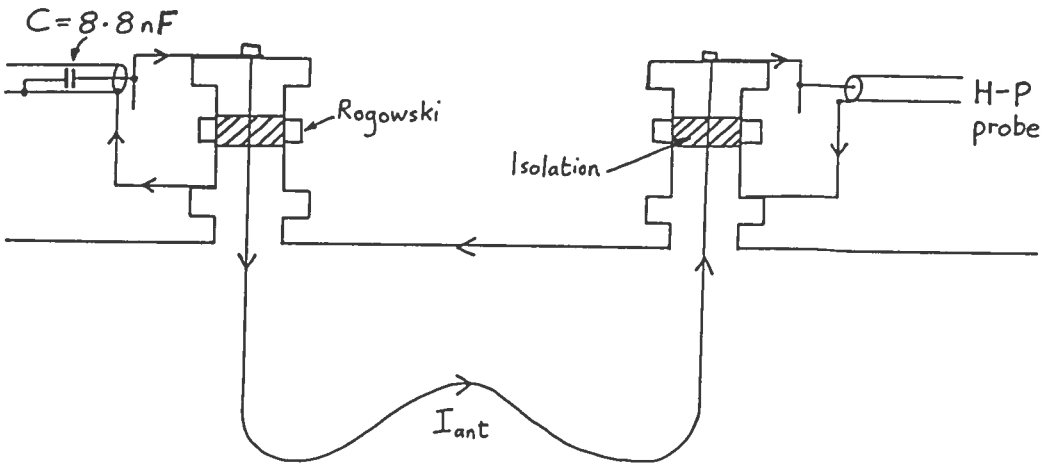

Figure 3.2 Modification to rf plugs for resonance measurement.

2 rf plugs were modified, one with an internal known capacitor 8.8 nF and the other to connect to the H-P impedance meter. The inductance 42 nH of the probe and capacitor plug is subtracted from the circuit inductance (resonance at 2.54 MHz) giving L_{pair} = 404 nH. The combined inductance for three isolated pairs in parallel is therefore 135 nH. Because of the mutual inductance of the bars, the total inductance will be higher by 30% or so. Therefore $L_{ant}(4) = 155 \pm 20$ nH.

Method 5 By changing the number of cables (hence varying the characteristic impedance Z_o of the line) we can estimate L_{ant} by method 1 above, and the consistency of the results is a test of the validity of the model in section 1. Table 3.2 was drawn up:

TABLE 3.2

No. of cables	Characteristic Impedance	Resonant Frequency	L'ant for partial Antenna (nH)	Fraction of Antenna	Lant for whole Antenna (nH)
18	50/9	2.017*	174	1	174
12	50/6	1.682	275	2/3	183
6	50/3	1.265	506	1/3	169
4	50/2	1.135	526	1/3	175
4	50/2	1.139	544	1/3	181
4	50/2	1.138	546	1/3	182

* On this day, the resonant frequency had changed from 2.033 MHz to 2.017 MHz. Only the cable arrangement had been changed.

The values for L_{ant} are consistent for a range of factor 4 in ω^2 and Z_o, thus confirming the model in Section 1. The average of these values gives $L_{ant}(5) = 177 \pm 10$ nH.

Reconciliation between estimated values for L_{ant}
See figure 3.3.

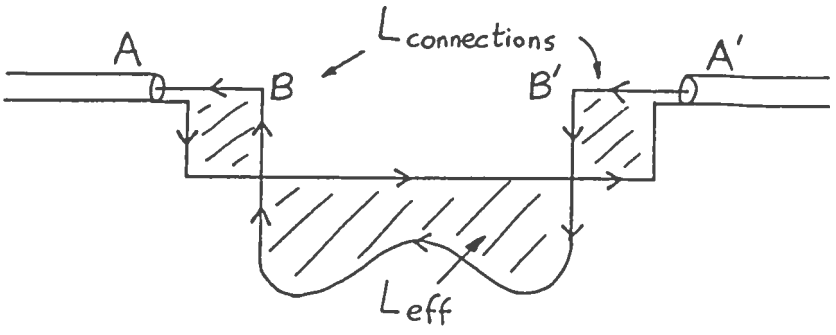

Figure 3.3 Definition of L_{ant} and L_{eff}.

Methods 1,4,5 measure the inductance between AA', using different techniques. This is the inductance seen at the cable ends and so is L_{ant} for the purposes of Section 1.

Methods 2,3 measure the inductance across the antenna terminals BB', again by different methods. Table 3.3 compares these values:

TABLE 3.3

Whole antenna L_{ant} (nH)	Effective antenna L_{eff} (nH)
$L_{ant}(1) = 174 +/- 20$	$L_{ant}(2) = 98 +/- 10$
$L_{ant}(4) = 155 +/- 20$	$L_{ant}(3b) = 105 +/- 10$
$L_{ant}(5) = 177 +/- 10$	

Note $L_{ant}(3a)$ is false because $L_{ant} = 165$ nH must be used for the calculation of Z_{magic}, and not L_{eff}.

We see that, within each group, there is good agreement. Therefore:

$L_{ant} = 165 +/- 15$ nH which is the relevant inductance for Section 1 and

$L_{eff} = 100 +/- 10$ nH which is the inductance associated with the feedthroughs and the antenna itself and does not include the cable connections to the terminals.

Now that all the important circuit elements have been measured, we can continue with antenna loading measurements.

SECTION 4 PRELIMINARY ESTIMATIONS OF R_{ant}

Measurement 1 As before, all the measurements are made on antenna 1 using the H-P vector impedance meter (at the input to the matching circuit) to avoid probe calibration errors. Table 4.1 shows a frequency scan of the impedance and phase.

TABLE 4.1

f(MHz)	Zgen	ϕgen	Rant = $Z_{magic}^2 \cos\phi / Z_{gen}$
1.8	19.7	80.9	82.7
1.9	33.3	75.8	83.3
1.95	50.3	68.5	86.2
1.975	66.7	61.0	87.9
2.0	94.8	46.5	89.8
2.015	117.7	30.5	91.7
2.025	130.6	15.8	93.1
2.034 (Resonance)	134.6	0.5	94.7
2.04	131.7	-9.8	95.8
2.05	119.8	-25.0	97.7
2.075	82.3	-49.3	104.5
2.1	58.7	-60.7	112.4
2.15	36.4	-71.7	121.2
2.2	25.2	-77.0	129.1
2.3	15.06	-80.7	170.0

Fig. 4.1 plots the deduced antenna vacuum loading from

$$R_{ant} = Z_{magic}^2 I_{gen} \cos\phi_{gen} / V_{gen} = Z_{magic}^2 . \cos\phi_{gen} / Z_{ant}$$

using the simple model of Section 1. The loading is not constant, but rises with frequency as did the loading measured by G Besson's probes in Section 1 Fig. 1.2

Measurement 2 Secondly, the resonant frequency was altered by adding small capacitors or inductances in parallel with the capacitor C. At resonance, only the real part of the impedance Z_{res} is measured, and $R_{ant} = Z_{magic}^2/Z_{res}$. We plot the deduced loading on Fig. 4.1.

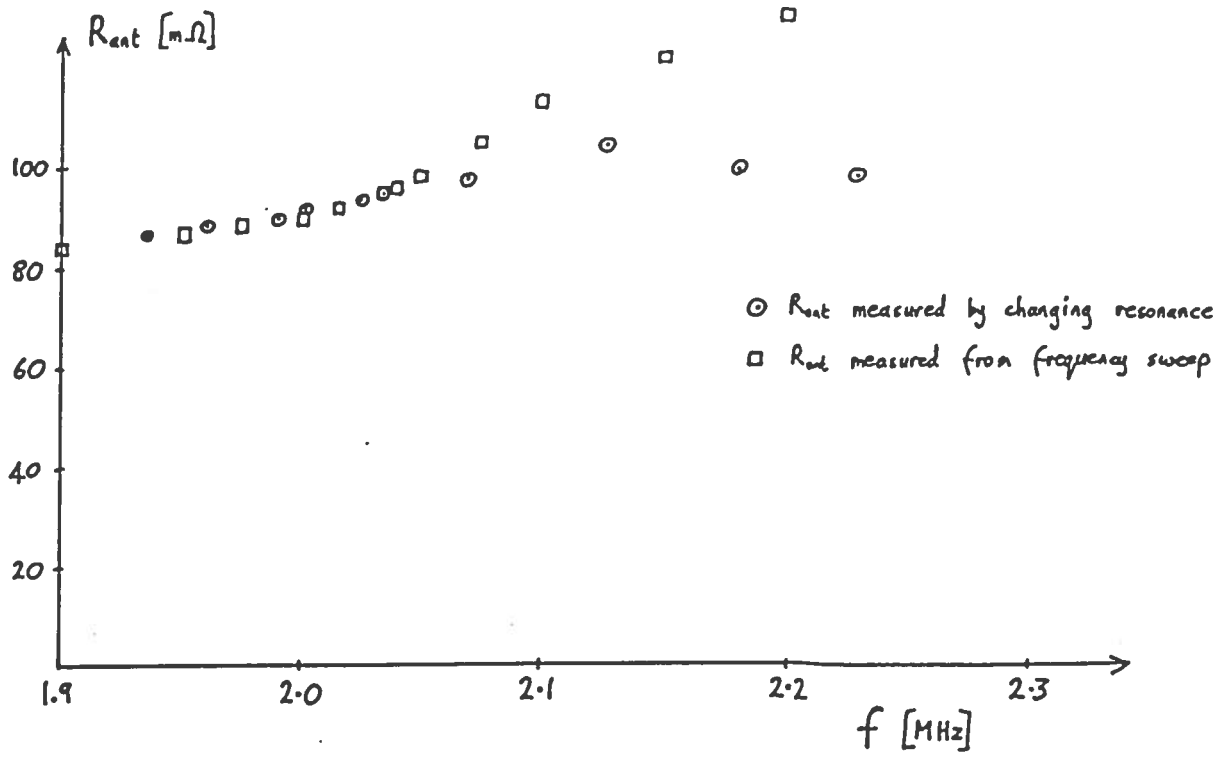

Figure 4.1 R_{ant} measured by two methods

Conclusion The vacuum loading as deduced from a frequency sweep (either static or dynamic, with a fixed resonant frequency as normal) increases strongly and monotonically with frequency. The loading from the different-resonance measurements increases only due to the skin effect (although approximately double this increase is found; the error remaining may be due to errors in the values taken for L_{ant}, cable length, Z_o, velocity in the cable and the assumption of ideal cables). There is therefore a clear discrepancy with respect to the frequency sweep method ie R_{ant} measurements made during a frequency sweep (and therefore, off-resonance) are incorrect. This will be resolved in the following section.

SECTION 5 CORRECTION FOR L_{ser}

The final circuit of Section 1 was:

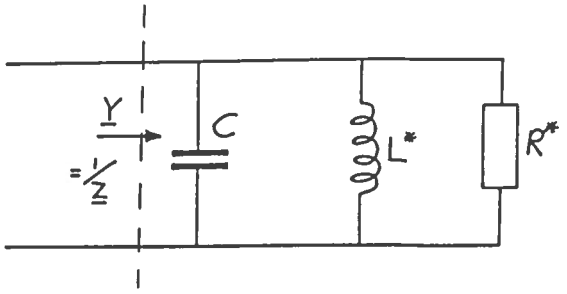

and $R_{ant} = Z_{magic}^2.Re(\underline{Y})$.

The identification of a series inductance L_{ser} between this circuit and the probes means that we actually measure $\underline{Y}_o$:

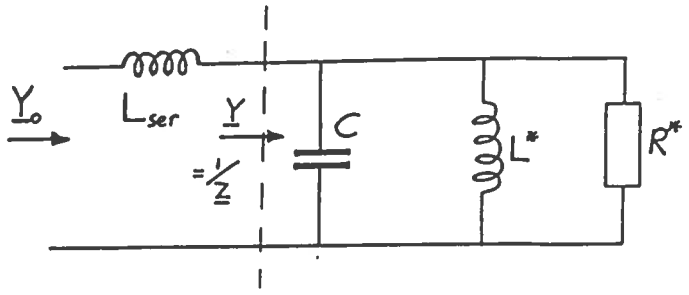

ie

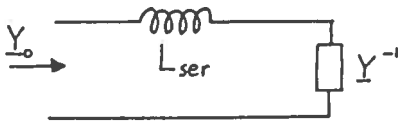

ie We measure $\underline{Y}_o$, but require $\underline{Y}$. Therefore:

$\underline{Y}_o = 1 / (j\omega L_{ser} + 1/\underline{Y}) = \underline{Y} / (j\omega L_{ser}\underline{Y} + 1)$ ie:

$\underline{Y} = \underline{Y}_o (1 + j\omega L_{ser}\underline{Y}_o)^{-1}$ is the transformation to apply. Rationalising:

$\underline{Y} = \underline{Y}_o (1 + j\omega L_{ser}\underline{Y}_o^*) / (1 + j\omega L_{ser} (\underline{Y}_o^* - \underline{Y}_o) + \omega^2 L_{ser}^2 Y_o^2)$

$\underline{Y} = (\underline{Y}_o + j\omega L_{ser} Y_o^2) / (1 + 2\omega L_{ser}(\underline{Y}_o)_{Im} + \omega^2 L_{ser}^2 Y_o^2).$

Re-arranging the denominator and taking real parts, we have:

$$(\underline{Y})_{Re} = (\underline{Y_o})_{Re} / ((1 + \omega L_{ser}(\underline{Y_o})_{Im})^2 + \omega^2 L_{ser}^2 (\underline{Y_o})_{Re}^2).$$

But $\omega L_{ser}(\underline{Y_o})_{Re} = \omega L_{ser} / R_{eq} = \omega L_{ser} / 135$ approx. $<< 1$ (for f < 3 Mhz) so:

$$(\underline{Y})_{Re} = (\underline{Y_o})_{Re} (1 + \omega L_{ser}(\underline{Y_o})_{Im})^{-2} = (\underline{Y_o})_{Re} (1 - \omega L_{ser} Y_o \sin\phi_o)^{-2},$$ and finally:

$$(\underline{Y})_{Re} = (I_{gen} \cos\phi_{gen} / V_{gen}) (1 - \omega L_{ser} I_{gen} \sin\phi_o / V_{gen})^{-2}$$ therefore:

$$R_{ant}(corrected) = R_{ant}(original) . (1 - \omega L_{ser} I_{gen} \sin\phi_o / V_{gen})^{-2}.$$

Using L_{ser} = 158 nH, Fig. 5.1 shows the correction applied to the data from the frequency sweep of Fig. 4.1 - the antenna loading trace is rotated about the value at resonance, thus levelling the loading trace. A computer plot (see PHACOR.FTN in appendix), using the circuit above, shows the effect of L_{ser} on the loading measurement (Figs.5.2 and 5.3). The changes to the phase, current and voltage measurements are surprisingly small, demonstrating the difficulty of making accurate measurements during a frequency sweep. Results of real measurements are presented in Section 7.

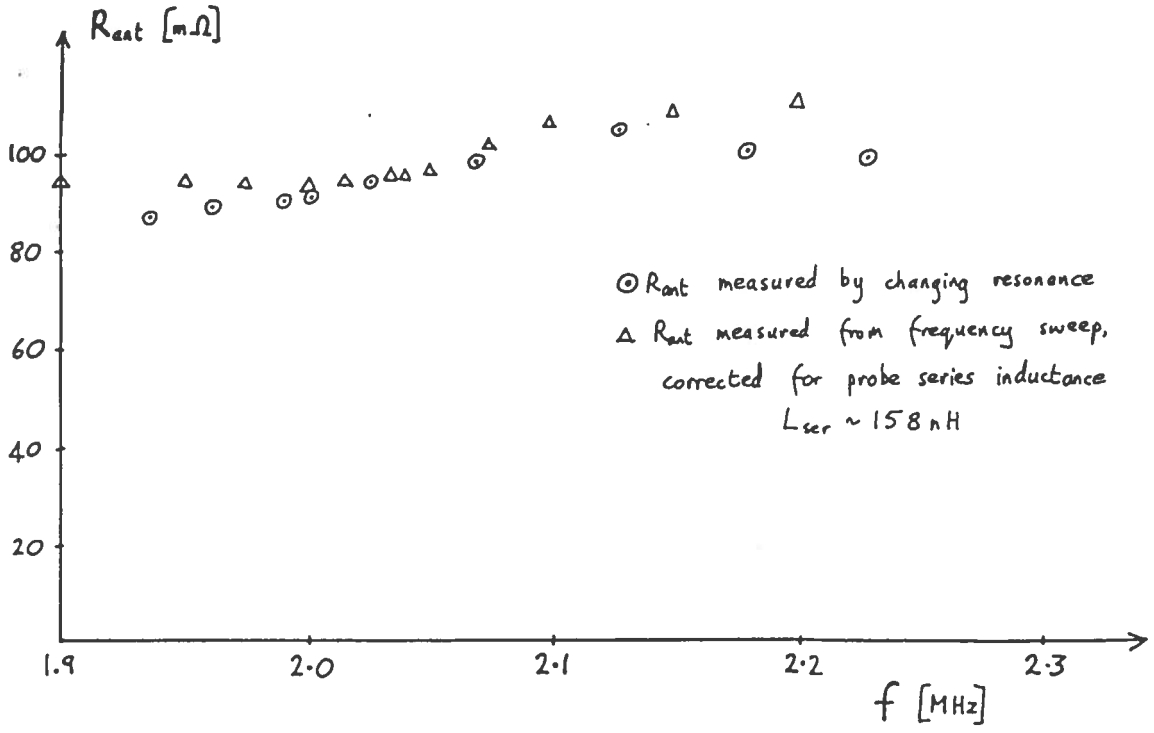

Figure 5.1 L_{ser} correction applied to data of fig. 4.1.

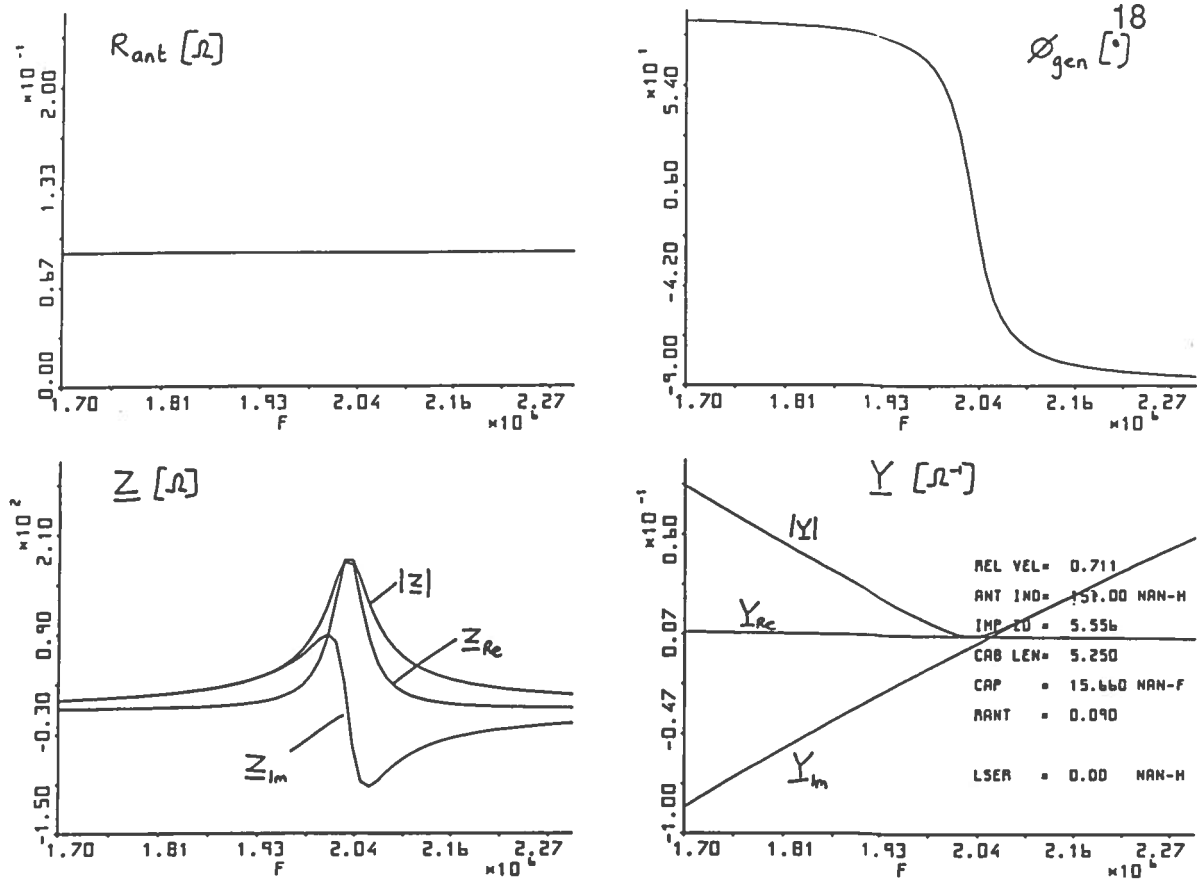

Figure 5.2a Computer plot of R_{ant} for the ideal circuit of Section 1.

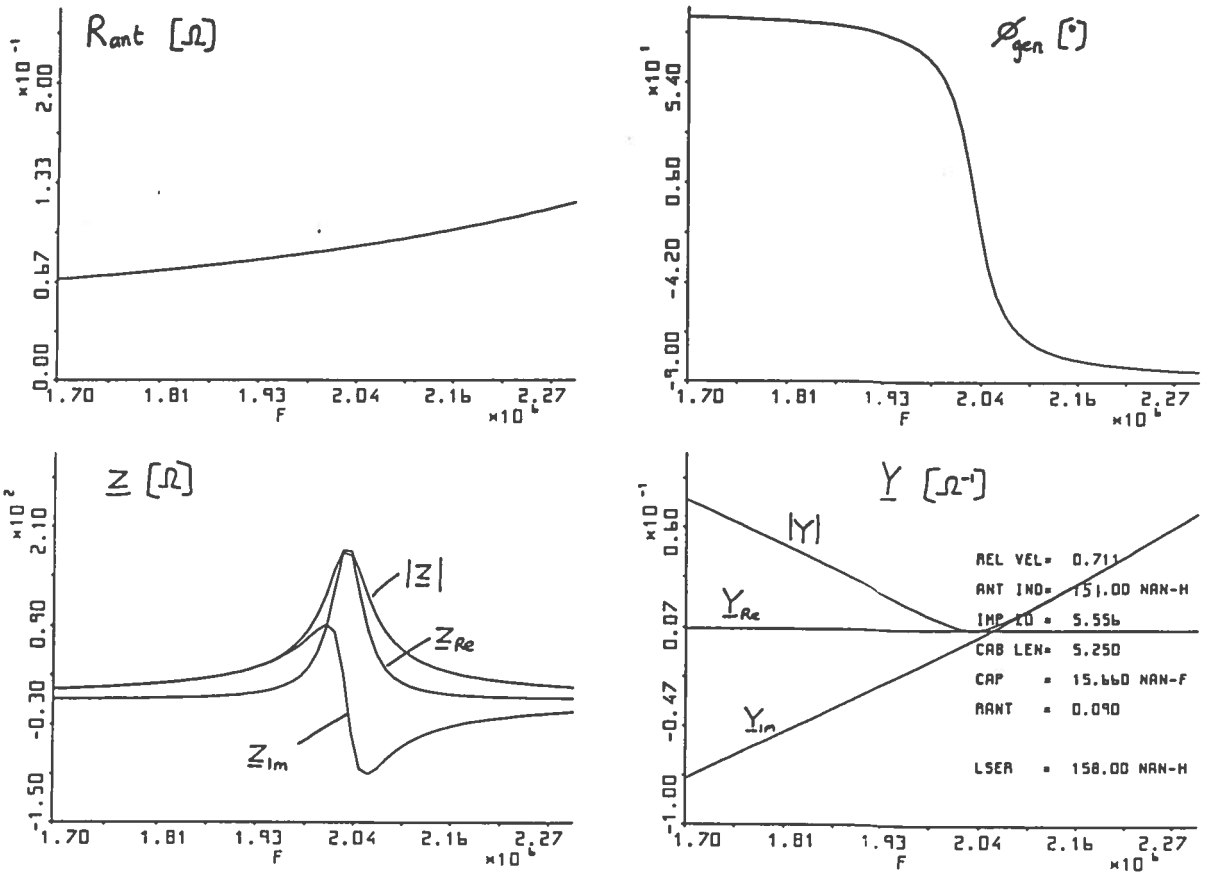

Figure 5.2b Computer plot of R_{ant} including probe series inductance L_{ser}.

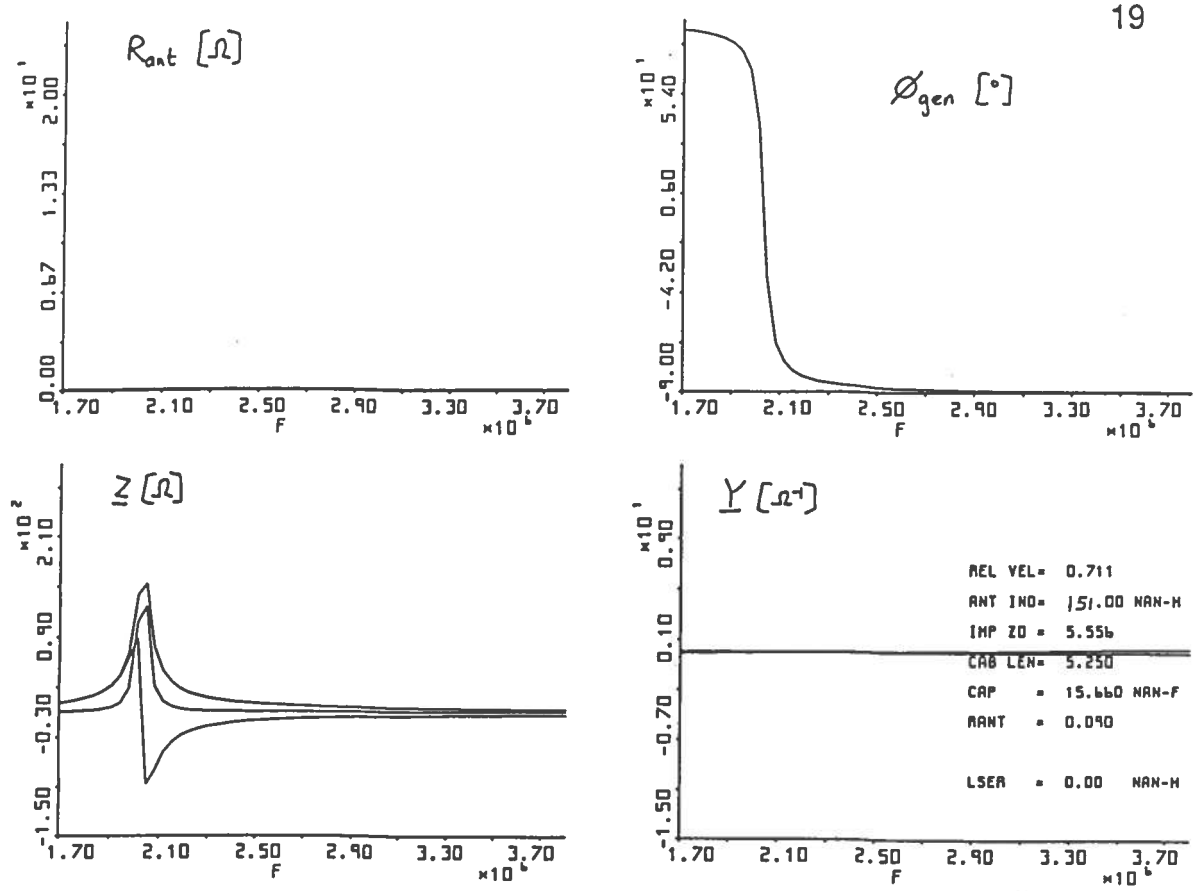

Figure 5.3a Computer plot of R_{ant} for the ideal circuit of Section 1, as for Fig.5.2a but with different scaling.

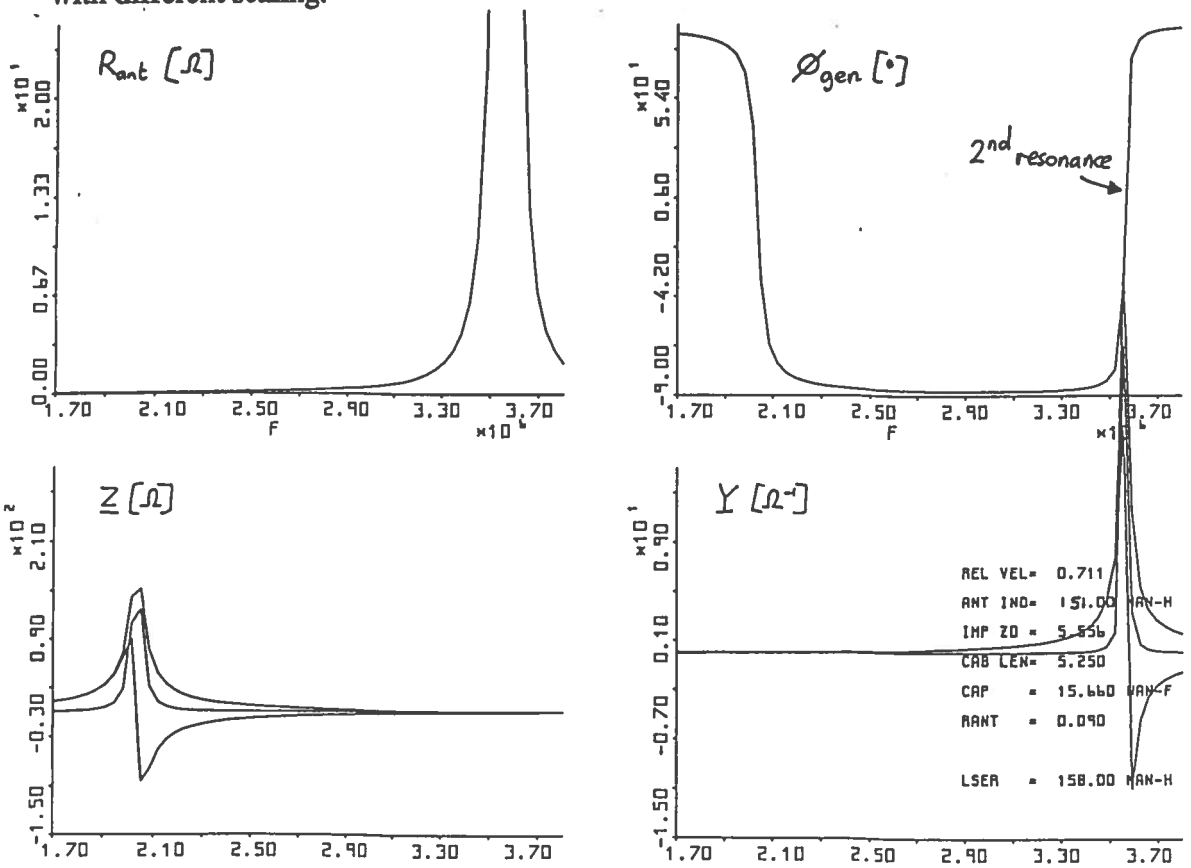

Figure 5.3b Computer plot of R_{ant} including probe series inductance L_{ser}, as for Fig 5.2b, but also showing second resonance.

SECTION 6 OTHER CORRECTIONS TO R_{ant}

The full circuit considered is (compare the simple circuit Section 1):

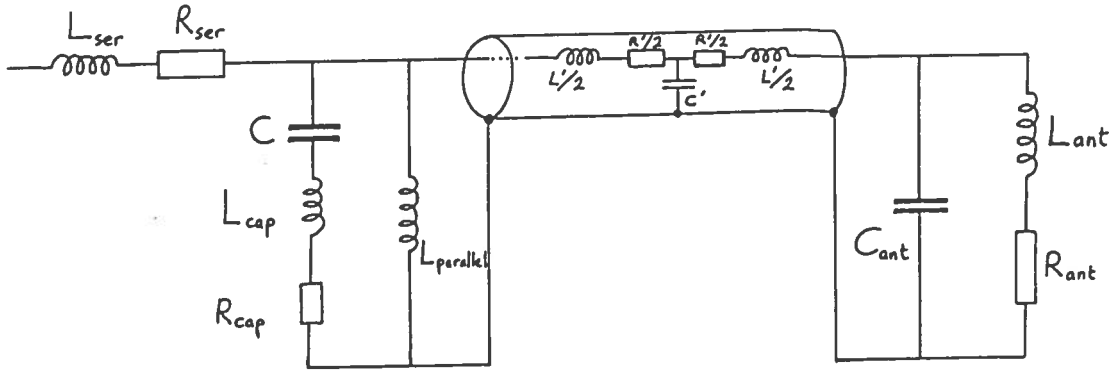

The contribution to errors introduced by each 'parasitic' component is considered in turn below:

*6.1 L_{ser}, the series inductance associated with the probes, has been treated in the previous section and significantly alters the estimation of $R_{ant}(f)$.

*6.2 R_{ser} is the small resistance of the probe connection to the tuning capacitors C. Its effect can be calculated by replacing $j\omega L_{ser}$ by $j\omega L_{ser} + R_{ser}$ in Section 4. We obtain:

$$(\underline{Y})_{Re}(\text{corrected}) = ((\underline{Y}_o)_{Re} - R_{ser}\, Y_o^2) / ((1 + \omega L_{ser}(\underline{Y}_o)_{Im})^2 + R_{ser}^2\, Y_o^2)$$

The effect of R_{ser} is to artificially increase R_{ant}(estimated) on both sides of the resonance.

*6.3 $L_{parallel}$ Two large inductances have been added to each antenna, connecting each capacitor plate to the cable screens (torus earth). This shorts dc potentials to ground. The rf resonant frequency, however, is independent of whether these inductances are connected or not. Their inductance (approx 470 μH) is much larger than L_{eq}, the cable transformed antenna inductance, and so $L_{parallel}$ can be ignored for rf calculations.

*6.4 L_{cap}, the inductance associated with the tuning capacitor system (boîte d'accord) affects the resonant frequency; it is lower than that which would be estimated from C and L_{eq} alone:

$$\omega_{res}^2 = 1 / (C\,(L_{eq} + L_c)).$$

The real part of the admittance, and therefore the measurement of R_{ant}, is not altered.

*6.5 C_{ant} It was suggested that the antenna may have a stray capacitance to the torus. C_{ant} modifies Z_{ant}, and when cable-transformed, modifies Z_{magic} - this is the only effect of C_{ant} on the calculation of R_{ant}. We obtain

$$Z_{magic}(\text{corrected}) = (\omega L_{ant} + \delta Z_o (1 - \omega^2 C_{ant} L_{ant})) / (1 + \delta^2)^{.5}$$

(compare with Z_{magic} from Section 1). If we take C_{ant} even as high as 500 pF, Z_{magic} changes by <.5%. This stray capacitance, then, introduces negligible error into the measurement of R_{ant} and can be ignored.

*6.6 R_{cap} The effective series resistance of the tuning capacitor system was gauged to be about 10 mΩ. Since R_{ant} is deduced from the real part of the admittance of the total circuit, R_{cap} could cause errors. We find that R_{ant} is overestimated by an amount:

$$\delta R_{ant} = (Z_{magic}\, \omega C)^2 R_{cap} = R_{cap} / 2 = 5\ \text{m}\Omega \quad \text{at 2 MHz.}$$

This is simply an error in the vacuum loading result and is automatically subtracted when the plasma loading is calculated. However, the ω^2 dependence of the correction means that a fractional residual error of $2\delta\omega/\omega$ of this correction persists for a frequency sweep range $\delta\omega$. For a typical sweep of 1.7 - 2.3 MHz, $2\delta\omega/\omega = 0.3$ and so the final error in the plasma loading is a false increase of only about 3 mΩ. This may nevertheless be important for small plasma loading in the presence of screens.

*6.7 Non-ideal cables Up until now, the cable resistance has been assumed to be a lumped resistance included in the antenna resistance to from an effective vacuum loading resistance. The real cable resistance is, however, distributed along the cable and thus the cable-transformed loading is changed. To evaluate any errors incurred by assuming a lumped cable resistance, we adopt a T-section description of the cable as given by G Collins:

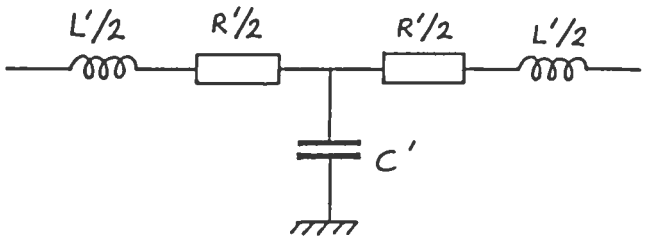

For the asymmetric single cable we have $Z_o = 50\Omega$, C = 96 pF/m, L = 0.24 μH/m.
For a 2 x 18 cable symmetric transmission line:
L' = 26.7 nH/m = 140 nH for 5.25m, C' = 864 pF/m, $Z_o = 5.5556\Omega$
$R' = 6.32\ f_{MHz}^{0.552}$ mΩ/m = $50\ (f_{MHz}/2)^{0.552}$ mΩ for 5.25m (from G Collins' GC1)

Note that the cable resistance 50mΩ is the major contribution to R_{vide}.

In the equation for Z_{eq} (Section 1), we simply replace Z_o and γ by the complex impedance and complex phase delay:

$$Z_o = (L'/C')^{0.5}\ (1 - jR'(f)/2\omega L'), \text{ and } \gamma = \omega\ (L'/C')^{0.5}\ (R'(f)/2\omega L' + j).$$

Programme CABLES.FTN (see appendix) plots the cable-corrected vacuum loading as a ratio to the total lumped effective antenna resistance, $R_{effective} = R_{ant} + R_{cables}$ (set equal to 80mΩ here), using our standard defintion of Z_{magic} (unaffected by ideal/non-ideal cables) - see fig. (6.1). This is then the error in R_{vide} due to the ideal cable assumption. There are two effects:

a) that the corrected resistance is less because parts of the cable resistance are now transformed by shorter lengths of cable (and this reduction effect becomes more important at higher frequency because the cable length is a larger fraction of λ), and:

b) this trend is reversed (and almost compensated) by the increase in cable resistance due to the skin-effect. The imaginary part of Z_{eq} is changed by < 0.1%. This offset value of R_{vide} is automatically accounted for by making a vacuum shot measurement and we are left with a small (5%) apparent increase in R_{vide} due to the non-ideal cables.

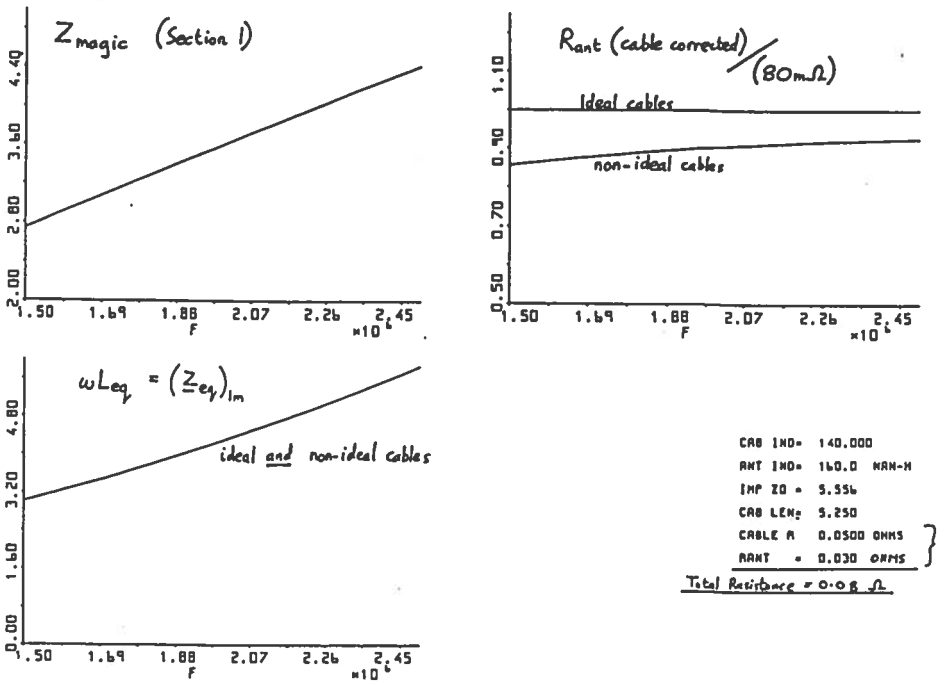

Figure 6.1 The effect of non-ideal cables on the estimation of R_{ant}.

*6.8 Instrumental measurement errors Here we prematurely consider errors due to the probe measurements themselves. Since

$$R_{ant}/ Z_{magic}^2 = I_{gen} \cos\phi_{gen} / V_{gen},$$

errors in I_{gen} and V_{gen} simply add to the total error in R_{ant} and therefore to the plasma loading $R_{pl} = R_{ant} - R_{vide}$. An error in the phase angle $\phi = \tan^{-1} (Y_{Im}/Y_{Re})$ could be due to a poor phase measurement or to probe cables of unequal lengths. For the latter case, the error $\phi = \delta l.f.2\pi/v$ (where δl is the cable length discrepancy) is proportional to frequency. Ignoring for the moment the correction due to L_{ser}, for a given phase error:

$$R_{ant} = I_{gen} \cos (\phi - \phi_{err}) Z_{magic}^2 / V_{gen},$$

where ϕ is the true phase, and $\phi - \phi_{err}$ the measured phase, then

$$R_{ant}(\text{corrected}) = R_{ant}(\text{measured}) / (\cos\phi_{err} + \sin\phi_{err} \tan\phi), \quad \text{therefore:}$$

$$R_{ant}(\text{corrected}) = R_{ant}(\text{measured}) / (\cos\phi_{err} + \sin\phi_{err} Y_{Im} / Y_{Re}).$$

This correction reduces the estimate of R_{ant} on both sides of the resonant frequency - see Section 7.3 for an example.

*Study of complete circuit using network programme AMPERE+

+Courtesy Ph Marmillod - see appendix for AMPAL.FTN

Aim: To build up the circuit from its simplest elements to fully include all of the above components mentioned above, whilst investigating the constancy of R_{ant} (deduced from the standard equation $R_{ant} = (\underline{Y})_{Re} . Z_{magic}^2$) as a function of frequency.

Since the line is short ($l<<\lambda$), we can well represent the line by a single T-section à la G Collins (no change to the results was found for a line made up of 5 T-sections and the single T-section input impedance was equal to the line characteristic impedance for up to 6.5 MHz). Non-ideal cables are simply represented by transferring the cable contribution to R_{vide} back into the T-section arms although the skin-effect on the resistance is not included. In all cases, the 'true' vacuum loading is $R_{ant} + R_{cables} = 80m\Omega$; deviations from this represent errors when using the simple model $R_{ant} = Y_{Re} . Z_{magic}^2$. The following series of figures shows the effect of each of the components discussed previously, and Table 6.1 is a summary. The final figure includes all identified circuit components. Note that the probe series inductance causes by far the largest errors. With the correct choice for this inductance, the curve R_{ant} v f can be fairly well flattened with the simple correction described in Section 5. Since all extra components act to increase R_{ant} as a function of frequency (even the non-ideal cable

case, if the skin-effect is included), the experimental measurements of Section 1 are seen to be reasonable. For future frequency-swept measurements, it would seem fair to assume that the real R_{ant} varies only due to the skin-effect, and apply the corrections above until the measured vacuum loading is indeed approximately constant. The graph in Fig 6.9, using the complete circuit, demonstrates the important check that the plasma loading is correctly deduced ie that $R_{plasma} = R_{ant} - R_{vide}$ is proportional to the antenna resistive load after the transformation of the circuit and application of the probe corrections.

TABLE 6.1 Summary of corrections to theory of Section 1

Element added to circuit	Effect on system	Error for frequency sweep	Error on R_{plasma} at const. frequency
L_{ser} (6.1)	Changes measure of Y seen by probes	Large. False increase in R_{ant} with frequency	Zero at resonance
R_{ser} (6.2)	Changes measure Y seen by probes	Increases R_{ant} on both sides of resonance (small)	Zero at resonance
$L_{parallel}$ (6.3)	Shorts dc potentials to ground	None	None
L_{cap} (6.4)	Changes resonant frequency	None	None
C_{ant} (6.5)	Slightly modifies Z_{magic}	Negligible	Negligible
R_{cap} (6.6)	Modifies Y_{Re}	False increase of 3mΩ	Zero
Non-ideal cables (6.7)	Changes R_{cable}	False increase of 5% in R_{ant}	Zero
Phase error (6.8)	False interpretation of Y_{Re}	Monotonic increase or decrease in R_{ant}	Changes constant of proportionality

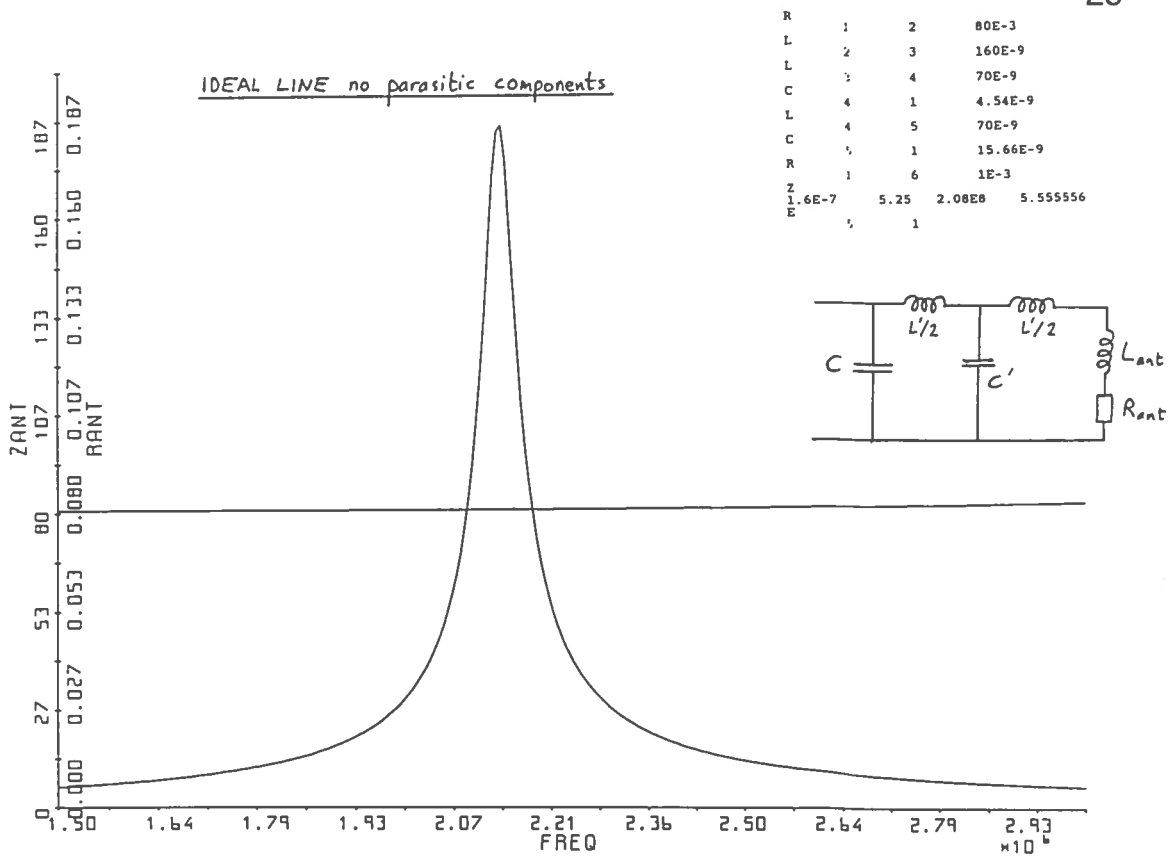

Figure 6.2 Idealised circuit of Section 1 with T-section for transmission line.

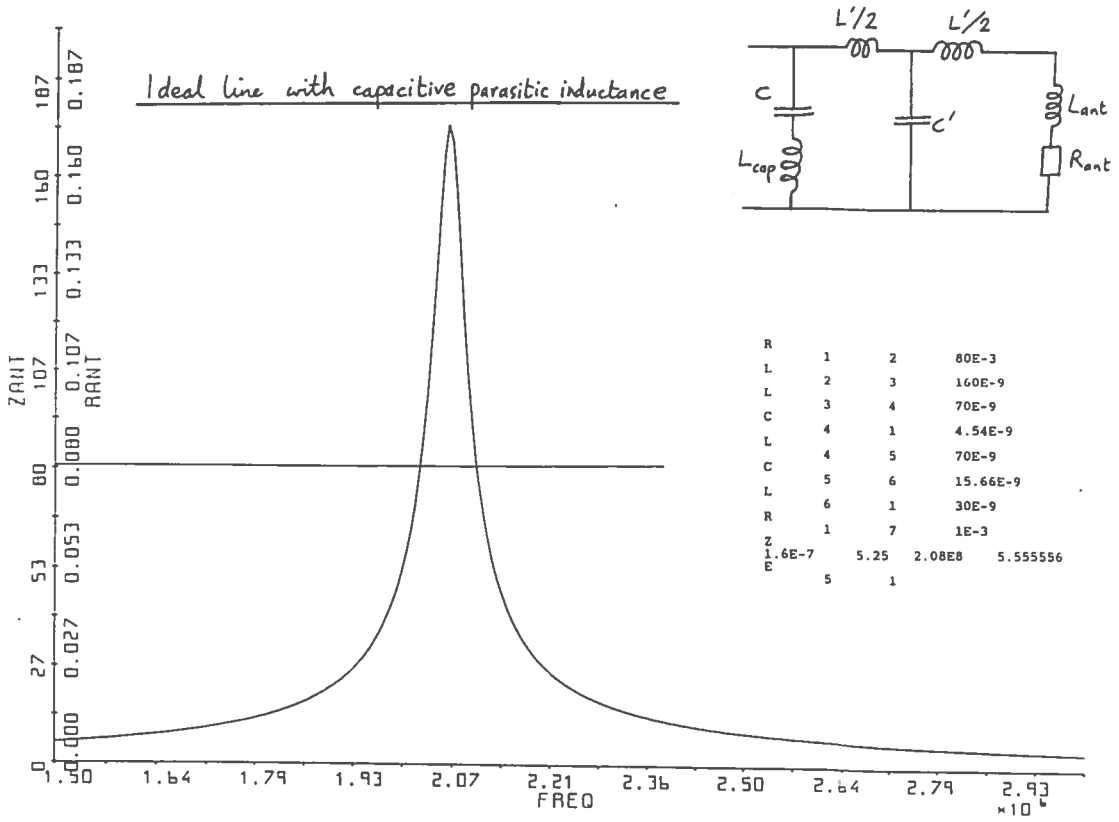

Figure 6.3 Add in L_{cap}, which merely shifts the resonant frequency.

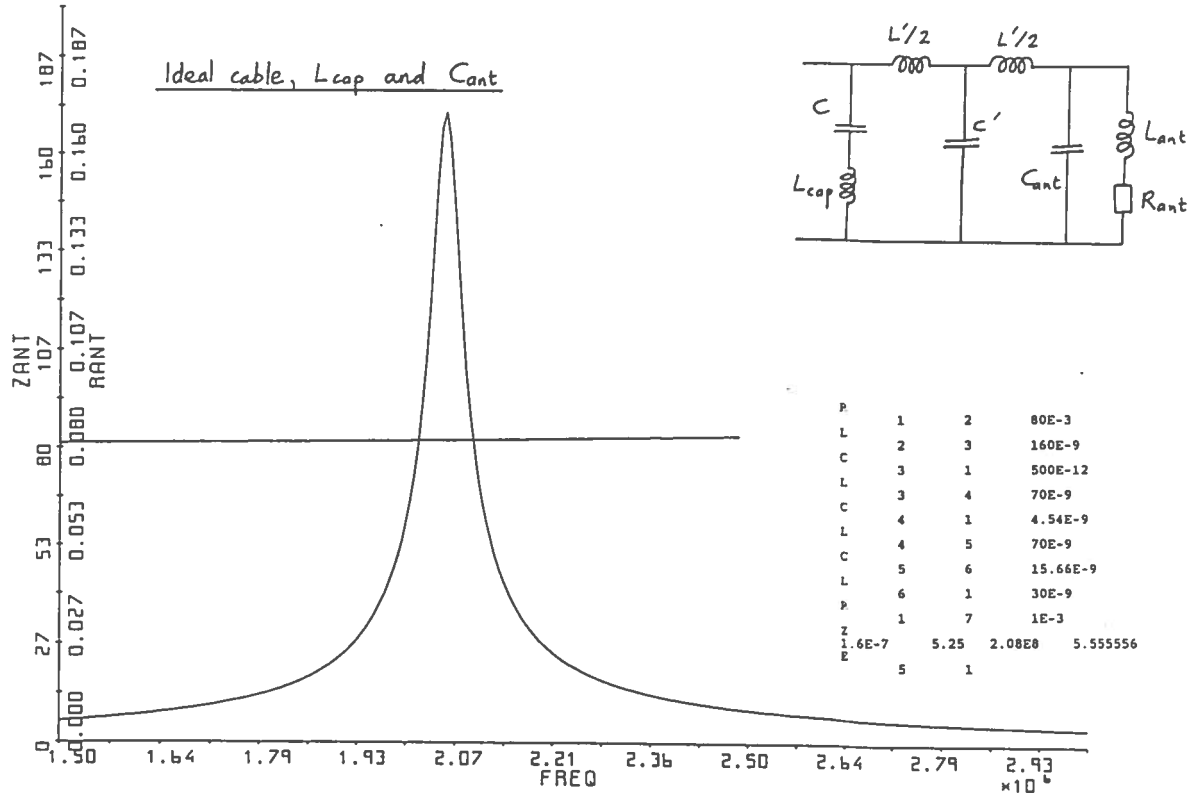

Figure 6.4 Negligible effect of C_{ant}.

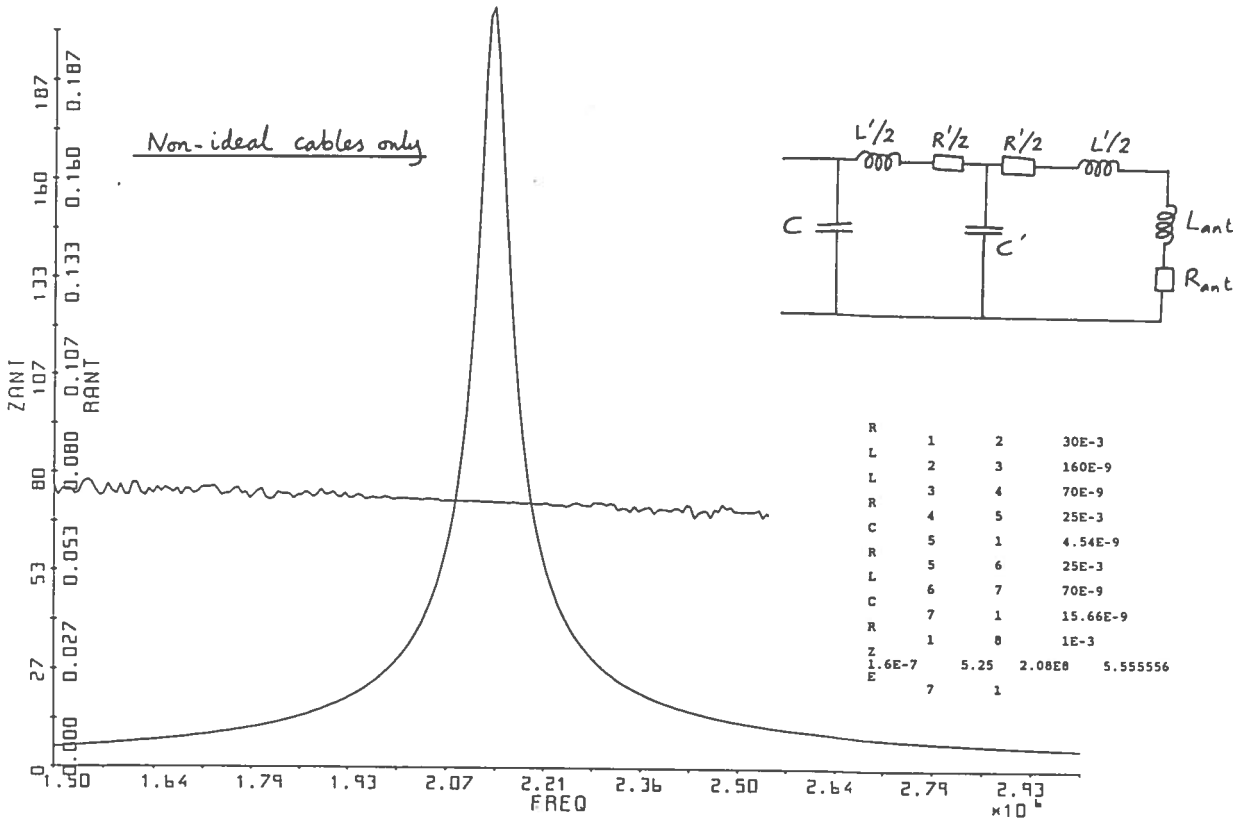

Figure 6.5 Effect of non-ideal cables, modelled by the T-section.

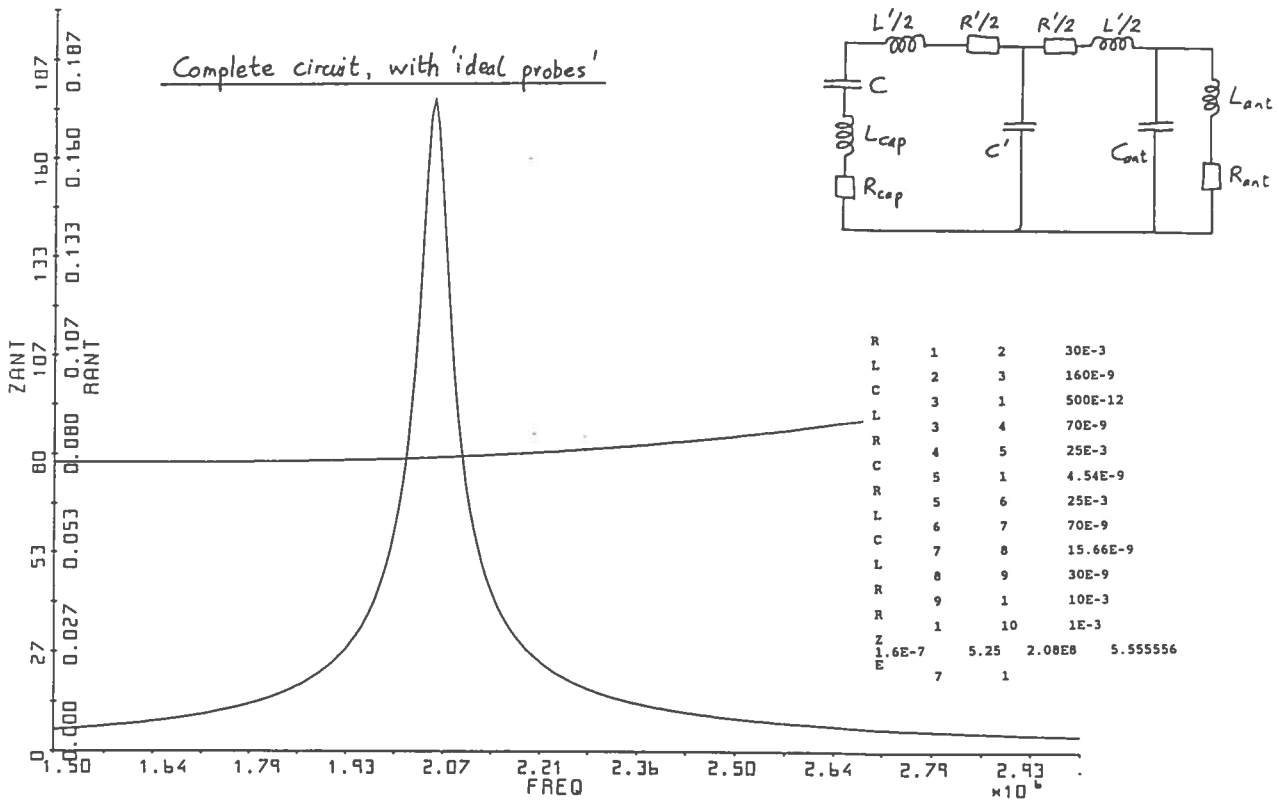

Figure 6.6 Final R_{ant} which would be measured with ideal probes.

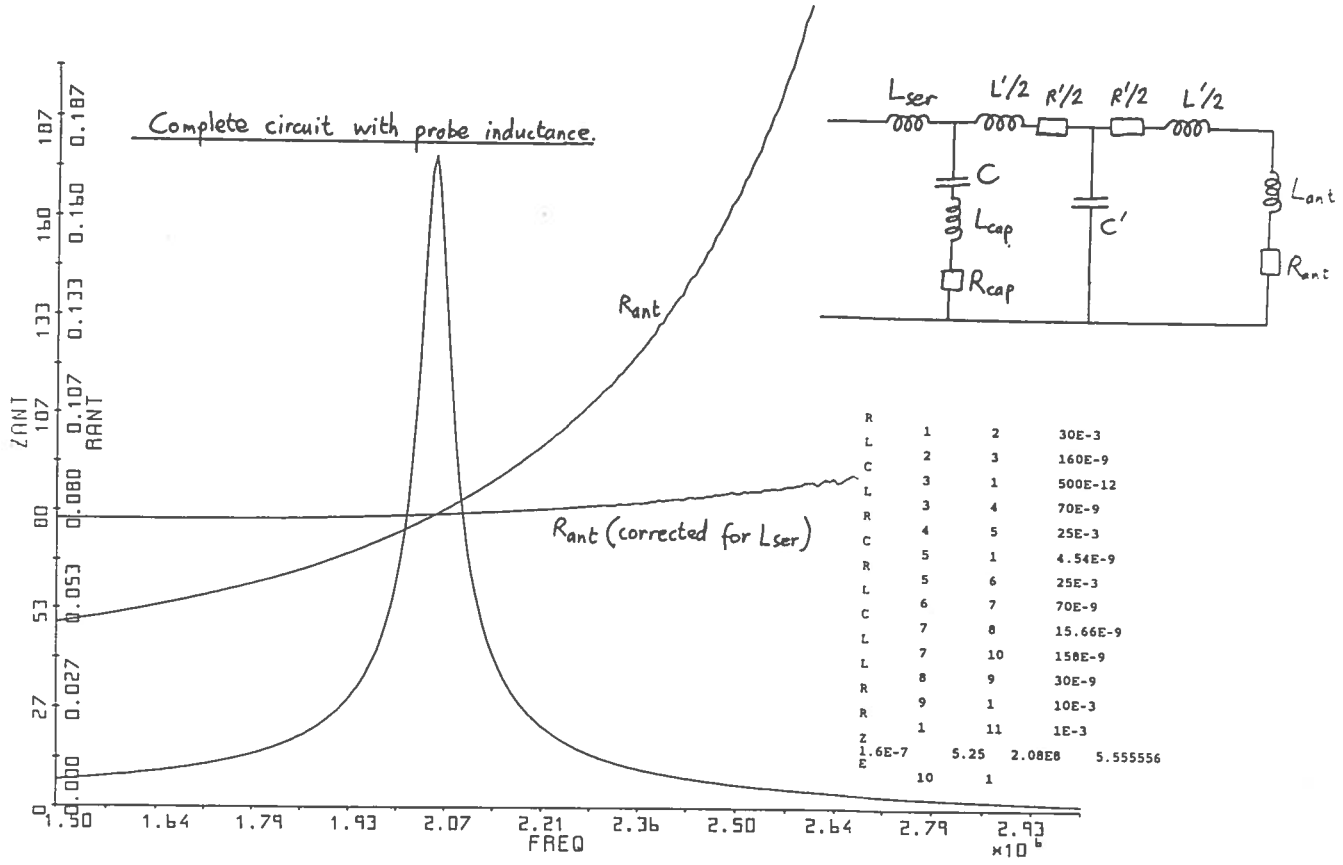

Figure 6.7 Allowing for the probe inductance L_{scr}.

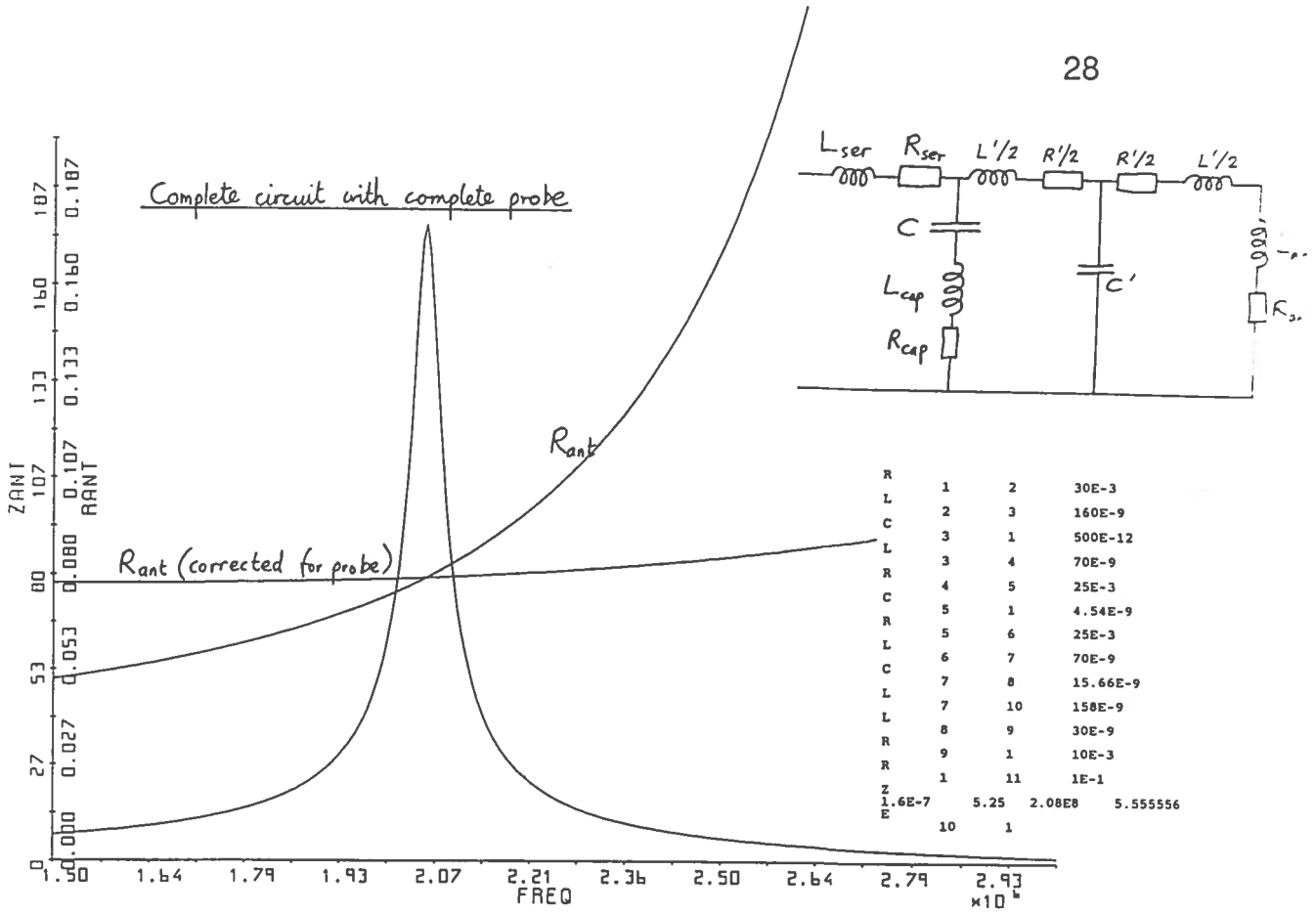

Figure 6.8 Best possible R_{ant} measurement with correction for probe.

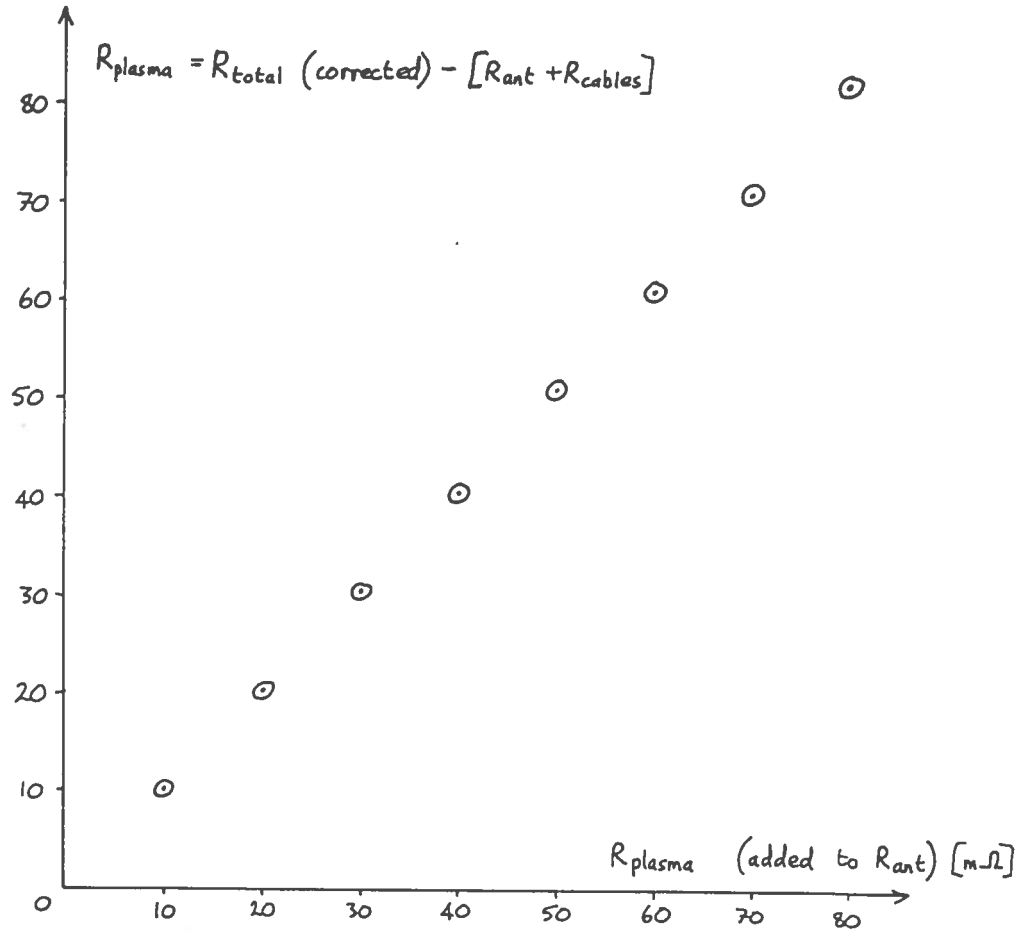

Figure 6.9 To show that R_{plasma}(deduced) is proportional to the load at the antenna.

PART 2 EXPERIMENTAL RESULTS

SECTION 7 MEASUREMENTS USING THE ENI AMPLIFIER

7.1 Probe circuits

a) To measure generator current I_{gen} into the matching circuit.
Two Rogowskis (10 turns on PVC torus, R = 27mm, r = 8mm), each with a nominal sensitivity of 190 mV/A at 2 MHz, are wired differentially and connected via two 39Ω resistors (it was found necessary to improve the impedance seen at the cable input) into a 2 core coaxial cable (labelled 'red') which is terminated in the screened room by another pair of 39Ω resistors. The signal, dI_{gen}/dt, is halved by the termination method, but doubled by the differential configuration.

b) To measure generator voltage V_{gen} at the matching circuit.
Two capacitors, nominally 27 pF, are connected to the cable screen via 39Ω resistors, again to improve the cable input termination impedance. The differential signal is fed by a twin core cable (labelled 'green') to the Faraday cage and is of nominally equal length to the 'red' Igen cable.

All probes, constructed by G Besson, are screened within a compartmented copper box and are virtually-earthed for rf frequencies to the antenna circuit earth (= torus earth via the 5.25m cable screens) by 2 nF capacitors. Their calibration is described below.

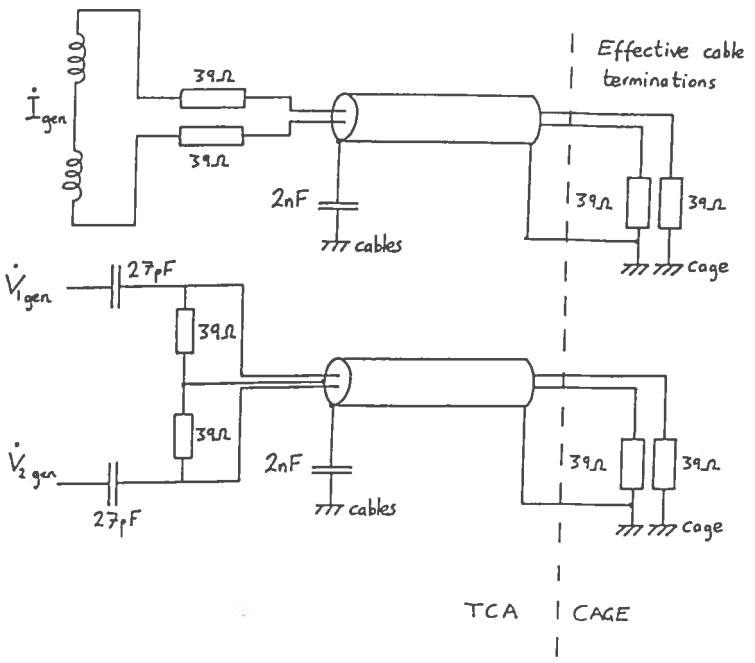

7.2 Calibration of probes using calibration resistance and mélangeur.

A swept-frequency, constant amplitude sine wave (from the Rohde-Schwarz generator) into the ENI rf amplifier produced sufficient voltage on a 114Ω calibration resistor (phase angle < 0.5° at 2 MHz) for the probes to be connected directly into the mélangeur (ie attenuation = 1). The mélangeur was used here in preference to the usual rf measurement acquisition amplifiers because there are no problems of non-linearity from diode rectifiers and the phase measurement is more reliable. For the frequency sweeps, the 'X' output of the Rohde-Schwarz generator was acquired in preference to FUN(54) from µ14, because the latter trace often has 'glitches'. The antenna current measurement was made asymmetrically (single pole), but the voltage, since it is not a floating measurement, was measured differentially using two mélangeur input channels. Preliminary attempts to combine the two voltage signals into one using a ferrite transformer always introduced small (1-2°) but important phase errors with respect to the current channel (even when a compensation transformer was installed into the current line) and therefore were not used in any of the experiments presented here. For all the work with the ENI generator, the probes of antenna 1 were used. The traces in Fig.7.1 were generated as follows:

I (A) = 0.97 x (signal from mélangeur) x 2.03/f (MHz)
V (V) = 17.5 x (difference in signals from mélangeur) x 2.03/f (MHz)

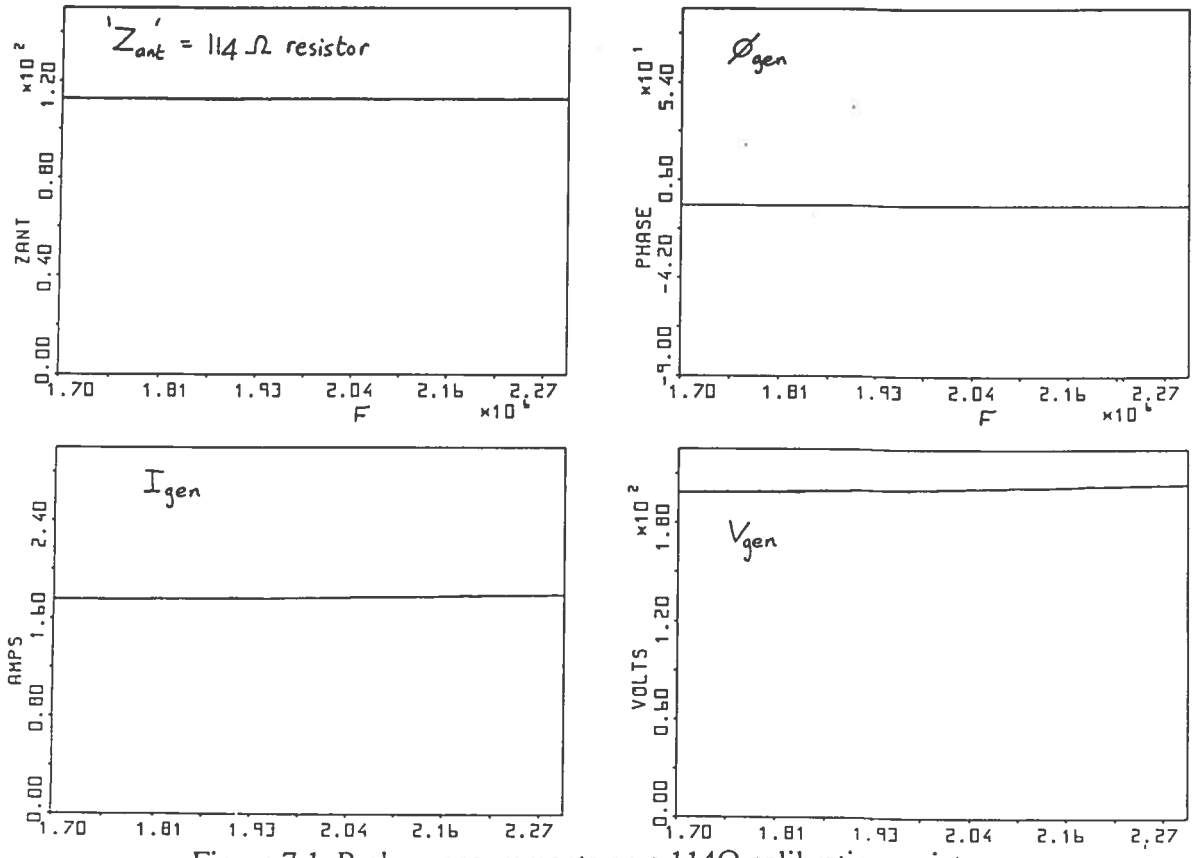

Figure 7.1 Probe measurements on a 114Ω calibration resistor.

The calibration factors were estimated using a Tektronix probe for the current, and the voltage from ohms law for the calibration resistor. We see from Fig.7.1 that the phase = 0° and Z = 114 Ω for the whole frequency range (I and V change slightly because of the frequency response of the ENI amplifier), thus confirming that the probes perform as good differentiators for this frequency range. We can therefore have confidence in the probe/mélangeur system for variable frequency and constant load.

7.3 Probe measurements on antenna using mélangeur and ENI amplifier

The calibration resistor was then replaced by the antenna. The experiment is now exactly as for a real frequency-swept AW heating experiment, except that the ENI generator replaces AFCO. Fig. 7.2 shows the raw signals for each (sin,cos) pair of I, V_1, and V_2 along with the sawtooth-swept frequency 'X' output. Fig 7.3 shows the reconstructed I_{gen}, V_{gen} traces along with their phase difference, and the magnitude, real and imaginary parts of the antenna impedance. Note that the matching circuit Q = $\omega/\delta\omega_{45o}$ = 50 approximately. These agree very well with the circuit models of Part 1. Fig.7.4 shows the real part of the admittance, the calculated Z_{magic} (according to Section1) and the antenna resistance $R_{ant} = Y_{Re}.Z_{magic}^2$ (see appendix for SWE.THT). After correcting for the probe series inductance (Section 5), the final R_{ant} is obtained. This is 90+/-10 mΩ over a 1.5-2.5 MHz frequency range - note the importance of the L_{ser} correction. For a better comparison with the original data see Fig. 7.5 which compares the R_{ant} trace over the original frequency range of Fig.1.2 (Section 1).

A shot in which the cable lengths from the I and V probes were slightly different (approx 50cm) is shown in Figs. 7.6 and 7.7, which demonstrate the large error in R_{ant} due to a phase offset error of only 2°. The correction algorithm of Section 6.8 was applied to Y_{Re} before the final correction due to L_{ser}. (continued)

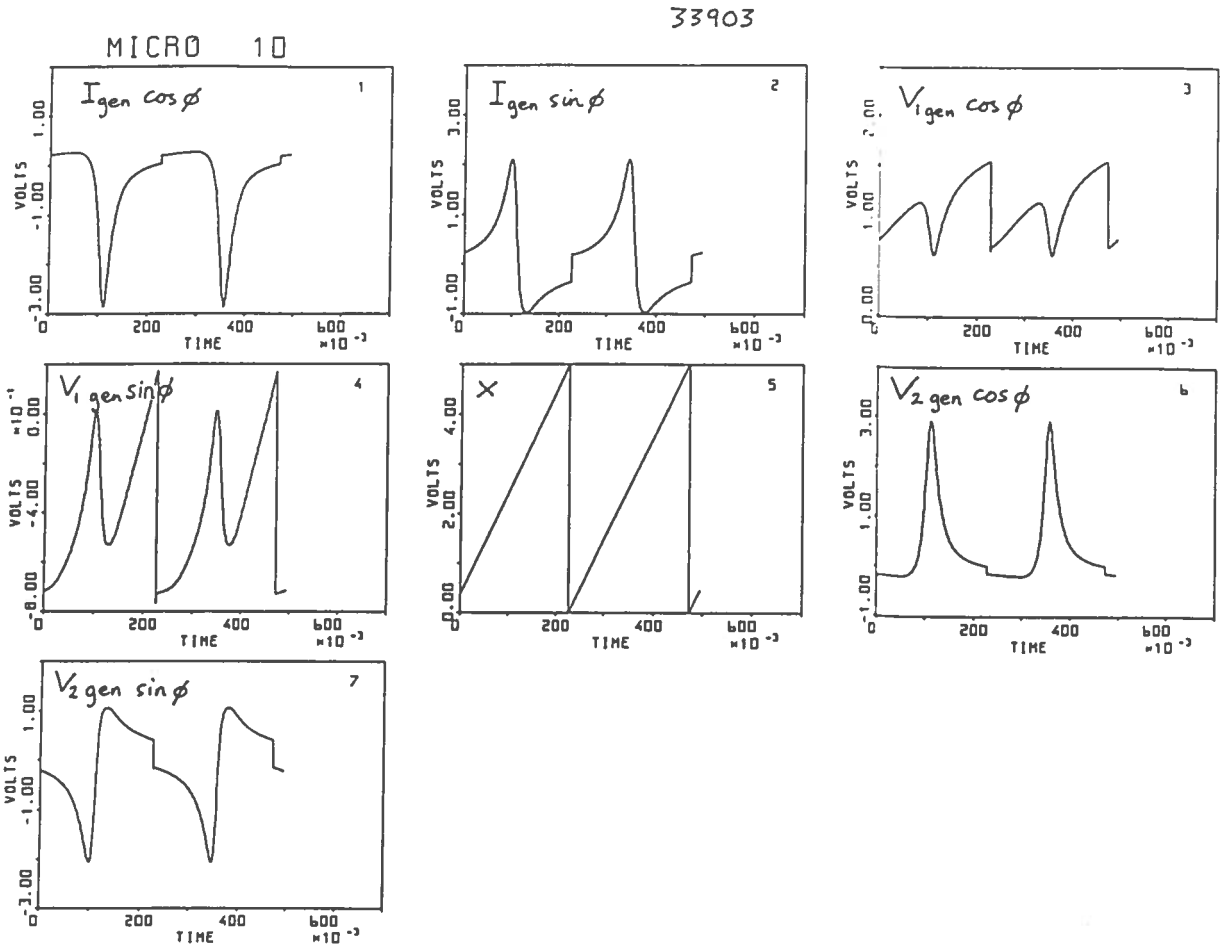

Figure 7.2 Raw signals from mélangeur for frequency-sweep with ENI generator.

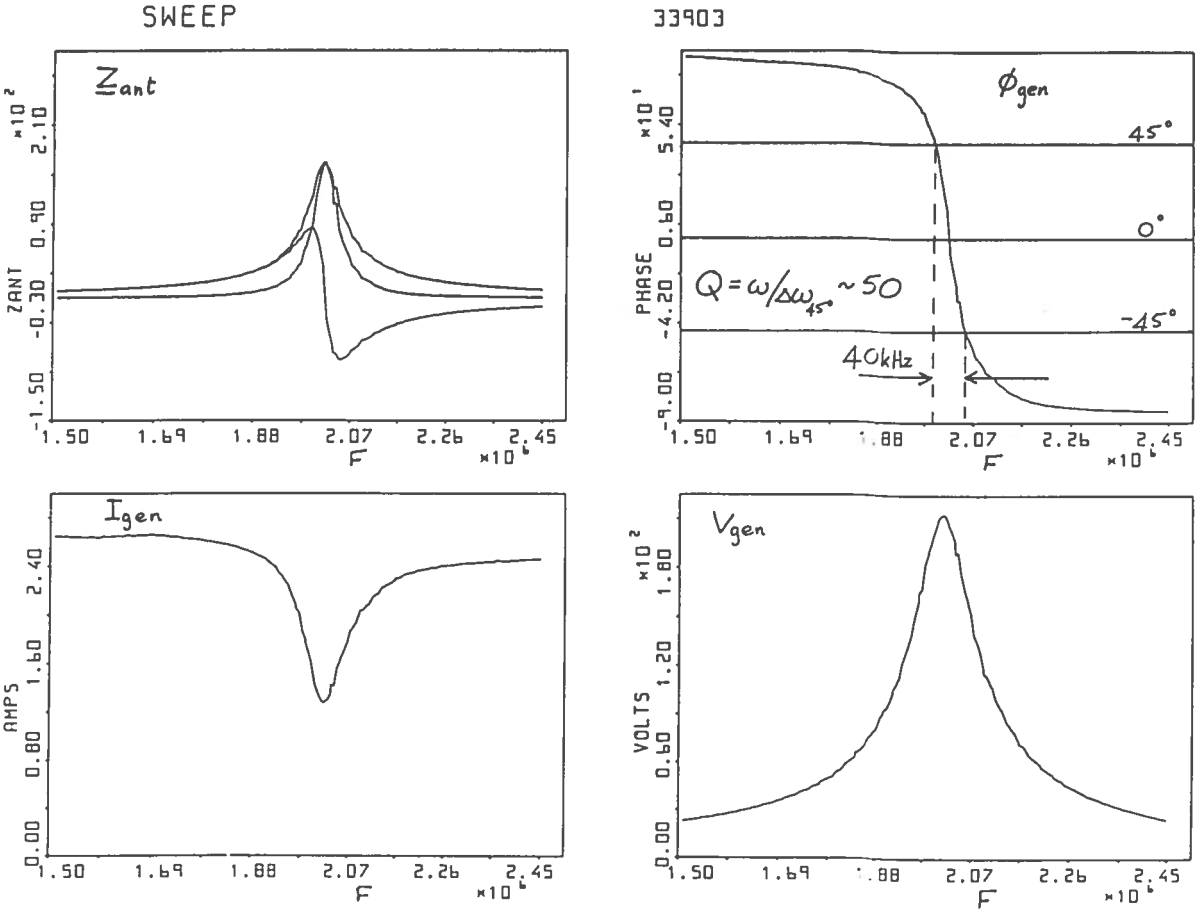

Figure 7.3 Reconstructed probe signals and deduced antenna impedance.

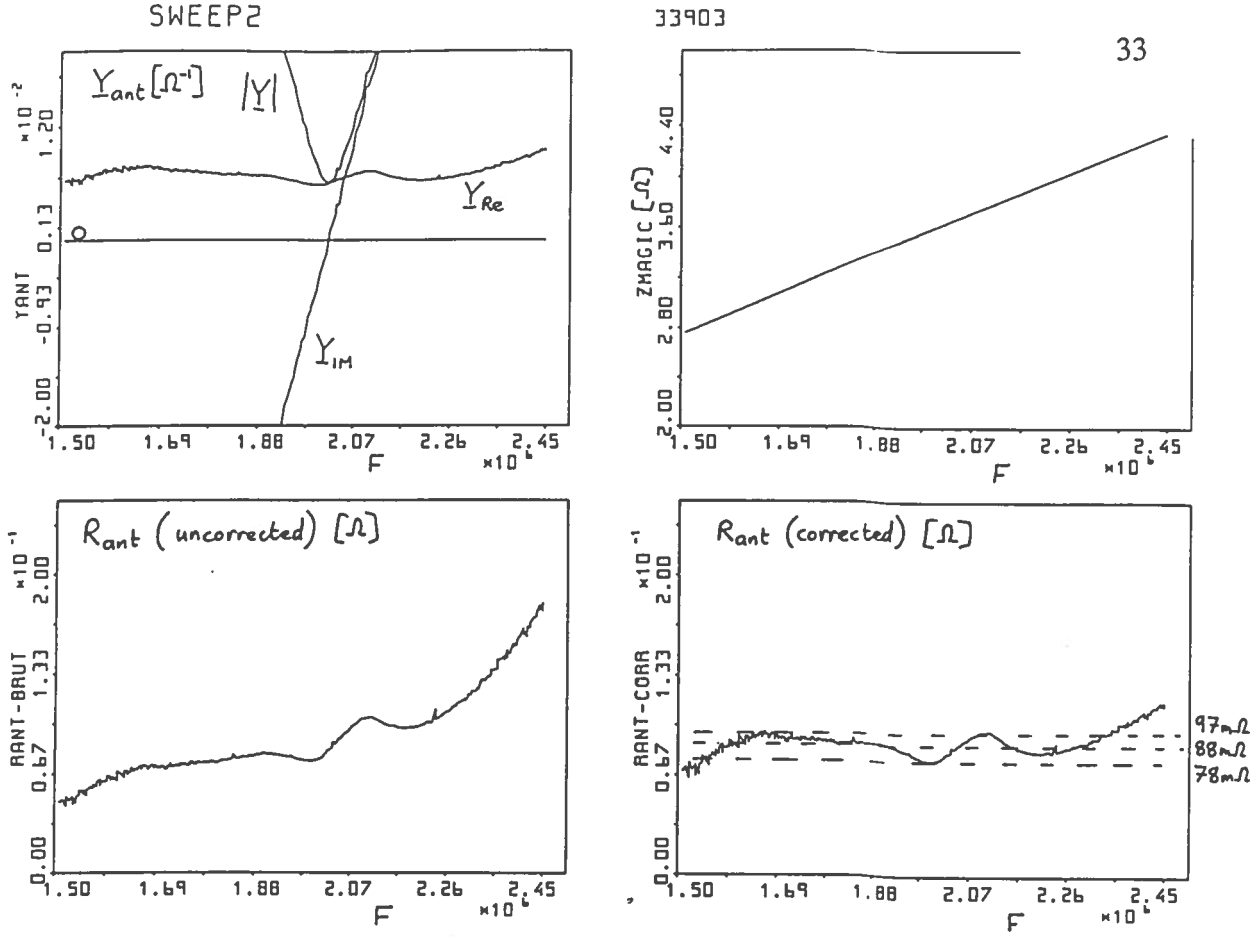

Figure 7.4 Calculation of R_{ant} from data shown above.

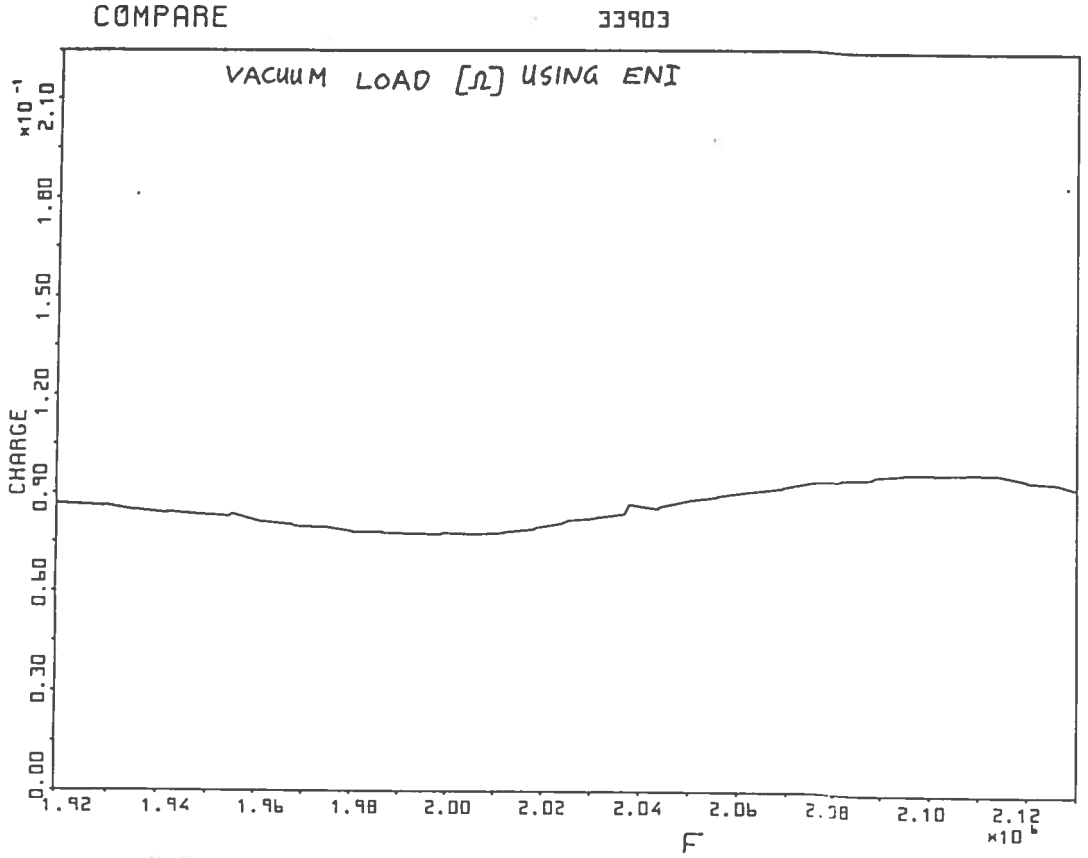

Figure 7.5 R_{ant} on a different scale to be compared with fig.1.2.

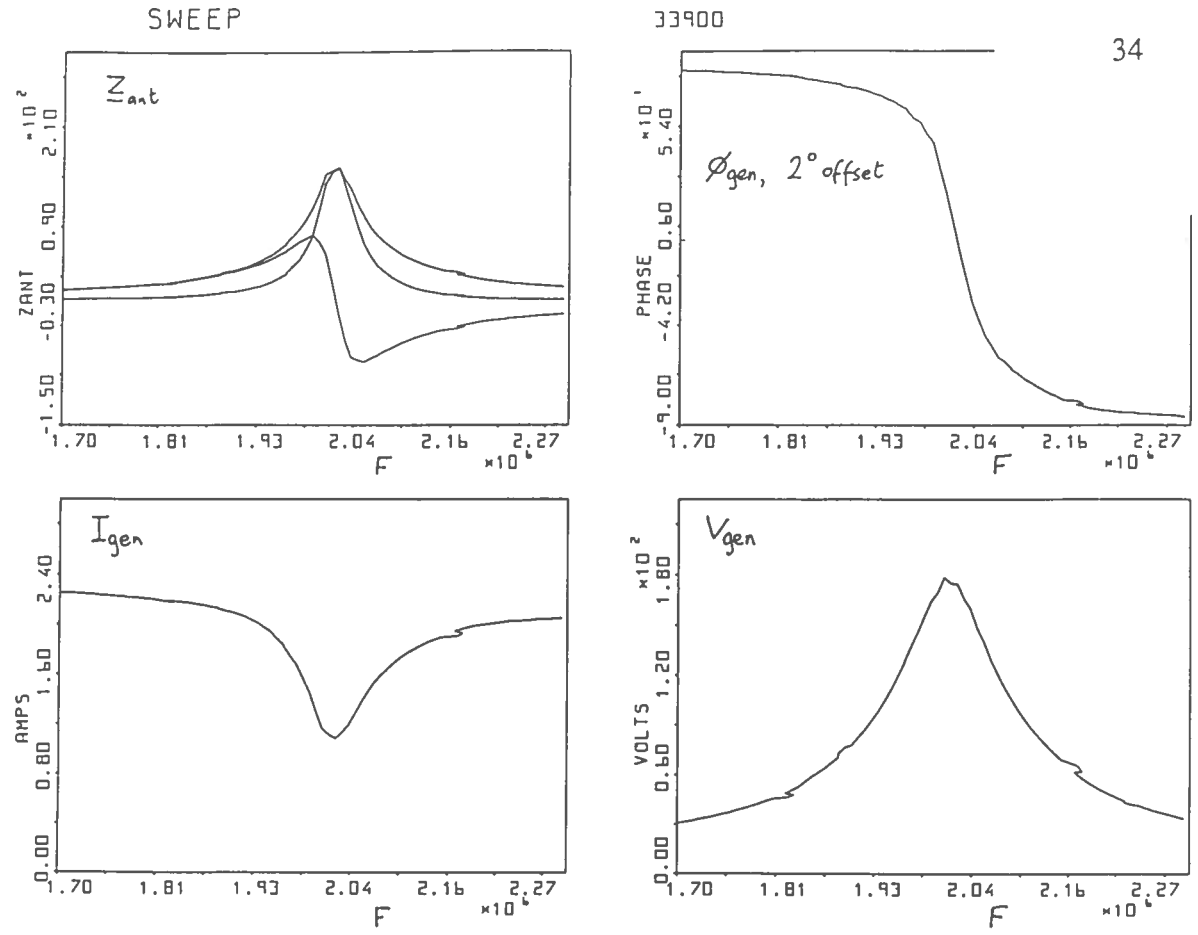

Figure 7.6 Data for a shot with a 2° phase offset.

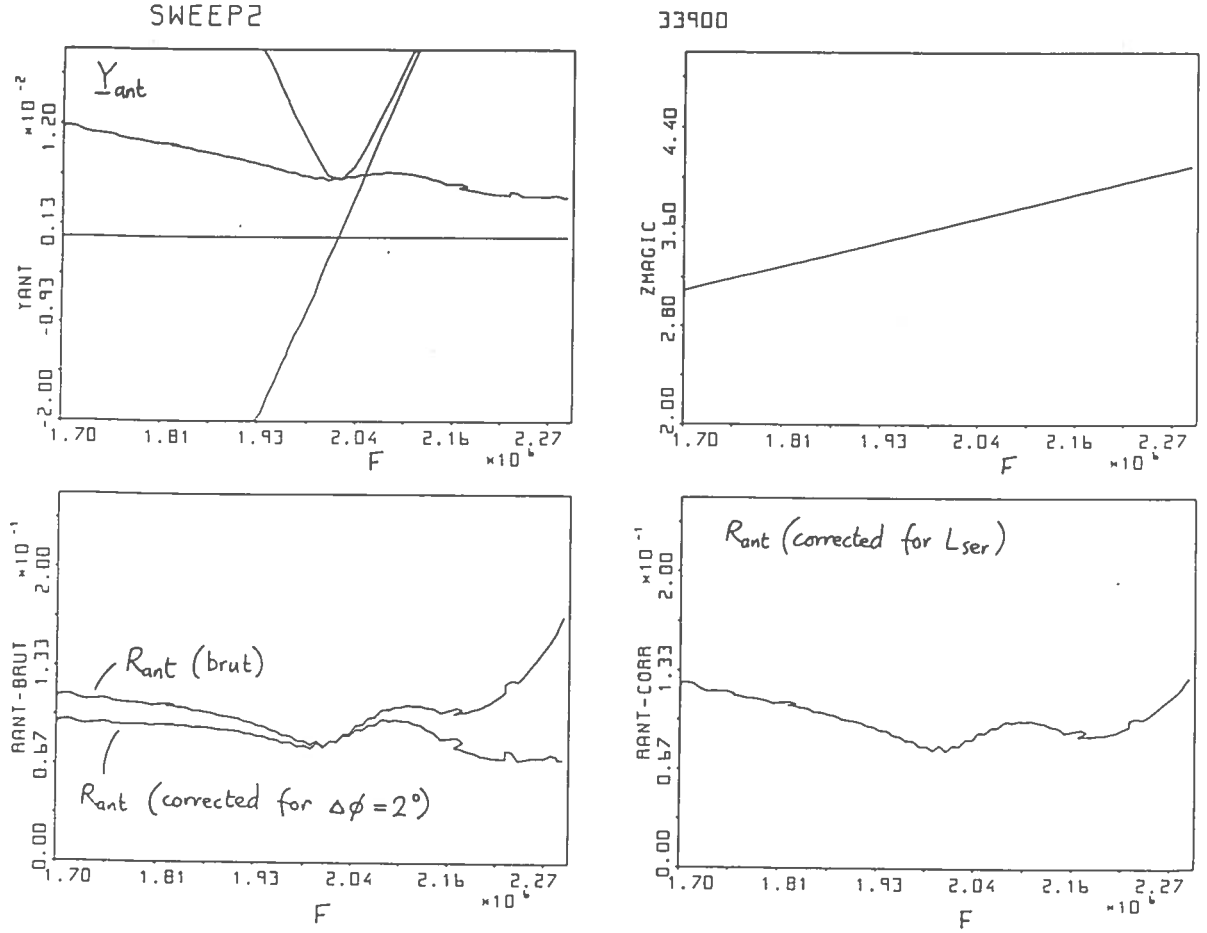

Figure 7.7 Showing the correction necessary for the 2° offset.

The double hump in R_{ant} was a constant feature of these measurements. No combination of the parasitic elements displayed in Figs.6.2 to 6.8 could reproduce this behaviour. The error is perhaps due to a slight phase non-linearity in the probe/mélangeur system, as was estimated using a delay line of one wavelength at 2 MHz (Fig. 7.8), although it becomes difficult to distinguish between a phase non-linearity in the mélangeur and one in the delay line.

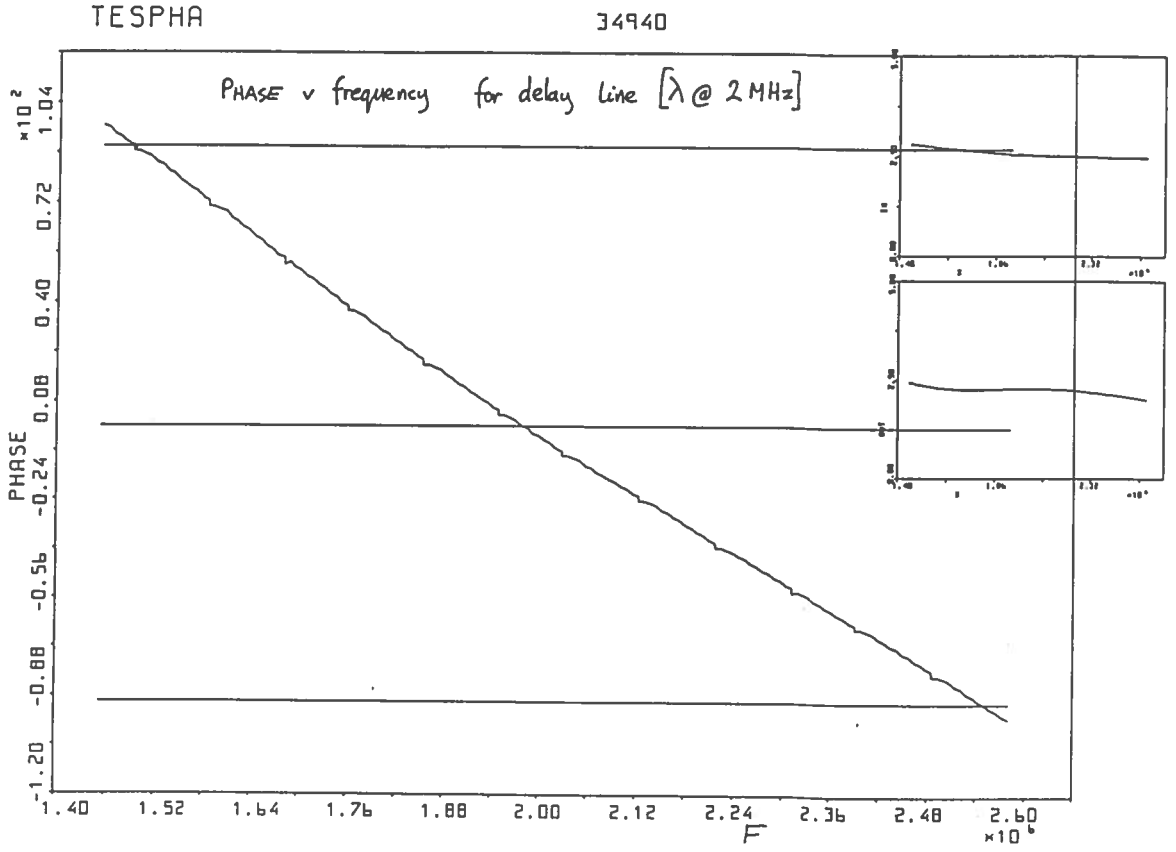

Figure 7.8 Estimation of possible phase non-linearity in measurement system.

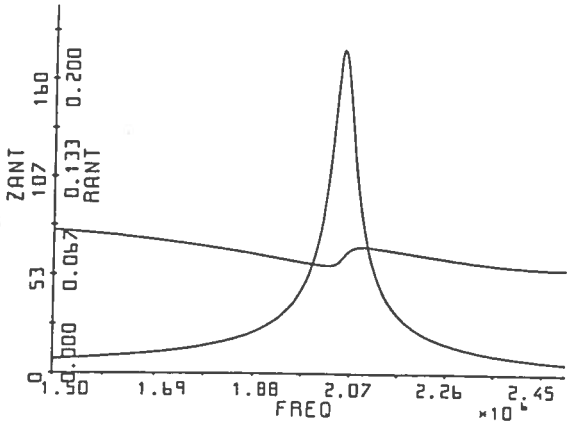

Figure 7.9 Model with phase error

However, a phase error of this form inserted into the program AMPERE (used to produce figs.6.2 to 6.8) can reproduce the features observed in the experimental loading curve (compare figs. 7.4 and 7.9). In the final analysis, it becomes meaningless to apply a whole series of corrections, each of which has a significant uncertainty associated with it. Fig. 7.4 is the best swept-frequency measuement of R_{vide} made to date.

SECTION 8 MEASUREMENTS USING AFCO

The final step is to replace the ENI generator with AFCO (Amplitude- and Frequency-Controlled Oscillator), for which attenuators (1/10.4) were used to reduce the probe signals to acceptable levels for the mélangeur.

8.1 Calibration of probes on the 114Ω calibration resistor.

Using the system as for the ENI generator, including the Tektronix current probe and 114Ω resistor, the probes for antennae 2 and 6 were also calibrated for the circuit with attenuators. The plots in fig. 8.1 show the ever-present AFCO oscillations, with the Tektronix probe signal superposed. NB this is at fixed frequency. We find for the probes of antenna 2:

I (A) = 11.6 x (signal from mélangeur) x 2.03/f (MHz)
V (V) = 183 x (difference in signals from mélangeur) x 2.03/f (MHz)

and for antenna 6:

I (A) = 12.4 x (signal from mélangeur) x 2.03/f (MHz)
V (V) = 197 x (difference in signals from mélangeur) x 2.03/f (MHz),

demonstrating the tolerances of the probe construction and attenuator components.
Fig.8.2 shows a frequency sweep under identical conditions on the calibration resistor. Significant departures (outside the obvious saturation and low signal regions) occur which show the deterioration in the quality of the measurement once AFCO is used as the rf source. The reason for this was never fully understood - it may be due to a poor frequency response or frequency stability in the AFCO system (which, after all, is much more extensive than the ENI amplifier!), leading to a dephasing between the mélangeur reference (Rohde-Schwarz 'pilote') and the probe signals at the output of AFCO during a frequency sweep. Perhaps the mélangeur reference should be taken from the AFCO output rather than its input, although this would require signal conditioning before a satisfactory reference could be obtained because of the large dynamic range involved. The probes themselves are known to be reliable from the results presented in section 7.3. More probably, the difference in quality between the ENI and AFCO results is that the ENI is a broad-band amplifier, whereas AFCO itself has a narrow frequency band approximately centred on the matching circuit resonance. The convolution of these two high-Q circuits means that signal level is even more severely reduced with AFCO as a source than with the ENI, away from resonance, thus increasing any error due to offsets and small-signal non-linearity.

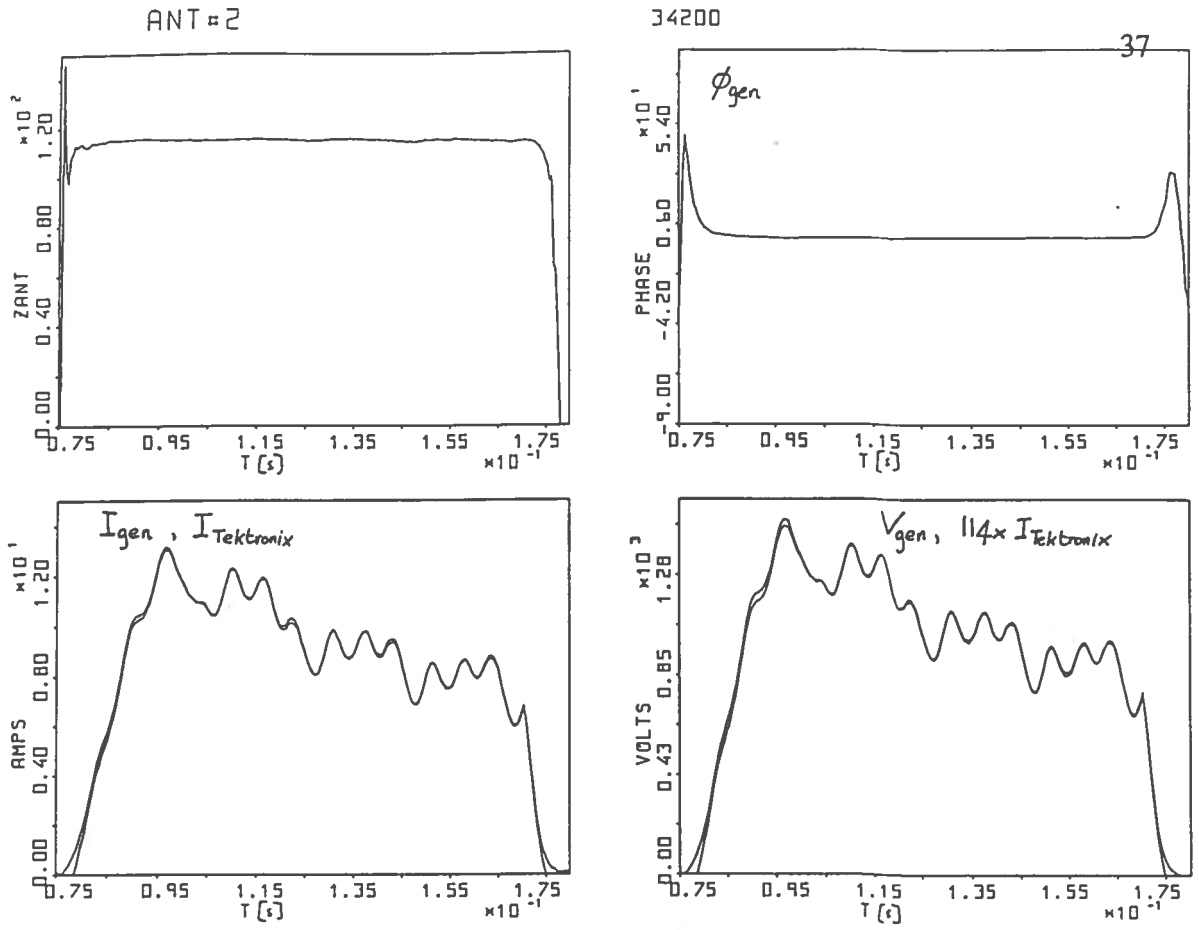

Figure 8.1 AFCO (2.03 MHz) on calibration resistor 114Ω

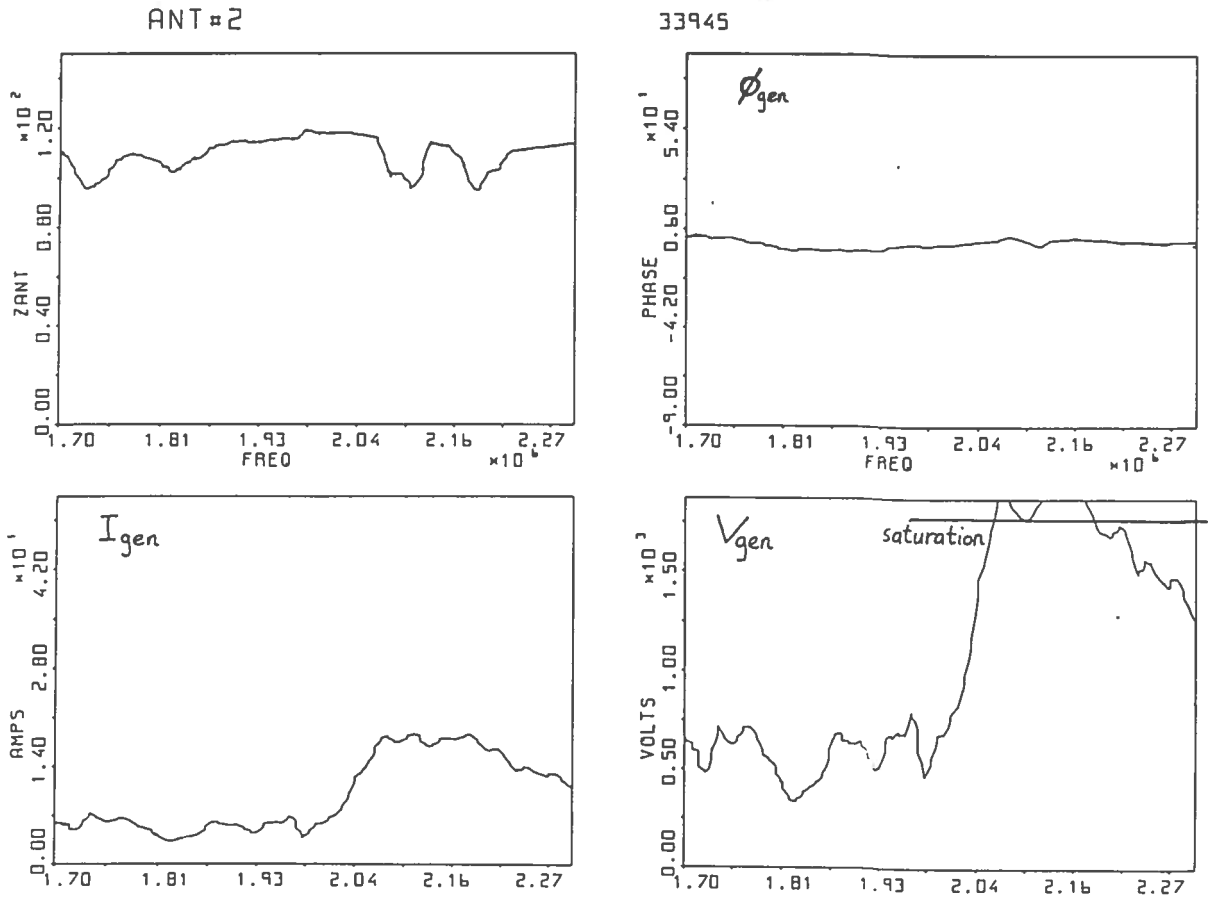

Figure 8.2 AFCO (frequency sweep 1.7 - 2.3 MHz) on calibration resistor 114Ω

Effect of toroidal field on rf measurements.

With previous rf probes, the apparent rf vacuum loading depended strongly on the presence or absence of the toroidal field B_ϕ during the vacuum shot. This was found to be largely due to saturation of the ferrite core used in the old Rogowskis. To ascertain the B_ϕ effect with the new system, two shots, with/without B_ϕ were studied, in which one probe system was connected to antenna 2 (Fig.8.3) whilst the probes of antenna 6 were connected to the calibration resistor (Fig.8.4). In this way, the relative contributions of the B_ϕ sensitivity of the probes and antenna circuit could be separately evaluated. From the superposition of the shots with and without B_ϕ shown in figs.8.3 and 8.4, we can deduce that:

i) The probe/mélangeur system is completely unaffected by the toroidal field, and
ii) The matching box, cable and antenna circuit suffer a small change due to B_ϕ: both the phase and esimated vacum loading have small increments. This introduces an error of only 2% into R_{vide} and is probably a real effect due to a change in the effective skin depth of the conductors in the magnetic field.

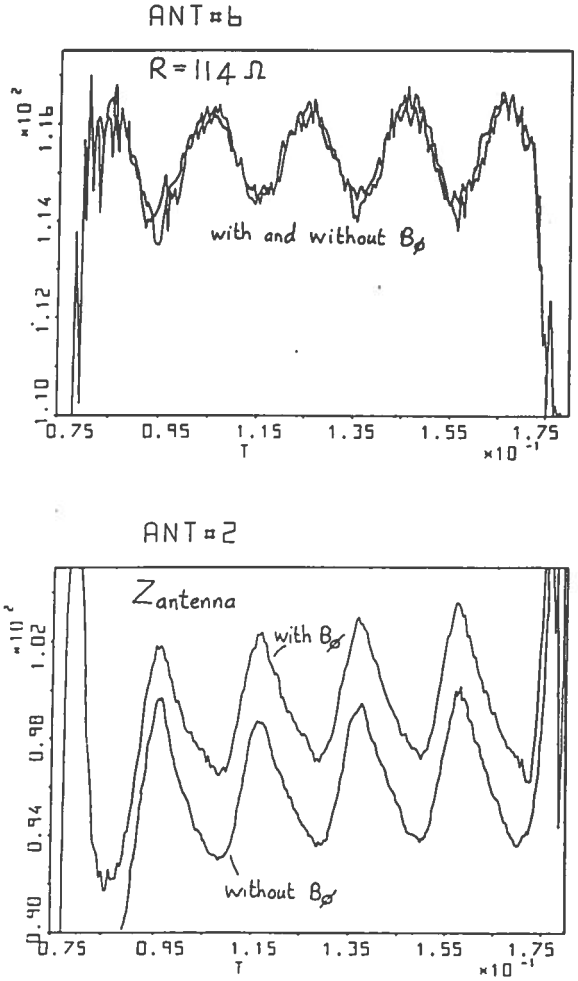

Figure 8.3 (top) Probes on 114Ω +/– B_ϕ,

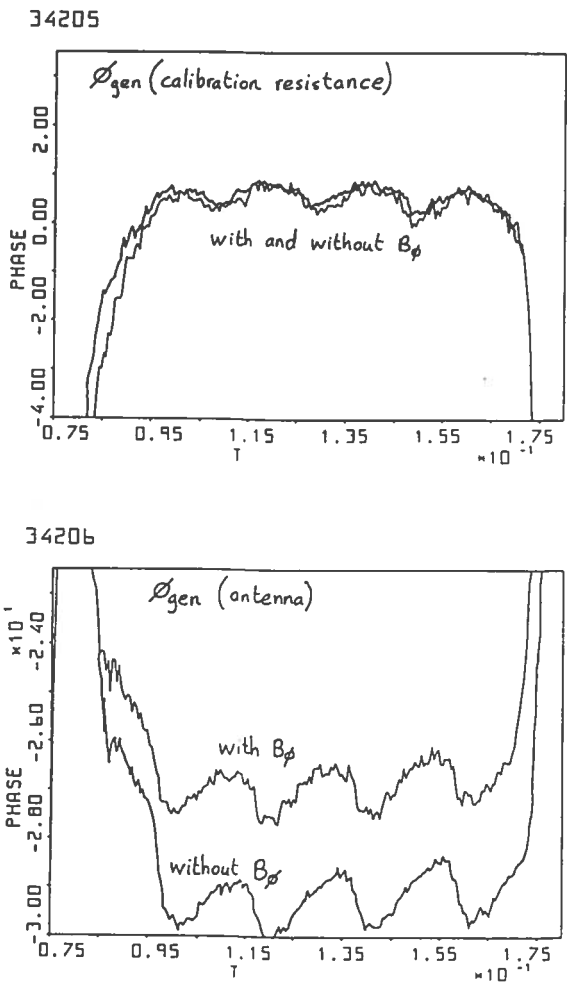

Figure 8.4 (bot) Probes on antenna +/– B_ϕ

8.2 Probe measurements on the antenna using mélangeur and AFCO

This is the complete antenna/probe system as would be used in normal operation, except that the mélangeur is used to measure I_{gen}, V_{gen} and ϕ_{gen} instead of the purpose-built rf amplifiers for reasons of non-linearity of the rectifiers in the latter system. Fig. 8.5 shows the raw data acquired for a 100ms sweep from 1.7 - 2.3 MHz. There is no saturation of the mélangeur or acquisition. The step-like nature of the traces is due to the Rohde-Schwarz frequency-stepping, as shown in output 'X' in the last box. Fig.8.6 shows the deduced phase and impedance, again of lower quality than with the equivalent fig.7.3 using the ENI amplifier (probably for the same reason as above ie that the AFCO narrow band amplification reduces signal level off-resonance faster than with the ENI as rf source). The current trace I_{gen} may seem bizarre, but it is the correct form of Igen given the resonance curve of V_{gen} (imposed by AFCO), convoluted with the resonance envelope of the matching circuit (as shown by Z_{ant}). Fig.8.7 shows this more clearly. Basically, the resonance frequency of AFCO does not coincide exactly with that of the matching circuit; a discrepancy of 40 kHz in 2 MHz is significant for such high-Q resonances. Fig.8.8 is the equivalent of fig.7.4, showing the final corrected R_{vide} for 1.7 - 2.3 MHz. The loading is essentially the same as for fig.7.4, but with larger deviations, especially at the extremes of the sweep. The 'hump' feature at the resonant frequency remains since the same probe/cable/mélangeur system is used. For a final comparison with the original data of Section 1, fig.1.2, see fig.8.9. Given the various ill-defined corections and acute sensitivity to small phase errors and parasitic elements, this is the best R_{vide} v frequency trace obtained with the system described.

8.3 Estimation of R_{vide} with calibration resistors connected across the antenna

Earlier in Section 3, method 3, a technique was described in which known resistors, connected across the antenna terminals, modified the antenna impedance to permit of an estimate for L_{ant}. The original purpose of this technique, outlined here, was to add these known resistors and see if the estimated antenna loading at the matching box input changed as predicted, hence testing the transformation theory in Section 1.
From Section 3 method 3, we have

$R_{vide} = R_{vide} + (\omega L_{eff})^2 / R_{cal}$, by adding resistors $R = 3R_{cal}$ across the bar terminals.

Fig.8.10 shows R_{vide} measurements for a frequency sweep for which $R_{cal} = R/3 = 29\Omega$. Box 1 shows $R'_{vide} = I_{gen}.\cos\phi.Z_{magic}^2 / V_{gen}$, box 2 shows this R'_{vide} corrected for the probe series inductance as usual. Note that R_{vide} is considerably different from that of fig.8.8 (obtained with the normal antenna configuration). Box 3 shows $R_{vide} = R'_{vide} - (\omega L_{eff})^2/R_{cal}$. NB L_{eff} is not equal to L_{ant} for the reasons given in Section 3. The original R_{vide} of fig.8.8 is restored within the limits of signal

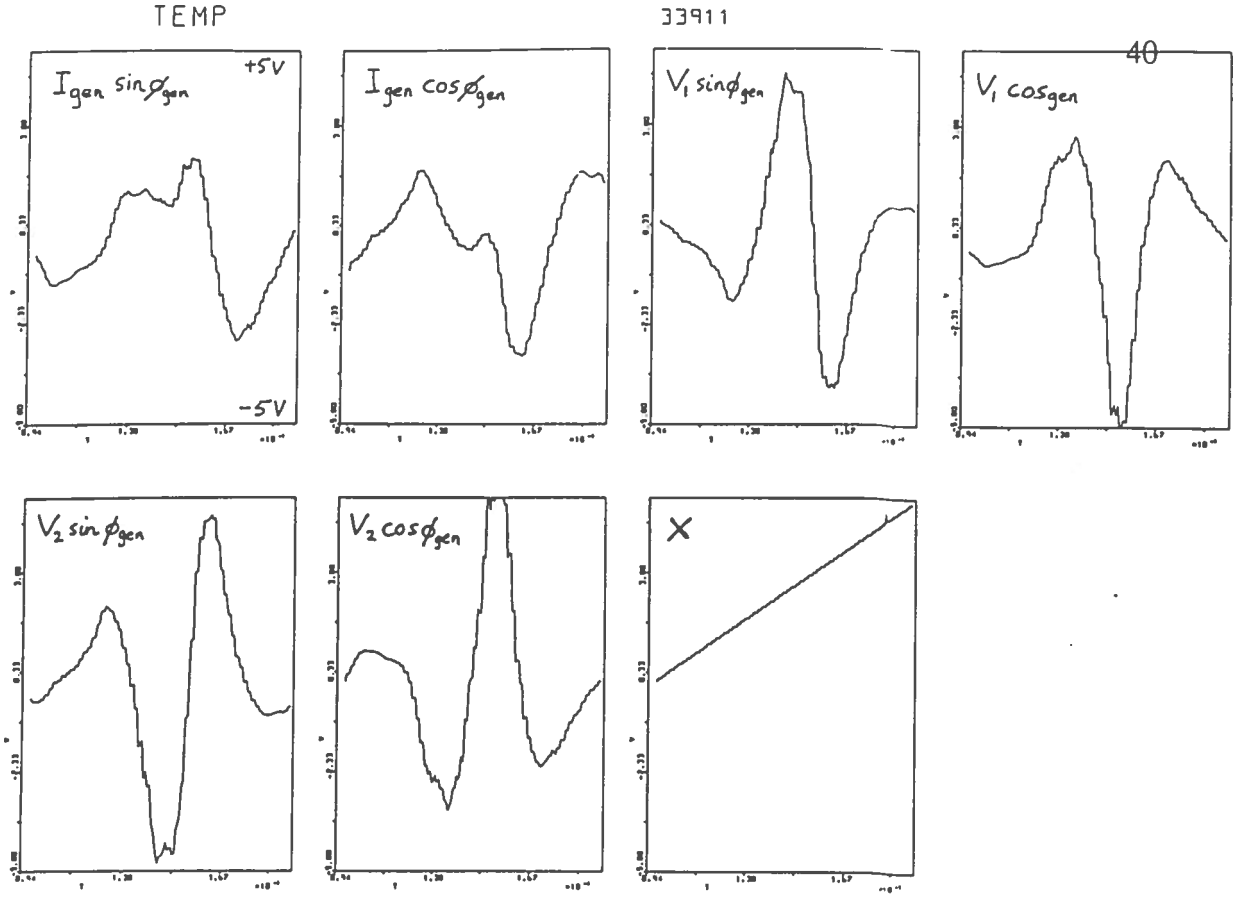

Figure 8.5 Raw data for frequency sweep with AFCO on antenna.

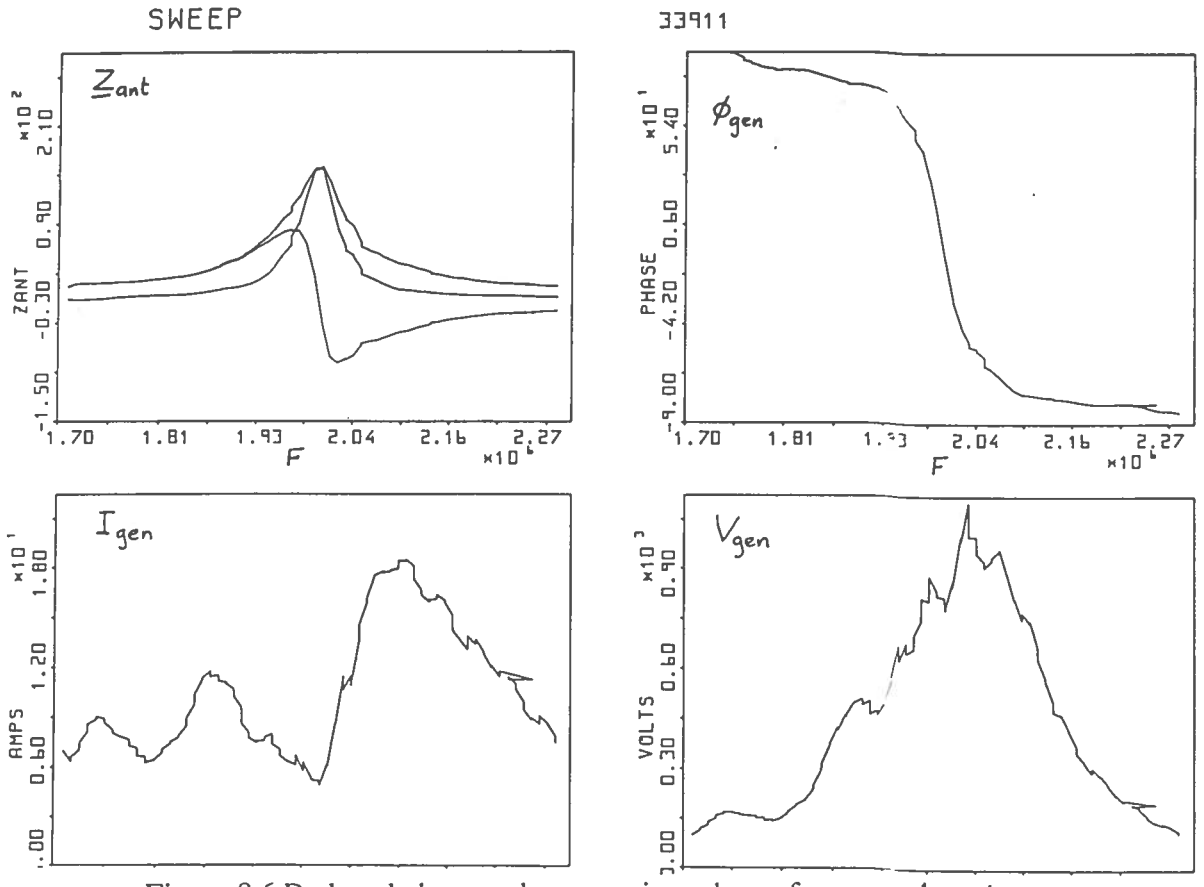

Figure 8.6 Deduced phase and antenna impedance from raw data above.

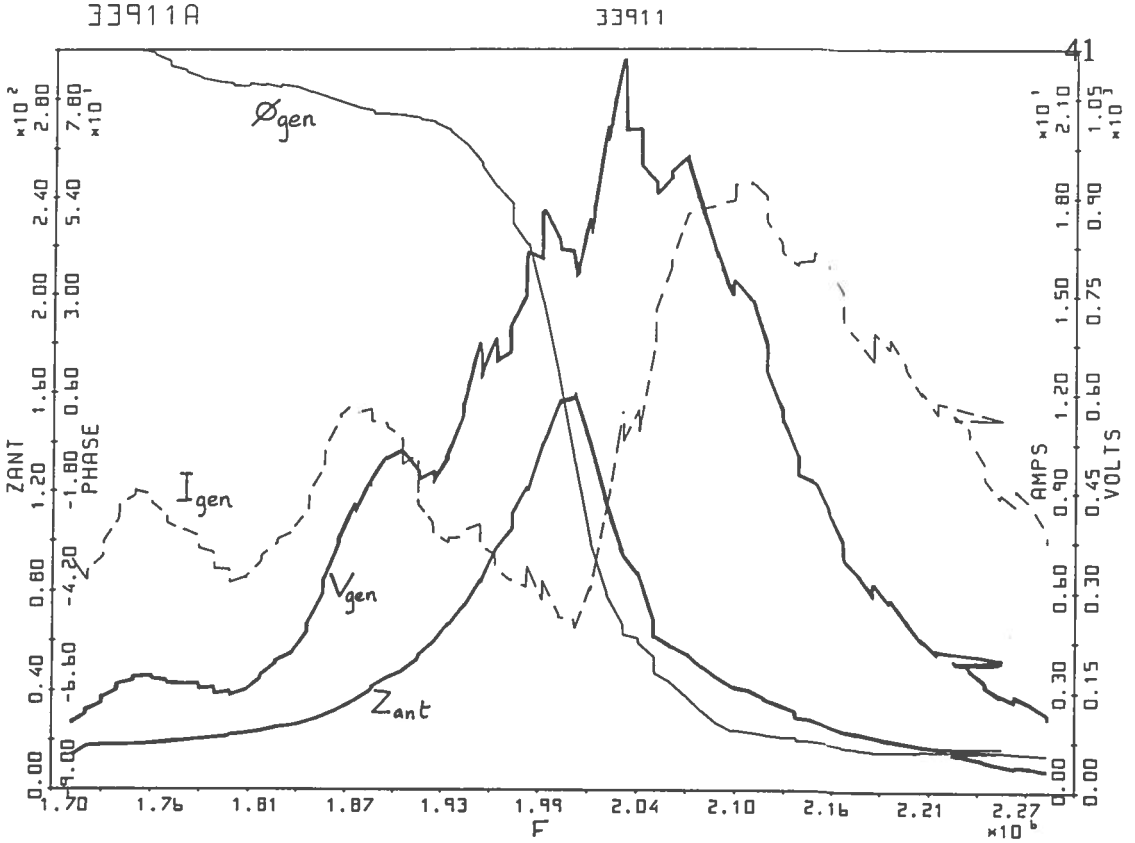

Figure 8.7 Showing displaced resonances of antenna and AFCO causing strange I_{gen}.

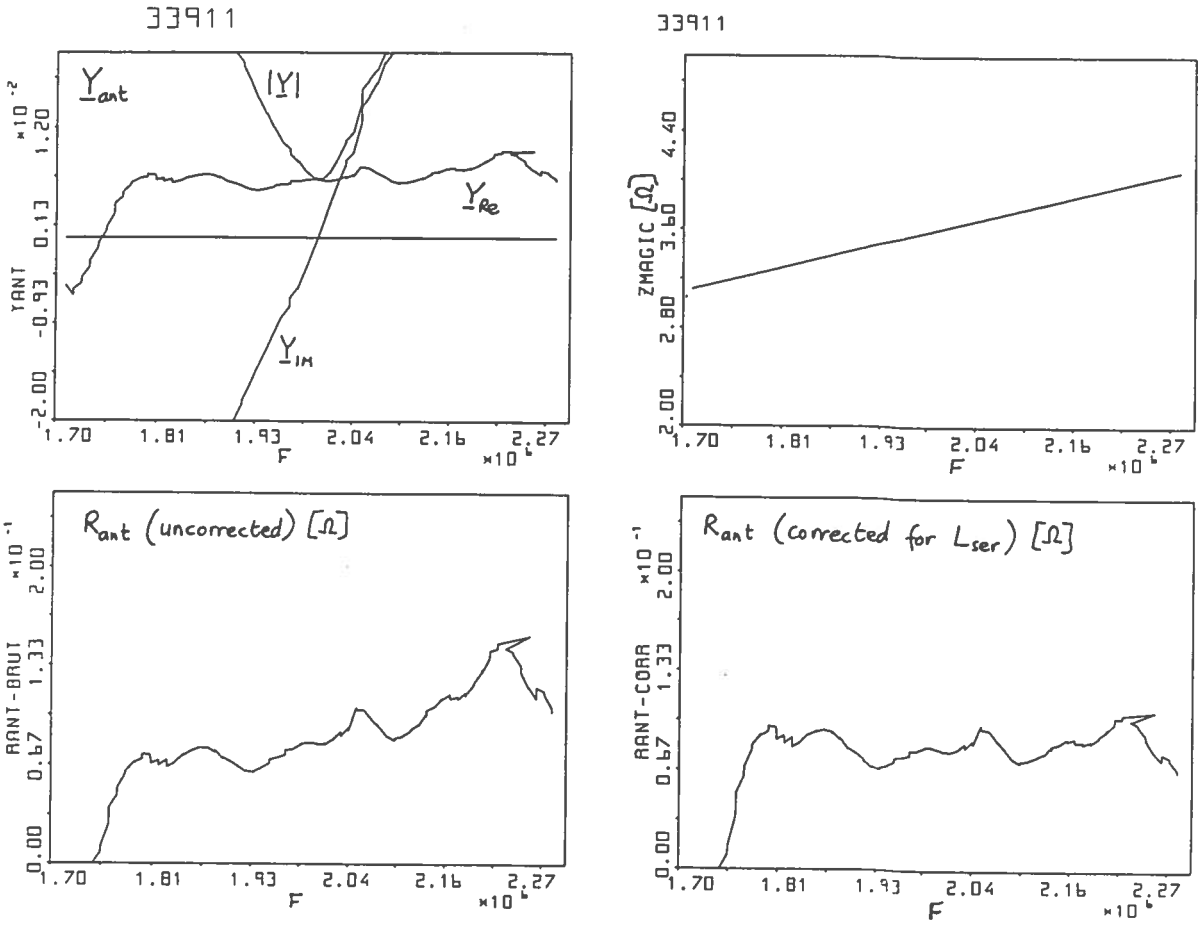

Figure 8.8 Estimation of R_{ant}(corrected).

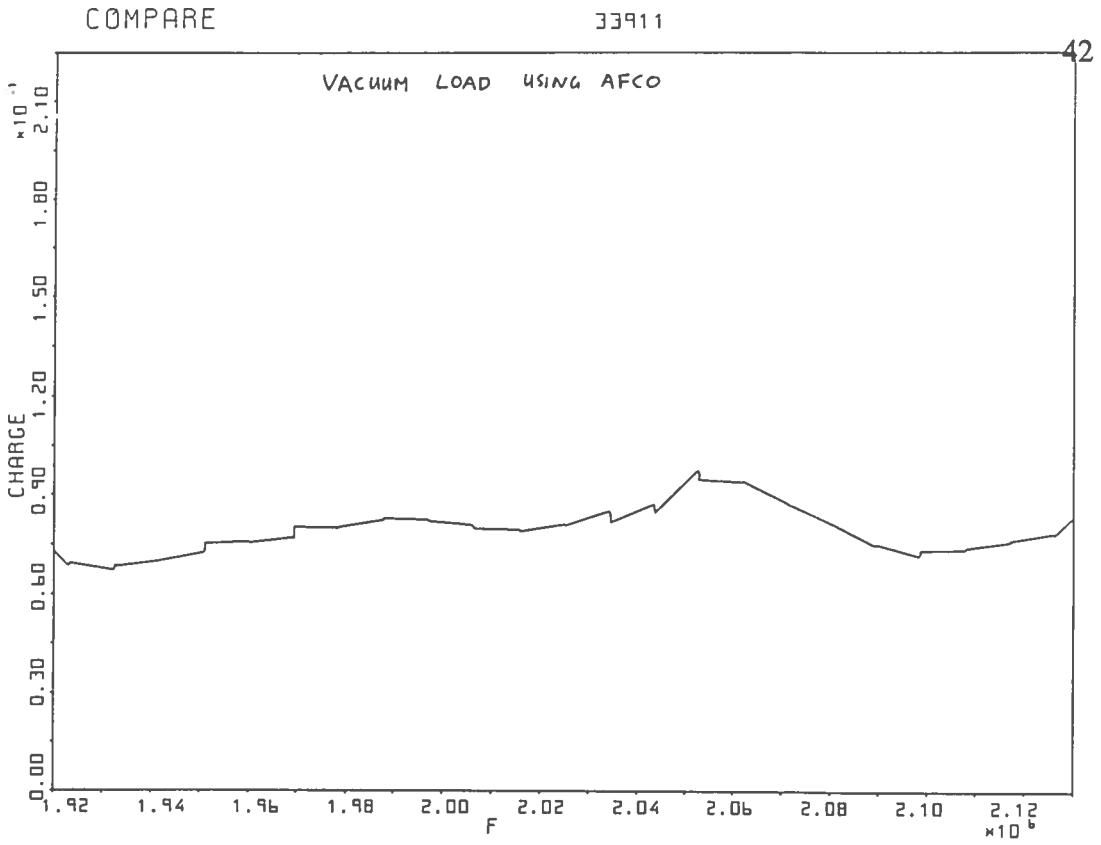

Figure 8.9 AFCO-estimated Rvide to be compared with figs. 7.5 and 1.2.

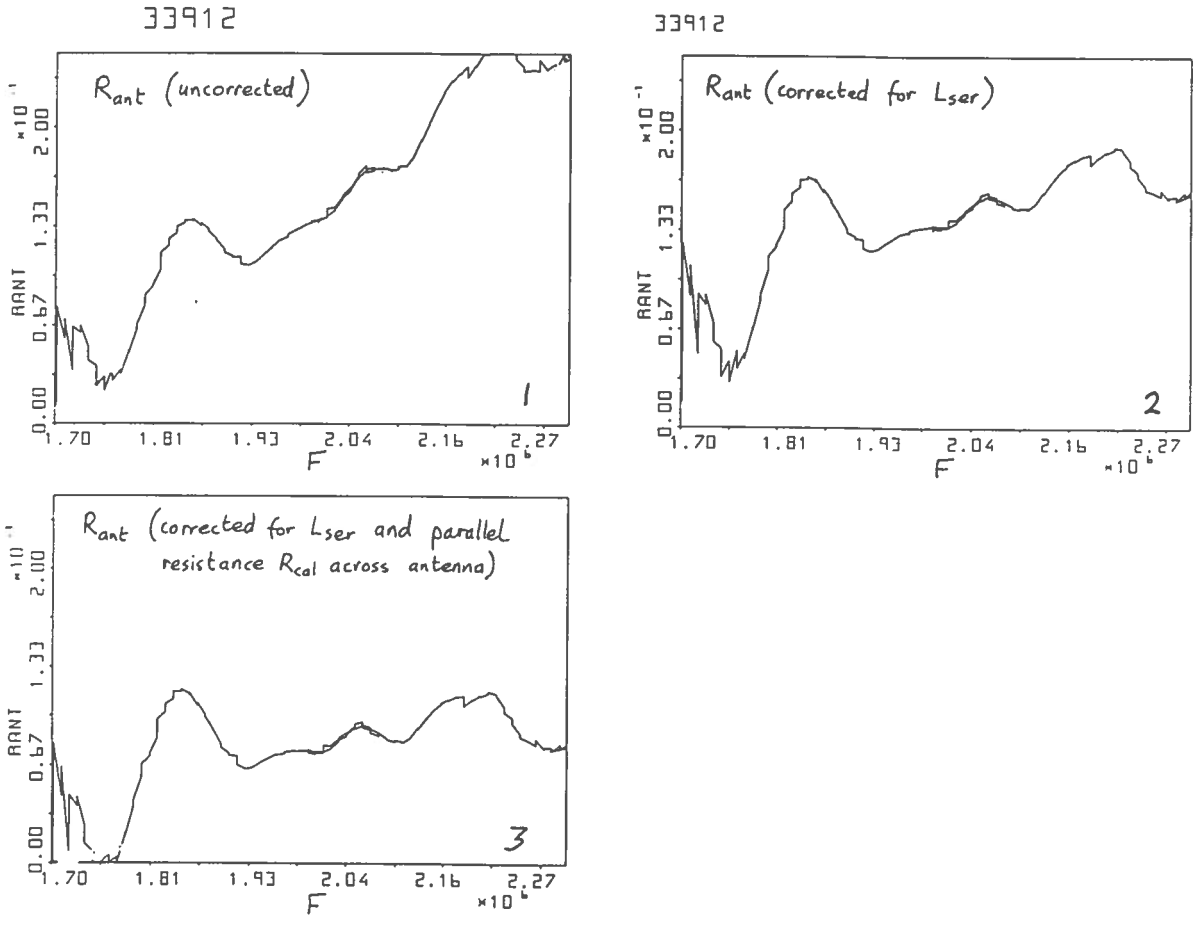

Figure 8.10 R_{ant} corrected for resistors in parallel across the antenna.

accuracy, thus confirming the validity of the complete measurement, associated theory and assumptions.

8.4 Some conclusions for R_{vide} measurements.

The basic problem is the high Q-factor both of AFCO and of the matching circuit, requiring accurate probes and acquisition (eg good linearity and negligible offsets) over a large dynamic range for a frequency sweep of more than a few tens of kHz. The Q of the matching circuit ($=\omega/\delta\omega_{45^o} = 50$) is necessarily high because circuit dissipation must be kept to minimum for high-power heating. Small errors in phase measurements lead to huge errors off-resonance. The combined effect of important, ill-defined parasitic components, instrumental offsets and non-linearity, phase errors, the high-Q resonant circuits of both AFCO and the matching network centred on slightly different resonant frequencies makes accurate estimations of R_{vide} over a large frequency range difficult.

The plasma loading is defined reasonably enough as $R_{pl} = R_{ant} - R_{vide}$. Indeed, it was demonstrated in Section 6.9 that the deduced load is proportional to the antenna loading. However, the inductance $L_{eff} = 100$ nH of the antenna responsible for the interaction with the plasma, is assumed to remain constant and unchanged by the presence of plasma. It may be that image currents of the antenna in the plasma could modify this inductance and hence change Z_{magic} and falsify R_{pl}(estimated) (Ph Marmillod, private communication). These image currents would tend to reduce the antenna inductance. If we assume that L_{eff} is reduced by 50% to 50 nH, the value of L_{ant} falls from 160 nH to 110 nH. If the same equations and corrections are used to estimate R_{pl} as for R_{vide} (as is always the case), we artificially overestimate R_{ant} by 40% over the whole frequency range (using AMPERE as described in Section 6), ie:

$R'_{ant} = 1.4\ (R_{pl} + R_{vide})$, therefore:
$R'_{pl} = R'_{ant} - R_{vide} = 1.4\ R_{pl} + 0.4\ R_{vide}$

Therefore, even if the real plasma loading, R_{pl}, is zero, we would still obtain a fictitious plasma loading $= 0.4\ R_{vide} = 35\ m\Omega$ approximately. This component would vary if the antenna inductance varied during the rf pulse. Fortunately, direct antenna measurements made at the antenna terminals (see following section) indicate that the antenna inductance probably changes by only 10% or so due to the plasma.
Nevertheless, values given for the plasma loading should be treated with scepticism, especially during a frequency sweep, since they are measurements of a very small resistance made, electrically-speaking, at a large distance from the antenna.

SECTION 9 DIRECT ANTENNA MEASUREMENTS

An attempt was made to measure the antenna voltage, current and hence loading and power, directly on the antenna ports.

9.1 Antenna Voltage and Current Probes

Fig.9.1 shows the probe circuits which are essentially the same as for the matching box probes.

$I_{ant}(A)$ = 74.3 x acquired signal (V) at 2 MHz
$V_{ant}(V)$ = 81.6 x acquired signal (V) at 2 MHz

The Rogowski is described by Ginesi (TP, 8éme semestre). The principal purpose of the voltage probes was to monitor the antenna phasing during travelling wave experiments - it should be remembered that, although all 8 antennae are powered by the same source, the phases at the antennae can be widely different if the resonant frequency and Q of each matching circuit are not identical because otherwise each ringing circuit transforms the AFCO voltage by different amounts. A resonant frequency mismatch of only 10 kHz in 2 MHz can detune the phase by 18°. The Rogowskis were installed on the input and output ports of one pair of antenna bars to measure:
a) the antenna current directly, and
b) the difference in current at input and output (called the default current) which might be lost, via the plasma, from the antenna circuit thus invalidating the rf loading and power estimates.

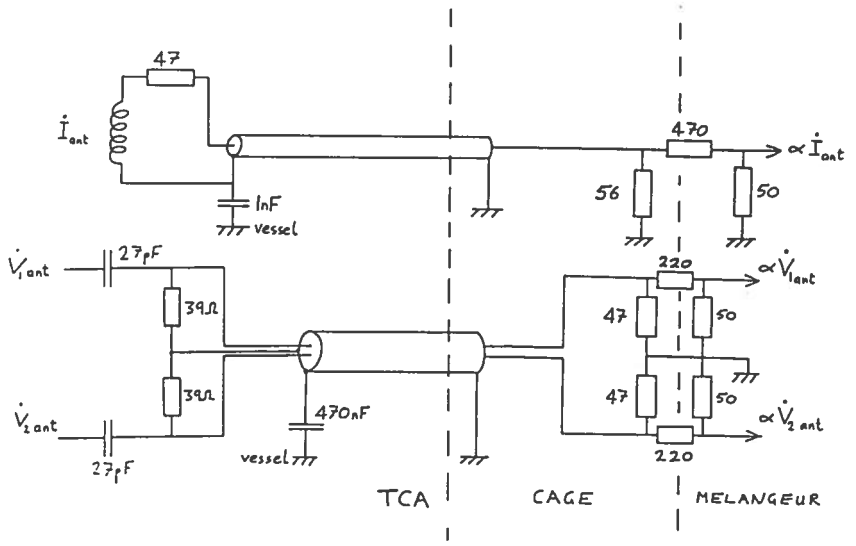

Figure 9.1 Antenna probes and attenuator circuits.

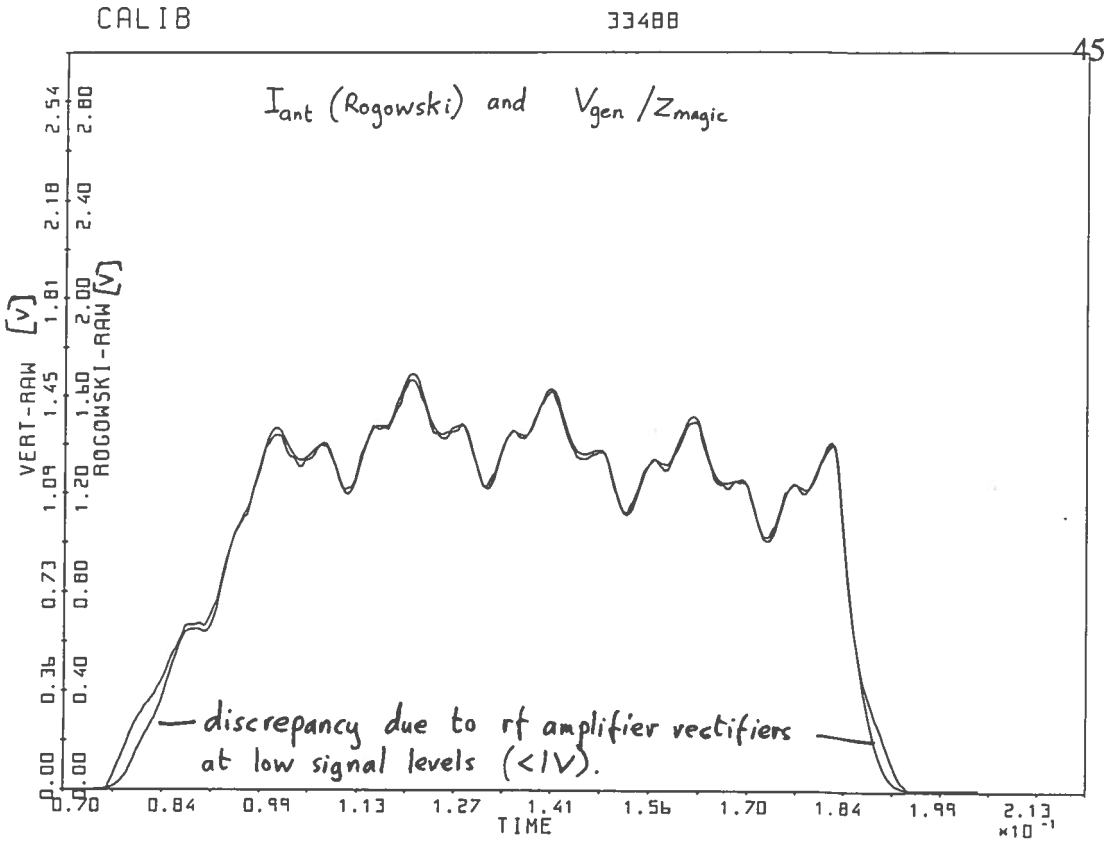

Figure 9.2 Comparison of two different measurements of I_{ant}.

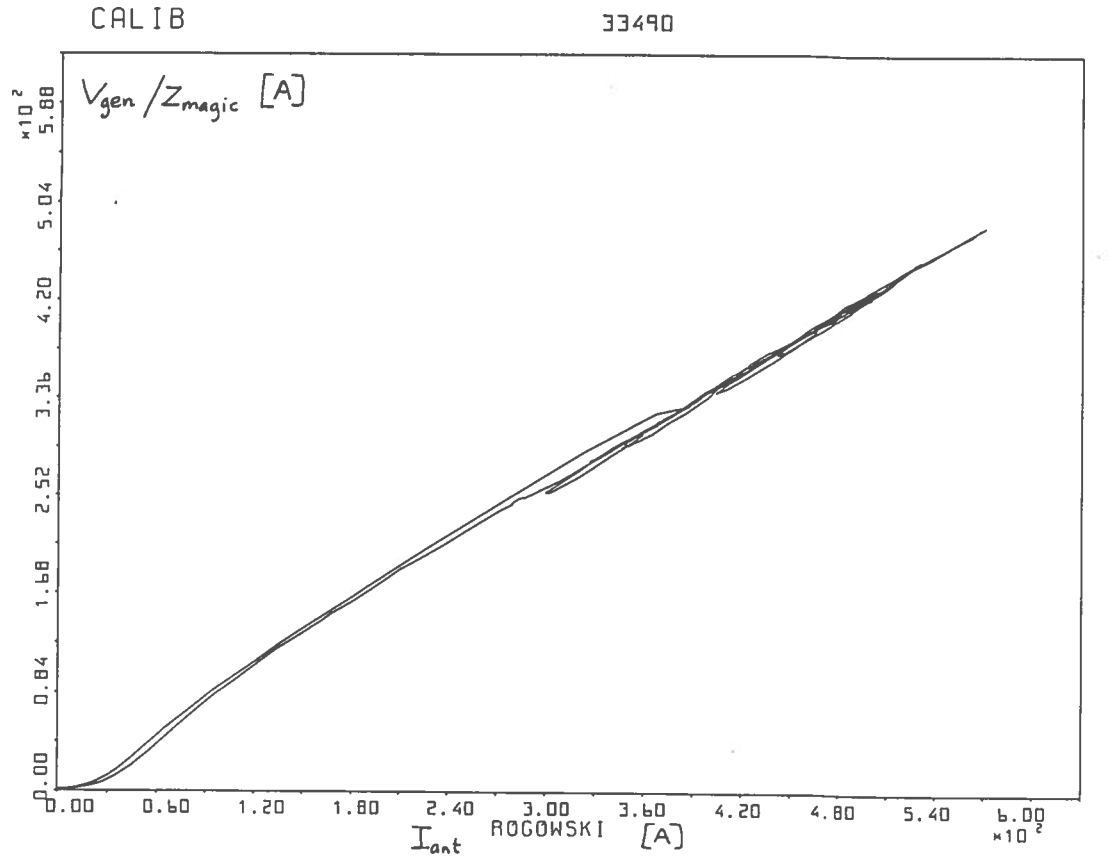

Figure 9.3 Linearity of the two measurements for a range of I_{ant}.

9.2 Comparison of antenna current measurements from two independent diagnostics

Fig.9.2 compares I_{ant} from the antenna Rogowski and V_{gen}/Z_{magic}, which is the antenna current if the transformation theory is correct. The Rogowski current is multiplied by 3 to approximate the total antenna current (one antenna comprises 3 pairs of bars). The curves agree remarkably well, even in absolute calibration. Fig.9.3 plots I_{ant}, deduced from both techniques, for a wider range of I_{ant}. The departure from linearity is due to the compensation for the rectification in G Besson's amplifier used here for the measurement of V_{gen}.

Note that the Rogowski measures dI_{ant}/dt at the antenna, whereas V_{gen} is the voltage at the matching circuit input. The agreement is therefore a good vindication of the circuit model in Section 1. Fig.9.4 shows the almost-identical current traces obtained from the Rogowskis on the input and output ports, thus demonstrating the reliability of the Rogowski circuits and the continuity of current in the rf circuit. However, some default current remains (several Ampères) and even though it is a relatively small component of the total current, it could be responsible for significant rf power losses in the antenna/plasma sheath (G Borg; private communication).

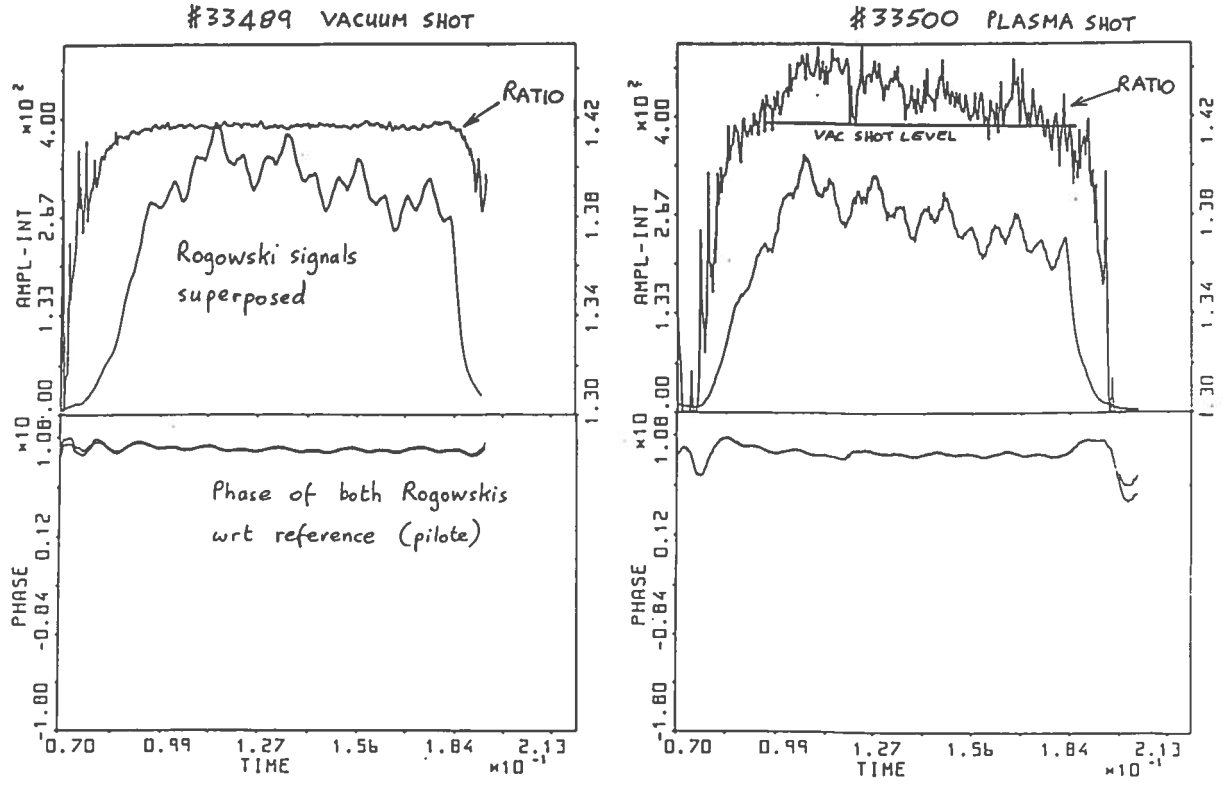

Figure 9.4 Comparison of in- and output antenna currents for vacuum and plasma shots

9.3 Direct Power Measurement at the Antenna

From the antenna current and voltage probes, we can directlly measure the antenna vector impedance and power dissipated by the antenna. The mélangeurs were again used since the measurement of phase must be very accurate as will be explained below. Because the mélangeur measures sin and cos components with respect to a reference, the most convenient algorithms are (B Marlettaz; private communication):

Total Power = Re (V_{ant}^{*} I_{ant}) = V_{ant} cosϕ_V I_{ant} cosϕ_I + V_{ant} sinϕ_V I_{ant} sinϕ_I, and

$\underline{Z} = V_{ant} \exp(j\phi_v) / I_{ant} \exp(j\phi_I)$, therefore:

$(Z)_{Re}$ = Total Power / I_{ant}^2 obviously, and:

$(Z)_{Im} = (V_{ant} \sin\phi_V . I_{ant} \cos\phi_I - V_{ant} \cos\phi_V I_{ant} \sin\phi_I) / I_{ant}^2$.

Fig.9.5 shows the impedance and phase at the antenna terminals. The impedance is almost entirely inductive (ϕ = 88°) and so Z = 1.25Ω = ωL_{eff} at 2 MHz giving L_{eff} = 100 nH as described in Section 3 method 2.

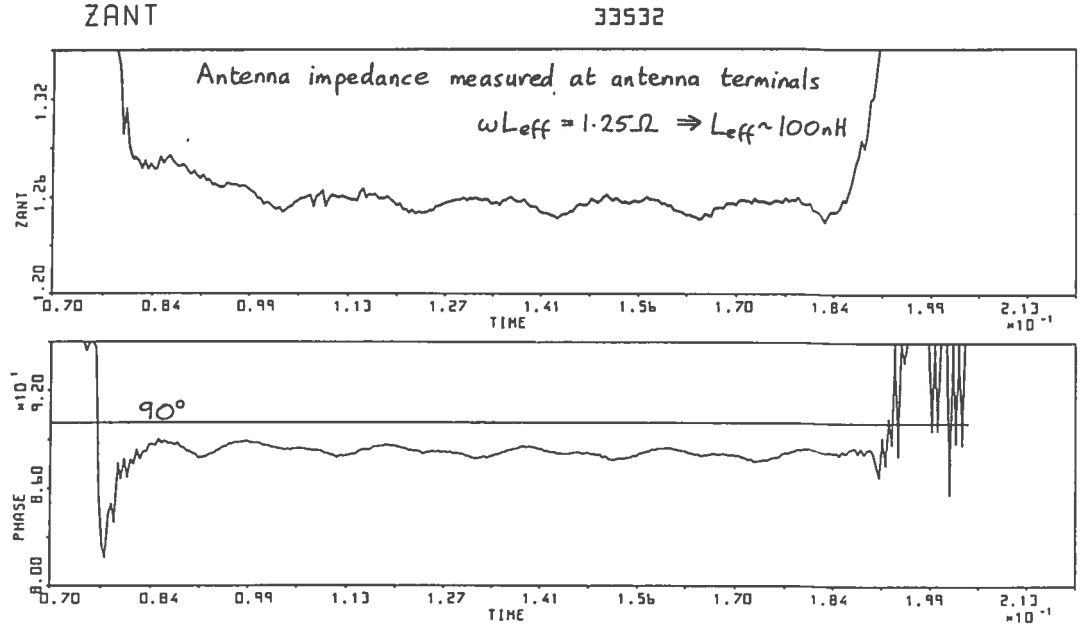

Figure 9.5 Impedance and phase at antenna terminals.

The basic difficulty of a direct measurement of power is that the real part of the impedance remains always small compared to the imaginary component, thus any change in the loading changes the phase by only 1 - 2° (Fig.9.6).

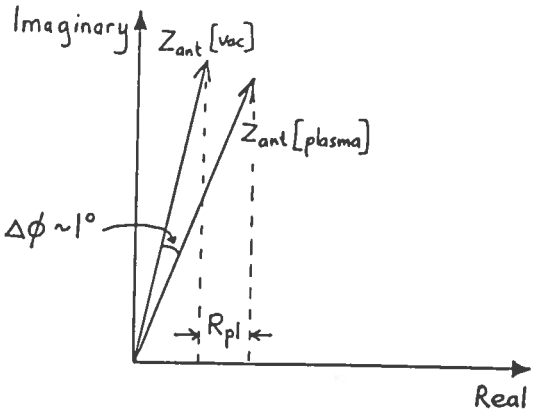

Figure 9.6 To show phase precision necessary for direct rf measurements.

Therefore a 10% precision in the loading requires a phase measurement to better than 0.1°. Devices such as a passive double-balanced mixer, using a diode ring, are especially designed for measuring small phase deviations from 90° (G Borg; private communication), and such a system could well be able to reliably measure plasma loading and power accurately. For the present fig.9.7 shows the best rf power and loading measurement compared with the 'conventional' rf values - the agreement is encouraging and further confirms the validity of the measurements made at the matching box (NB this was feasible only at fixed frequency; for swept frequency shots the phase errors quickly became intolerable).

9.4 Real-time RF Power Feedback

The power dissipated in the plasma is:

$$\text{Plasma Power} = \text{Re}\,(V_{ant}^{*}\, I_{ant}) - I_{ant}^2\, R_{vide}$$
$$= I_{ant}\cos\phi_I\,(V_{ant}\cos\phi_V - I_{ant}\cos\phi_I\, R_{vide}) + I_{ant}\sin\phi_I\,(V_{ant}\sin\phi_V - I_{ant}\sin\phi_I\, R_{vide})$$

- for direct measurements using the mélangeur. This algorithm could be easily implemented using only two analogue multipliers, with one adjustable constant R_{vide}, for use in an rf power feedback loop (B Marlettaz; private communication).

Equivalently, for measurements made at the matching box, the power in the plasma is:

$$\text{Power} = \text{Re}\,(V_{gen}^{*}\, I_{gen}) - I_{ant}^2\, R_{vide} = \text{Re}\,(V_{gen}^{*}\, I_{gen}) - V_{ant}^2\, R_{vide}/Z_{magic}^2$$
$$= V_{gen}\cos\phi_V\,(I_{gen}\cos\phi_I - V_{gen}\cos\phi_V\, R_{vide}/Z_{magic}^2)$$
$$+ V_{gen}\sin\phi_V\,(I_{gen}\sin\phi_I - V_{gen}\sin\phi_V\, R_{vide}/Z_{magic}^2)$$

- the advantage being that the phases are not close to 90° (for a few 10's of kHz around f_{res}); the disadvantage being that R_{vide}/Z_{magic}^2 is a function of frequency.

In the final analysis, we must ask ourselves just what the power measurement represents - feedback control of a power which consists of a large, possibly variable fraction wasted in the edge plasma or antenna/plasma sheath is of questionable value.

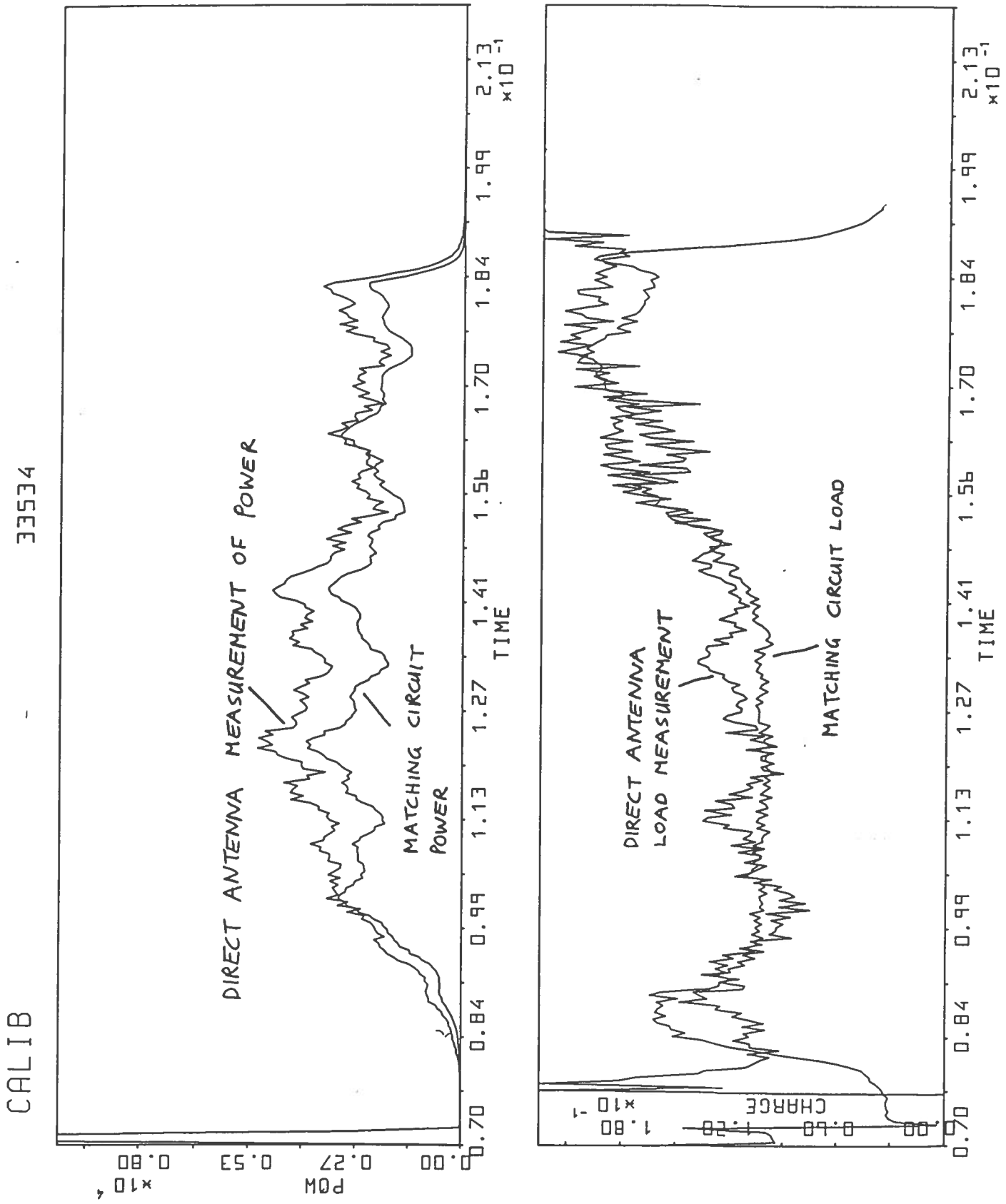

Figure 9.7 Direct and conventional power and loading measurements compared.

SECTION 10 CONCLUSIONS

This report analysed the circuit used to match the rf power to the antennae of TCA in an attempt to measure the plasma loading and rf power as a function of AFCO frequency. The basic equations are derived in Section 1 (see p6) and are valid for all frequencies (provided that $R_{ant} << \omega L_{ant}$), and not just the resonant fequency. However, the vacuum loading deduced from a frequency sweep (either shot-to-shot or dynamically) increases strongly and monotonically with frequency (see fig.1.2). The identification of a probe series inductance between the matching circuit and the probes means that a simple correction must be applied (see p17). This flattens the R_{ant} v frequency curve, and for future frequency-swept measurements, it would seem fair to assume that the real R_{ant} varies only due to the skin-effect, and apply the correction mentioned so that the measured vacuum loading is indeed approximately constant. Table 6.1, p24 summarises the effects of all the parasitic components considered. Fig.7.4 p33 and fig.8.8 p41 show the best R_{ant} estimations using the ENI amplifier and AFCO respectively as rf sources.

Various experiments have confirmed the validity of the circuit equations and improve confidence in the principle of the R_{ant} measurement. However, the combined effect of important, ill-defined parasitic components, instrumental offsets and non-linearity, phase errors, the high-Q resonant circuits of both AFCO and the matching network centred on slightly different resonant frequencies makes accurate estimations of R_{vide} over a large frequency range difficult because of the large dynamic range of the signals.

The probe system is completely unaffected by the toroidal field, although the matching box, cable and antenna circuit suffer a small change due to B_ϕ (see p38).

There is good agreement between direct antenna measurements and the conventional measurements (see fig 9.2 p45 for I_{ant} and fig. 9.7 p49 for power and load comparisons). Some default current (several Ampères) could be responsible for significant rf power losses in the plasma edge. In the final analysis, values given for the plasma loading should be treated with caution, especially during a frequency sweep, since they are measurements of a very small resistance made, electrically-speaking, at a large distance from the antenna.

Notes for the operator, example data and programmes are given in the appendices.

ACKNOWLEDGEMENTS

I gratefully acknowledge the assistance of Markus Pfister, without whose help and enthusiasm this work would never have seen the light of day.

APPENDIX CONSUMER GUIDE TO RF MEASUREMENTS

1) Parameters (See Section 1; and G Besson's notes for AFCO and amplifiers):

$I_{ant} = U_{gen} / Z_{magic}$

$Load = R_{plasma} = (Z_{magic}^2 . I_{gen} . \cos \phi / U_{gen}) - R_{vide}$

$Power = (U_{gen} . I_{gen} \cos \phi)_{tot} - (U_{gen} . I_{gen} \cos \phi)_{vide}$
equivalently: $= N_{ant} . I_{ant}^2 . (R_{tot} - R_{vide}) = N_{ant} . I_{ant}^2 . R_{plasma}$

(The latter power calculation is used because variations in $\cos\phi$, I_{ant} etc are automatically included in R_{vide}.)

NB all the above results hold on- and off-resonance - provided that $R_{ant} << \omega L_{ant}$.

$Z_{magic} = 0.435 + 0.531$ f(MHz) is sufficiently accurate for 2 - 3 MHz.

2) Programs available (see appendices for example output and software):
a) (5,1) SUPALF.FTN (J-M Moret) See pp 53 and 54
Functions: 53 - I_{ant} 47 - Load 46 - Power
b) (304,1) A.THT - same as above, but doesn't use MASK See p 55
c) (304,1) ALFVEN.THT - connoisseurs version, looks at every antenna. See pp 56-57
d) SLAVE 'p11' - Raw signals from G Besson's amplifiers. See p57

3) Constants 59, 60, 81.
*60 is the vacuum loading R_{vide}, = 88 mΩ (approximately). NB R_{vide} is different for each antenna, therefore 88 mΩ is an 8-antenna average. Different combinations of antennae would need different values for R_{vide}.
*59 is the MASK. Form +/- N.xyz (Real)
'N' used to define the amplifier gain for old shots (automatic for G Besson's amplifiers: set N = 0 arbitrarily)
'xyz': convert to binary, '1' means antenna signal <u>not</u> used ie for antennae 134578:
$00100010 = 034_{10} = xyz$
87654321 - antenna number
'+/-': negative sign means that 8 antennae are assumed to be supplying power, although only the measurements for the antennae defined by mask are used for the calculations - the final power includes all 8 antennae.
*81 is the phase offset, added to all phases in radians, to account for phase offsets in G Besson's amplifiers (which change somewhat with gain setting).

NOTES

*Artificial peaks in Load and Power at the beginning and end of the rf pulse are due to non-zero offset in the U_{gen} signal amplifier. They could be suppressed (as done by G Collins by imposing a threshold value on the signals, below which the Load and Power are set to zero), at the risk of losing data and the time-zero reference.

* Keep 'Rouge' and 'Vert' signals > 1V to avoid rectifier errors - use slave Page 11 to monitor this.

* Attention: the ' contraction', or I_{ant} feedback, changes with amplifier gain level setting.

* Gate the 'contraction' for after the G Besson amplifier calibration pulse to avoid AFCO power peaks and false calibration levels.

```
                U=MAX(WORK1(J)*GU,0.)
                WORK3(J)=WORK3(J)+U
C
CCC             I/U temporairement dans WORK1
C
                WORK1(J)=MAX(WORK2(J)*GI,0.)/U
5               CONTINUE
CCC
CCC     Cos dans WORK2
C
        CALL GTRACE(WORK2,230+I,NMIC,NIP,NPTS,LENGT,T1,DT,
     *                  IERR,SCALE)
        IF (IERR.NE.0) RETURN
C
CCC     facteur de conversion 1V = 20 degres
C
        GU=SCALE*.3491
C
CCC     (I cos / U)-tot dans WORK4
C
        DO 6 J=1,NPTS
6               WORK4(J)=WORK4(J)+WORK1(J)*COS(WORK2(J)*GU+CONSTS(61))
C
        NANT=NANT+1
2       CONTINUE
CCC
CCC
C
CCC     frequence dans WORK1 et WORK2

        CALL GTRACE(WORK1,16,NMIC,NIP,NPTSF,LENGT*2,T1F,DTF,IERR,SCALE)
        IF (IERR.NE.0) RETURN
        SCALE=1./(.9774*DTF-4.1E-6)
C
        DO 7 J=1,NPTS
                F=(J-1)*DT+T1                   !TEMPS
                I=(F-T1F)/DTF+1.5               !INDICE DANS WORK1
                IF (I.LT.2.OR.I.GT.NPTSF) THEN  !LE 1ER POINT EST FAUX
                        WORK3(J)=0
                        WORK4(J)=0
                ELSE
                        F=WORK1(I)*SCALE
                        ZMA=.435*F*1.541E-6
CC
                        I-avg dans WORK3 [A]
CCCC                    R-ant dans WORK4 [1E-4 Ohm]

                        WORK3(J)=10.*WORK3(J)/ZMA/NANT
                        WORK4(J)=WORK4(J)*ZMA*ZMA/NANT
                        END IF
7               CONTINUE
C
        IF (NS.EQ.53) THEN
C
CCC             I-ant [A]

                DO 8 J=1,NPTS
8                       W(J)=WORK3(J)
                RETURN
                END IF
        IF (NS.EQ.47) THEN
CCC
CCC             R-plasma [Ohm]

                DO 9 J=1,NPTS
9                       W(J)=MAX(WORK4(J)*1.E-4-CONSTS(60),0.)
                RETURN
                END IF
        IF (NS.EQ.46) THEN
C
CCC             P-rf [W]

                IF (CONSTS(59).LE.0.) NANT=8
                DO 10 J=1,NPTS
10                      W(J)=MAX(WORK4(J)*1.E-4-CONSTS(60),0.)*
     *                          FLOAT(WORK3(J))**2*NANT
                RETURN
                END IF
        RETURN
        END
```

SUPALF.FTN


```
C*SUPALF
        SUBROUTINE SUPALF(NS,W,IW,NW,NPTS,DT,T1,IERR)
C
CCC
        INCLUDE 'DK0:[250,1]COMM1.FTN'
        INTEGER*2       IW(1)
        REAL*4          W(1)
C
CCCC    FREQUENCE
C
        IF (NS.EQ.54) THEN
                CALL GTRACE(IW,16,NMIC,NIP,NPTS,LENGT,T1,DT,IERR,SCALE)
                IF (IERR.NE.0) RETURN
                SCALE=1./(.9774*DT-4.1E-6)
                T1=T1+DT
                NPTS=NPTS-1
                DO 1 I=NPTS+1,2,-1
1                       W(I-1)=IW(I)*SCALE
                RETURN
                END IF
C
CCC     ALFVEN, AMPLI GEORGE
C
        IF (NOPSNT.LT.31076) THEN
                IF (NW.LT.LENGT*3) THEN
                        IERR=1
                        RETURN
                        END IF
                NPTS=0
                NANT=0
                CALL ALFVEN(W(1),W(LENGT+1),W(2*LENGT+1),NANT,LENGT,
     *                  NPTS,DT,T1,0)
                IF (CONSTS(59).LT.0.) NANT=8
                DO 2 I=1,NPTS
                        IF (NS.EQ.53) W(I)=W(I+LENGT)
                        IF (NS.EQ.46) W(I)=.5*NANT*W(I)*W(I+LENGT)**2
2                       CONTINUE
CCCC
CCC     ALFVEN, AMPLI BESSON
C
        ELSE
                IF (NW.LT.LENGT*2) THEN
                        IERR=1
                        RETURN
                        END IF
                CALL ALFNEW(NS,W,IW(1),IW(LENGT+1),IW(2*LENGT+1),
     *                  IW(3*LENGT+1),NPTS,DT,T1,IERR)
                END IF
        RETURN
        END
C*ALFNEW
        SUBROUTINE ALFNEW(NS,W,WORK1,WORK2,WORK3,WORK4,NPTS,DT,T1,IERR)
CCC
CCC     W = WORK1(LENGT)-WORK2(LENGT)-WORK3(LENGT)-WORK4(LENGT)

        INCLUDE 'DK0:[250,1]COMM1.FTN'
        INTEGER*2       WORK1(1),WORK2(1),WORK3(1),WORK4(1)
        REAL*4          W(1)
C
        DO 1 J=1,LENGT
                WORK3(J)=0
1               WORK4(J)=0
        NANT=0
C
        DO 2 I=1,8
C
CCC             ANTENNE MASQUEE
CC
                J=ABS(INT(CONSTS(59)*1000.)).AND.2**(I-1)
                IF (J.NE.0) GOTO 2
CCC
CCC             U dans WORK1

                CALL GTRACE(WORK1,92+I,NMIC,NIP,NPTS,LENGT,T1,DT,
     *                  IERR,SCALE)
                IF (IERR.NE.0) RETURN
C
CCC             gain [10V]
CC
                RMIN=0.
                DO 3 J=1,NPTS
                        RMIN=MIN(WORK1(J)*SCALE,RMIN)
3                       CONTINUE
                J=-RMIN+.5
                GU=CONSTS(J+90)*SCALE/10.
C
CCC             I dans WORK2
CC
                CALL GTRACE(WORK2,84+I,NMIC,NIP,NPTS,LENGT,T1,DT,
     *                  IERR,SCALE)
                IF (IERR.NE.0) RETURN
C
CCC             gain [1E-4 Ohm]

                RMIN=0.
                DO 4 J=1,NPTS
                        RMIN=MIN(WORK2(J)*SCALE,RMIN)
4                       CONTINUE
                J=-RMIN+.5
                GI=CONSTS(J+95)*SCALE*1000.
C
                DO 5 J=1,NPTS
C
CCC                     U-tot dans WORK3
C
```

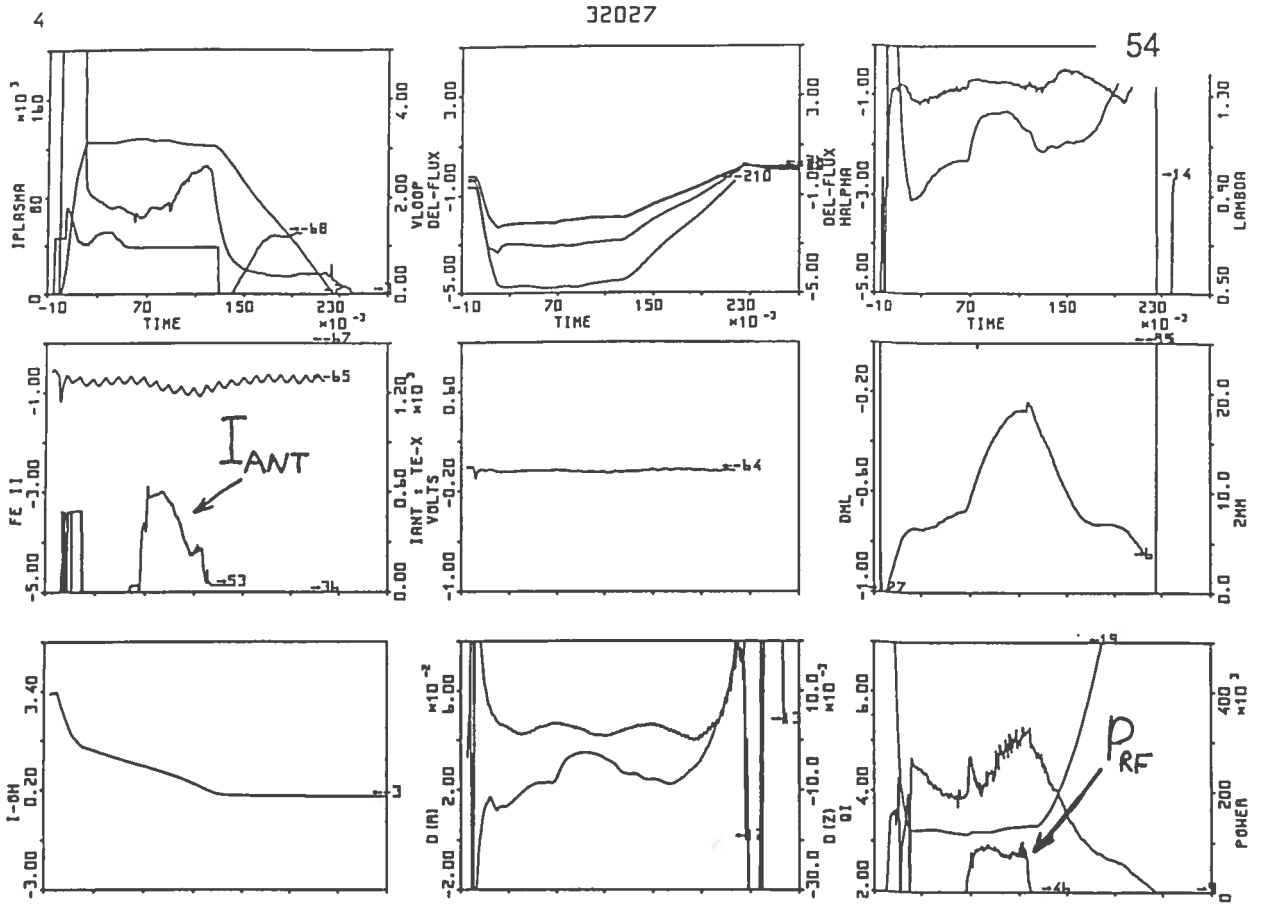

Slave Pages 2 and 4 showing rf parameters produced by SUPALF.FTN

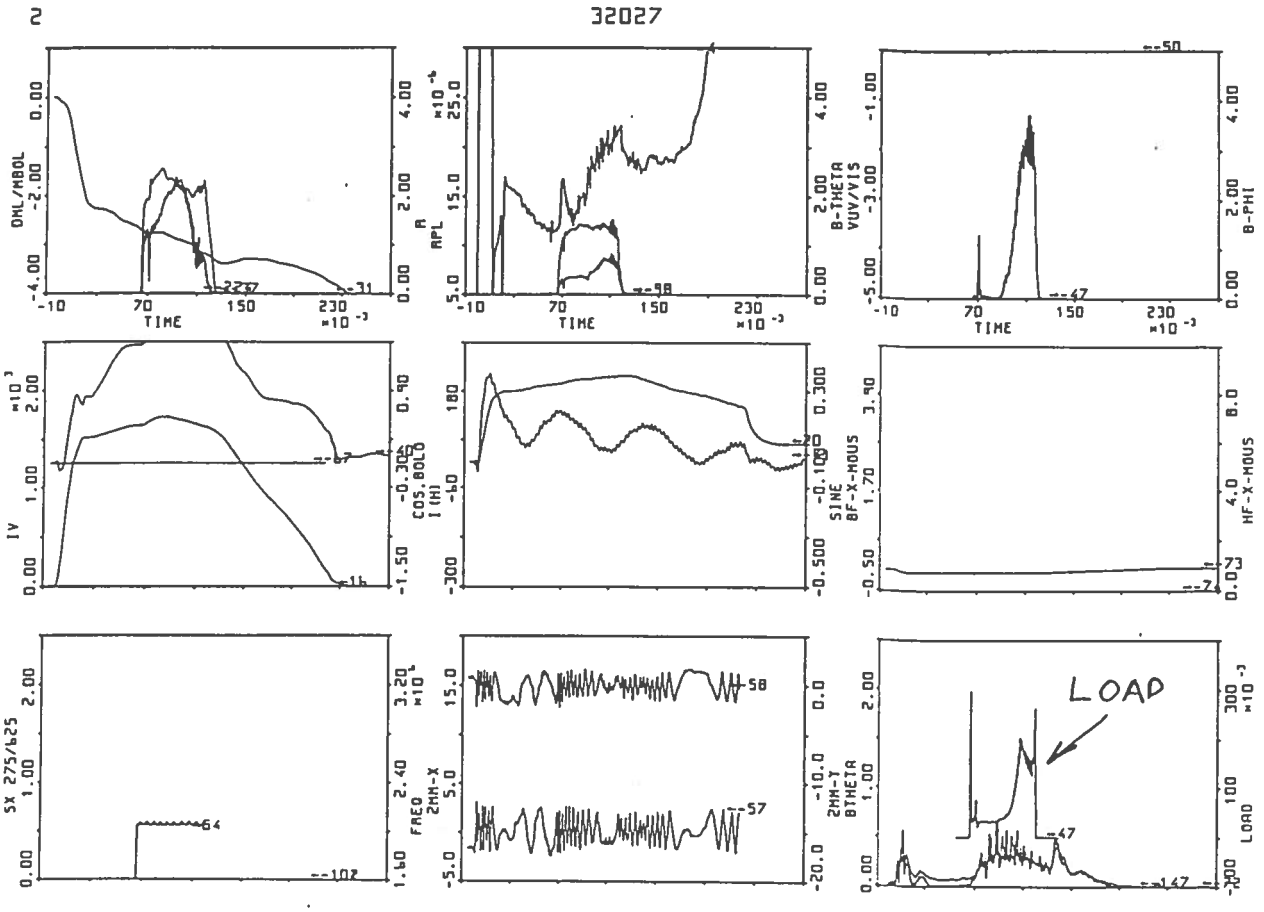

[304,1] A.THT

```
Spooling File:  A.THT  From  UIC=[304.1]  15:28:24 17-NOV-88

:CALCULATES Iant, LOADING AND RF POWER
CAL DEBUG(1)
CAL SHOT(ACCEPT('SHOT'))
:DEFINE AXES:
CAL AXIS(201,0.,750.,'IANT[A]')
CAL AXIS(202,0.,225.,'LOAD[MOHM]')
CAL AXIS(203,0.,150.E3,'RF-POWER[W]')
CAL AXIS(206,.05,.155,'TIME')
:DEFINE BOXES:
CAL BOX(1,1221,206,201)
CAL BOX(2,2221,206,202)
CAL BOX(3,3221,206,203)
U=FUN(-93)
:ABOVE USED TO KEEP SAMPLE FREQY HIGH
T=TIME(0)
F=FUN(54)
:(ZMAGIC...WILL NEED FULL FUNCTION FOR WIDE RANGE OF F)
Z=.435+(F*1.541E-6)
:INITIALISE:
N=0
UAV=0
LDAV=0
:DEFINE GAIN LEVELS::
:VERT:
GU[2:2]=956.
GU[3:3]=507.
GU[4:4]=208.
GU[5:5]=100.
:ROUGE:
GI[2:2]=8.83
GI[3:3]=4.28
GI[4:4]=1.96
GI[5:5]=1.
:LOOP OVER ANTENNAE:
LOOP
N=N+1
:VOLTAGE:
U=FUN(-92#N)
IU=EXT(U)
IU=IU[1]
IU=0#U[IU]+.5
U=U*GU[IU]
:CURRENT:
J=FUN(-84#N)
I=EXT(J)
I=I[1]
I=0#J[I]+.5
J=J*GI[I]
:PHASE:
PHI=FUN(-230#N)*20.+CON(81)*57.3
COPHI=COS(PHI/57.3)
:LOADING:
LD=Z*Z*J*COPHI/U
:SUM VOLTAGE AND LOAD:
UAV=UAV+U
LDAV=LDAV+LD
IF(N:EQ:8)
EXI
EIF
REP
:PRINT FINAL AVERAGED RESULTS:
CAL PAGE(3,'A')
CAL VALUE(N,'NO..ANT.USED',1)
:AVERAGE ANTENNA CURRENT:
CAL PLO(T,UAV/(N*Z),1)
:AVERAGE LOAD CORRECTED FOR VACUUM LOAD:
CAL PLO(T,1000.*((LDAV/N)#CON(60)),2)
:AVERAGE POWER PER ANTENNA (CORRECTED FOR VAC LOSSES):
POW=((LDAV/N)#CON(60))*(UAV/(N*Z))^2
IF(CON(59):GE:0)
CAL PLO(T,N*POW,3)
EIF
IF(CON(59):LT:0)
CAL PLO(T,8.*POW,3)
EIF
```

A

32027

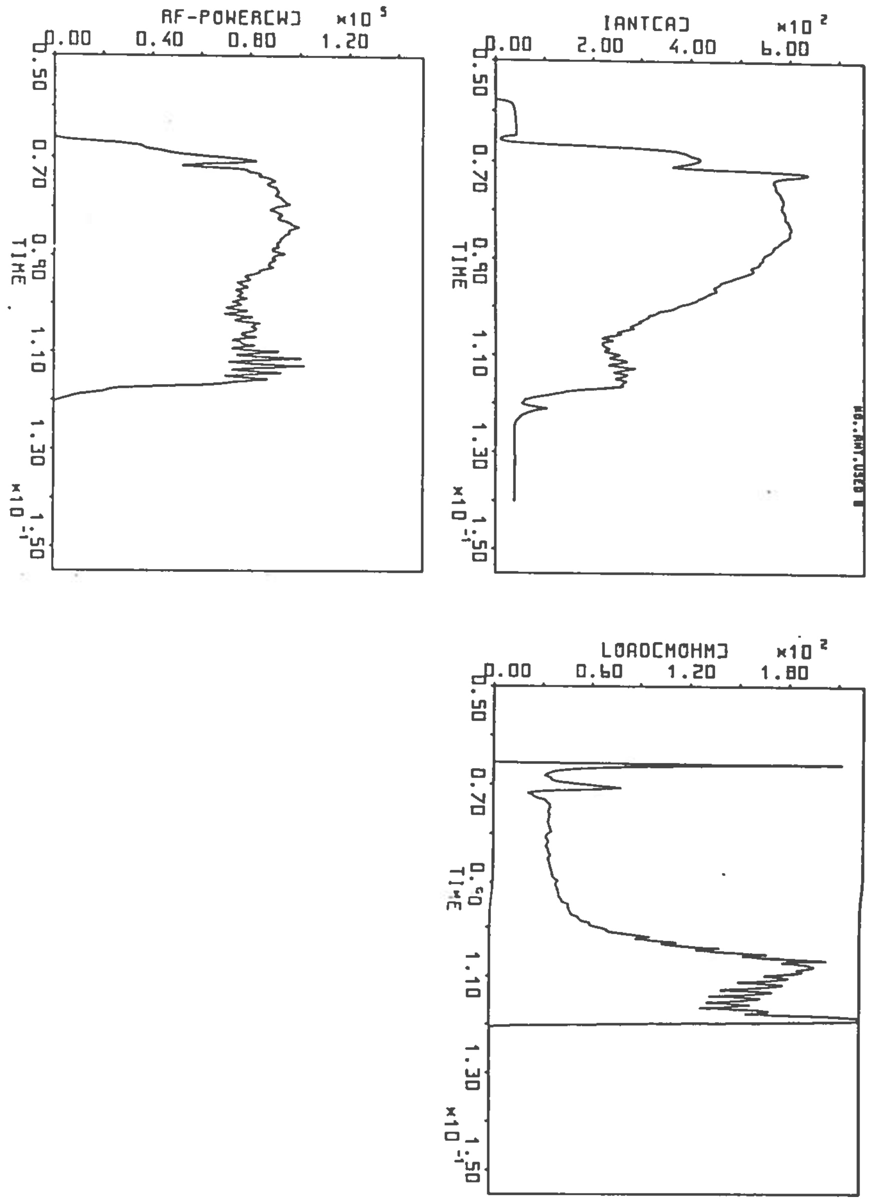

ANT

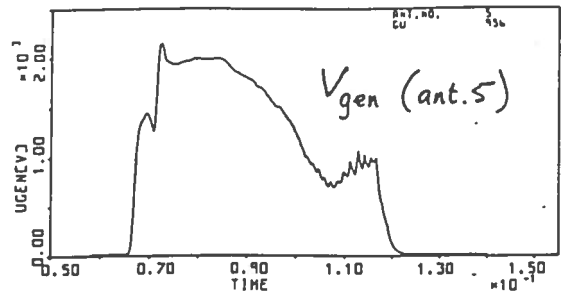

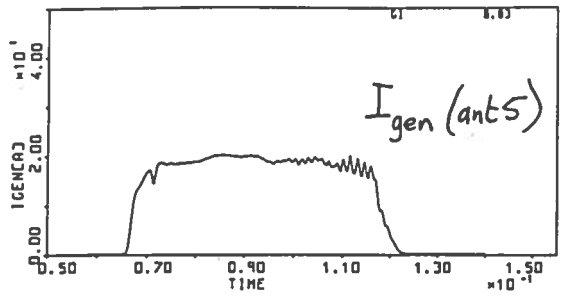

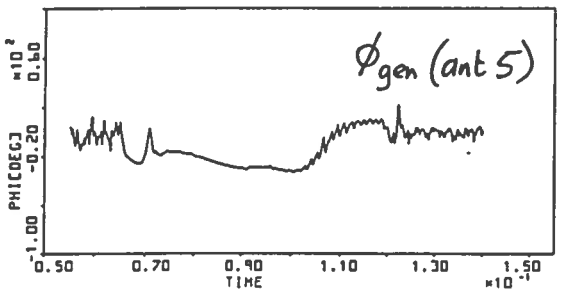

32027

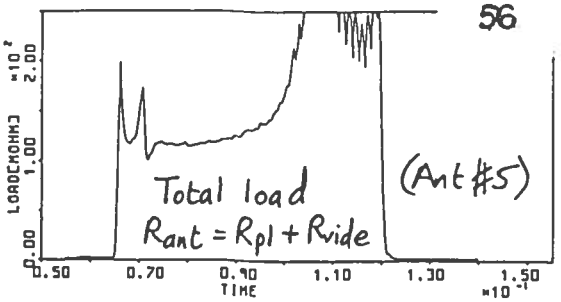

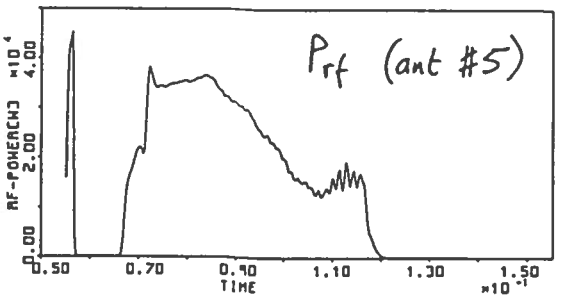

EXAMPLE OUTPUT FROM ALFVEN.THT.

ANTENNA #5 GIVEN HERE AS REPRESENTATIVE OF ALL ANTENNAE.

AVERAGED PARAMETERS FOR ALL ANTENNAE

ALFVEN

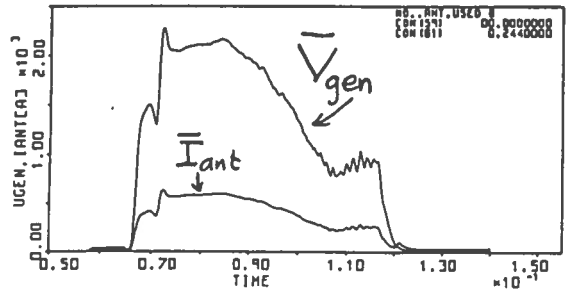

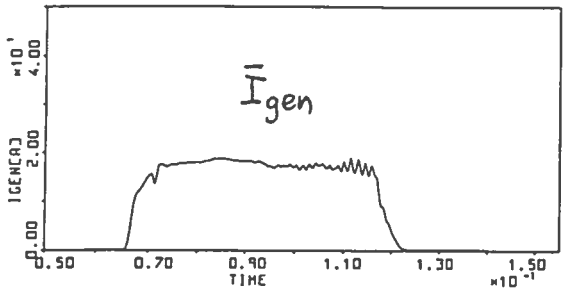

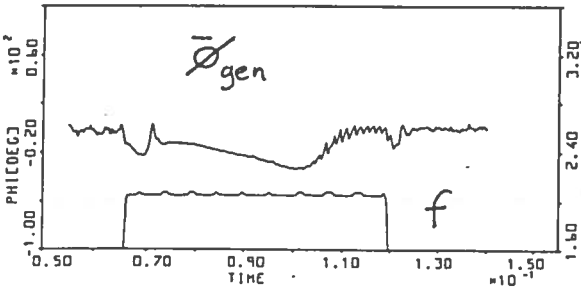

32027

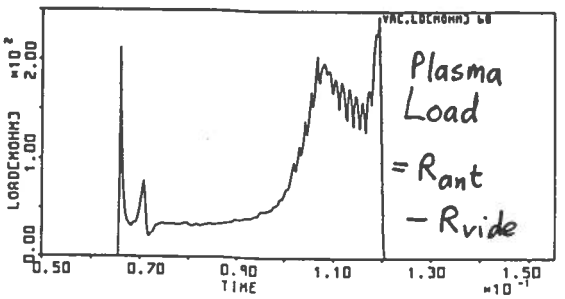

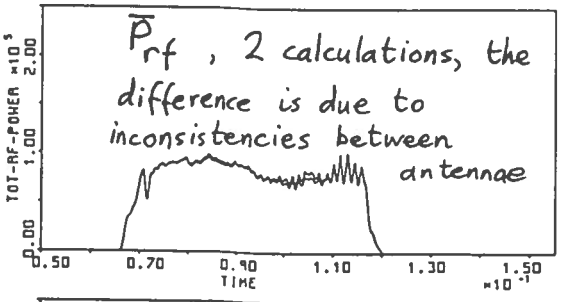

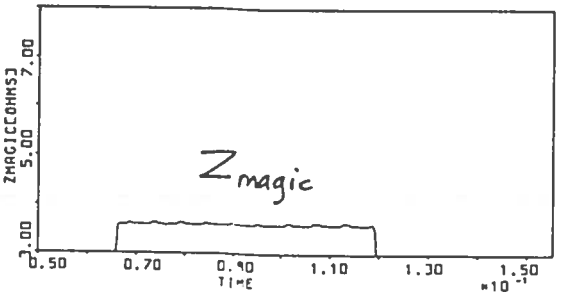

[304,1] ALFVEN. THT

```
Spooling File:  ALFVEN.THT  From  UIC=[304.1]  15:43:38 17-NOV-88

:ALFVEN.THT. TO PLOT ALL ANTENNAE AND THE FINAL AVERAGES.
:...PLOTS Igen. Iant. Ugen. phase. load. power.frequency. Zmagic
CAL DEBUG(1)
CAL SHOT(ACCEPT('SHOT'))
:DEFINE AXES:
CAL AXIS(201.0..2500..'UGEN[V]')
CAL AXIS(202.0..50..'IGEN[A]')
CAL AXIS(203.-100..100..'PHI[DEG]')
CAL AXIS(204.0..250..'LOAD[MOHM]')
CAL AXIS(205.0...5E5.'RF-POWER[W]')
CAL AXIS(206..05..155.'TIME')
:DEFINE BOXES:
CAL BOX(1.1231.206.201)
CAL BOX(2.3231.206.202)
CAL BOX(3.5231.206.203)
CAL BOX(4.2231.206.204)
CAL BOX(5.4231.206.205)
U=FUN(-93)
:ABOVE USED TO KEEP SAMPLE FREQY HIGH
T=TIME(0)
F=FUN(54)
:(ZMAGIC...WILL NEED FULL FUNCTION FOR WIDE RANGE OF F)
Z=.435+(F*1.541E-6)
:INITIALISE:
N=0
UAV=0
IAV=0
PHAV=0
LDAV=0
PAV=0
:DEFINE GAIN LEVELS:
GU[2:2]=956.
GU[3:3]=507.
GU[4:4]=208.
GU[5:5]=100.
GI[2:2]=8.83
GI[3:3]=4.28
GI[4:4]=1.96
GI[5:5]=1.
LOOP
N=N+1
U=FUN(-92#N)
IU=EXT(U)
IU=IU[1]
IU=0#U[IU]+.5
U=U*GU[IU]
J=FUN(-84#N)
I=EXT(J)
I=I[1]
I=0#J[I]+.5
J=J*GI[I]
PHI=FUN(-230#N)*20.+CON(81)*57.3
COPHI=COS(PHI/57.3)
LD=Z*Z*J*COPHI/U
P=U*J*COPHI
CAL PAG(3.'ANT')
CAL VAL(N.'ANT.NO.'.1)
CAL VAL(GU[IU].'GU =',1)
CAL VAL(GI[I].'GI =',2)
CAL PLO(T.U.1)
CAL PLO(T.J.2)
CAL PLO(T.PHI.3)
CAL PLO(T.1000.*LD.4)
CAL PLO(T.P.5)
UAV=UAV+U
IAV=IAV+J
PHAV=PHAV+PHI
LDAV=LDAV+LD
PAV=PAV+P
IF(N:EQ:8)
EXI
EIF
REP
:PRINT FINAL AVERAGED RESULTS:
CAL PAGE(3.'ALFVEN')
CAL VAL(N.'NO..ANT.USED'.1)
CAL VAL(CON(59).'CON(59)'.1)
CAL VAL(CON(81).'CON(81)'.1)
CAL VAL(1000*CON(60).'VAC.LD[MOHM]'.4)
CAL AXIS(201.0..2500..'UGEN.IANT[A]')
CAL PLO(T.UAV/N.1)
CAL PLO(T.UAV/(N*Z).1)
CAL PLO(T.IAV/N.2)
CAL PLO(T.PHAV/N.3)
CAL PLO(T.1000.*((LDAV/N)#CON(60)).4)
CAL AXIS(205.0..2.5E5.'TOT-RF-POWER')
POW=((LDAV/N)#CON(60))*(UAV/(N*Z))^2
POWVAC=N*CON(60)*(UAV/(N*Z))^2
IF(CON(59):GE:0)
CAL PLO(T.N*POW.5)
CAL PLO(T.PAV#POWVAC.5)
EIF
IF(CON(59):LT:0)
CAL PLO(T.8.*POW.5)
CAL PLO(T.8.*(PAV#POWVAC)/N.5)
EIF
CAL AXIS(201.3..8..'ZMAGIC[OHMS]')
CAL BOX(3.5234.206.59)
CAL BOX(7.6231.206.201)
CAL PLO(T.F.3)
CAL PLO(T.Z.7)
```

PAGE 11 : Raw data from G. Besson rf amplifiers.

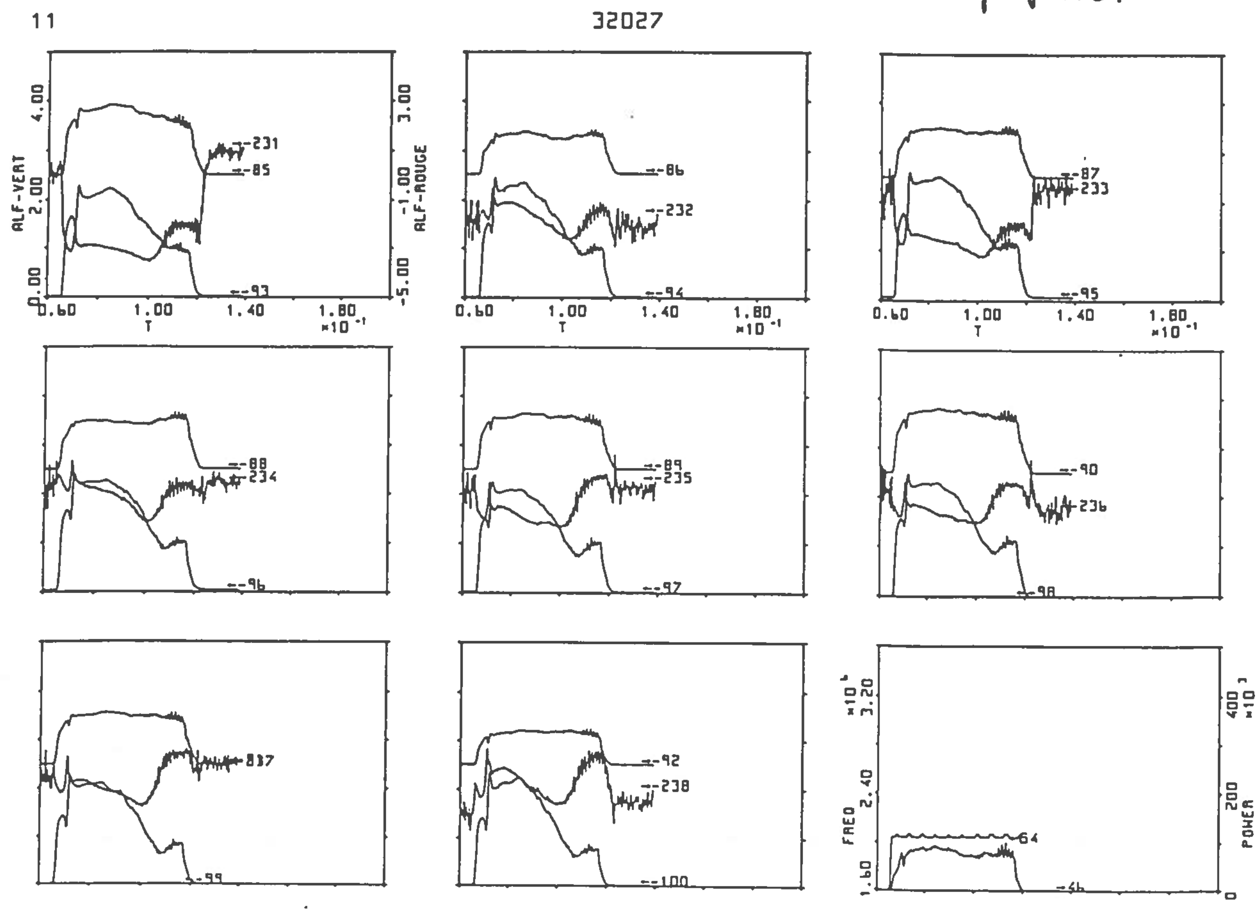

```
Spooling File:  PHACOR.FTN  From  UIC=[304,1]  17:43:04 29-AUG-88

      PROGRAM PHACOR
C Calculates Zmagic with and without ideal cables
C  and phase and impedance at input to ringing circuit:
C  series inductance on measuring probe and parallel
C  resistance options included.
      DIMENSION W(61),ZMAGIC(61),ZMAGGC(61),PHASE(61)
      DIMENSION ZINPUT(61),ZREAL(61),ZIMAGY(61)
      DIMENSION YREAL(61),YIMAGY(61),YMAG2(61),R(61)
      RCAL=0.
      CALL GETR('CAL-RES      ',.5,5,RCAL)
      CAP=15.66E-9
      CALL GETR('CAPACITOR    ',.5,5,CAP)
      RANT=90.E-3
      CALL GETR('R-ANTENNA    ',.5,5,RANT)
      CABLE=5.25
      CALL GETR('CABLE LEN    ',.5,5,CABLE)
      Z0=5.556
      CALL GETR('CHAR IMP Z0 ',.5,5,Z0)
      AI=193.E-9
      CALL GETR('ANT INDUCT L',.5,5,AI)
      SERL=158.E-9
      CALL GETR('SER INDUCT L',.5,5,SERL)
      FRAC=.711
      CALL GETR('FRAC LIGHT V',.5,5,FRAC)
      PI=3.14159
      C=3.E8
      CALL LGRGO(-1)
      DO 1 I=1,61
      P=1.7+FLOAT(I-1)*.035
      FREQ=P*1.E6
      W(I)=2.*PI*FREQ
      VEL=FRAC*C
      DUM=W(I)*CABLE/VEL
      D=TAN(DUM)
      WLANT=W(I)*AI
      TOP=WLANT+(D*Z0)
      BOT=SQRT(1.+(D*D))
      DEN=1.-(WLANT*D/Z0)
      ZMAGIC(I)=TOP/BOT
      ZMAGGC(I)=1.541E-6*FREQ+.435
      WLEQ=TOP/DEN
            IF(RCAL.NE.0)THEN
            RES=RANT+(WLANT**2)/RCAL
            ELSE
            RES=RANT
            ENDIF
C     TYPE *,'RES:',RES
      REQ=RES*BOT*BOT/(DEN*DEN)
      RSTAR=WLEQ*WLEQ/REQ
      YREAL(I)=1./RSTAR
      YIMAGY(I)=W(I)*CAP-(1./WLEQ)
      YMAG2(I)=YREAL(I)**2+YIMAGY(I)**2
C CORRN FOR LSER:
      DEN=1.-2*W(I)*SERL*YIMAGY(I)+YMAG2(I)*(W(I)*SERL)**2
      YIMAGY(I)=YIMAGY(I)-W(I)*SERL*YMAG2(I)
      YIMAGY(I)=YIMAGY(I)/DEN
      YREAL(I)=YREAL(I)/DEN
      YMAG2(I)=YREAL(I)**2+YIMAGY(I)**2
      TNPHI=-YIMAGY(I)/YREAL(I)
      ZINPUT(I)=SQRT(1./YMAG2(I))
      ZREAL(I)=YREAL(I)/YMAG2(I)
      ZIMAGY(I)=-YIMAGY(I)/YMAG2(I)
C     TYPE *,'ZINPUT,ZREAL,ZIMAGY:',ZINPUT(I),ZREAL(I),ZIMAGY(I)
      YMAG2(I)=SQRT(YMAG2(I))
      FRES=1./(2.*PI*SQRT(WLEQ*CAP/W(I)))
      PHASE(I)=ATAN(TNPHI)
      PHASE(I)=PHASE(I)*180./PI
C     TYPE *,'FREQ,RES FREQ,PHASE:',W(I)/(2.*PI),FRES,PHASE(I)
C     TYPE *,'WLEQ,D,TOP,DEN',WLEQ,D,TOP,DEN
      R(I)=YREAL(I)*ZMAGIC(I)*ZMAGIC(I)
1     CONTINUE
C     CALL APLOT(IBUF,ZMAGIC,61,1.7E6,.01E6,22,1.3,.4.875)
C     CALL APLOT(IBUF,ZMAGGC,61,1.7E6,.01E6,22,1.3,.4.875)
      CALL APLOT(IBUF,PHASE,61,1.7E6,.035E6,22,2,-90,.90.)
      CALL APLOT(IBUF,ZINPUT,61,1.7E6,.035E6,22,3,-150,.300.)
      CALL APLOT(IBUF,ZREAL,61,1.7E6,.035E6,22,3,-150,.300.)
      CALL APLOT(IBUF,ZIMAGY,61,1.7E6,.035E6,22,3,-150,.300.)
      CALL APLOT(IBUF,YREAL,61,1.7E6,.035E6,22,4,-15,.15.)
      CALL APLOT(IBUF,YIMAGY,61,1.7E6,.035E6,22,4,-15,.15.)
      CALL APLOT(IBUF,YMAG2,61,1.7E6,.035E6,22,4,-15,.15.)
      CALL APLOT(IBUF,R,61,1.7E6,.035E6,22,1,0,250E-1)
      CALL LORIG(0,.9.)
      CALL LTYPE(20,.3,1,.2,'LSER   =',0,.8)
      CALL LTYPE(20,.3,7,.2,'RCAL   =',0,.8)
      CALL LTYPE(20,.4,3,.2,'RANT   =',0,.8)
      CALL LTYPE(20,.4,9,.2,'CAP    =',0,.8)
      CALL LTYPE(20,.5,5,.2,'CAB LEN=',0,.8)
      CALL LTYPE(20,.6,1,.2,'IMP Z0 =',0,.8)
      CALL LTYPE(20,.6,7,.2,'ANT IND=',0,.8)
      CALL LTYPE(20,.7,3,.2,'REL VEL=',0,.8)
      CALL LNUMB(22,.3,1,.2,SERL*1.E9,0,.2)
      CALL LNUMB(22,.3,7,.2,RCAL,0,.2)
      CALL LNUMB(22,.4,3,.2,RES,0,.3)
      CALL LNUMB(22,.4,9,.2,CAP*1.E9,0,.3)
      CALL LNUMB(22,.5,5,.2,CABLE,0,.3)
      CALL LNUMB(22,.6,1,.2,Z0,0,.3)
      CALL LNUMB(22,.6,7,.2,AI*1.E9,0,.2)
      CALL LNUMB(22,.7,3,.2,FRAC,0,.3)
      CALL LTYPE(23.4,6.7,.2,'NAM-H',0,.5)
      CALL LTYPE(23.4,3.1,.2,'NAM-H',0,.5)
      CALL LTYPE(23.4,4.9,.2,'NAM-F',0,.5)
      CALL LGREND
      STOP
      END
      SUBROUTINE APLOT(IBUF,RBUF,NPTS,T1,DT,NTOT,NUM,AMIN,AMAX)
C-- IBUF IS AN INTEGER*2 ARRAY OF NPTS    T1=START TIME DT=DELTA TIME
      INTEGER IBUF(1)                  ! DUMMY LENGTH
      REAL RBUF(1)                     ! DUMMY LENGTH FOR REAL ARRAY
      REAL T1,DT                       ! REAL VARIABLES
      REAL AMIN,AMAX
C--
      CALL PARTSC(NTOT,NUM,XL,ZL,NN,NT)       ! SELECT PAGE 11 FIGURE 1
C--
      IF(ITYPE.EQ.1) THEN
      RMAX=FLOAT(IBUF(1))
      RMIN=RMAX
      ELSE
      RMIN=RBUF(1)
      RMAX=RMIN
      ENDIF
C--
      DO 100 I=2,NPTS
      IF(ITYPE.EQ.1) THEN
      RDUM=FLOAT(IBUF(I))
      ELSE
      RDUM=RBUF(I)
      ENDIF
C-- FIND THE MAX/MIN
      IF(RDUM.GT.RMAX) RMAX=RDUM
100   IF(RDUM.LT.RMIN) RMIN=RDUM
C-- SELECT THE INCREMENT OF THE AXES
      DX=FLOAT(NPTS-1)*DT/XL
      Z1=RMIN
      DZ=(RMAX-RMIN)/ZL
      IF(AMAX.NE.0.)THEN
      Z1=AMIN
      DZ=(AMAX-AMIN)/ZL
      RMIN=AMIN
      ENDIF
C-- PLOT THE AXES
      CALL LAXIS(0.,0.,XL,0.,T1,DX,99,'F     ',-6,NN,NT)
      CALL LAXIS(0.,0.,ZL,90.,Z1,DZ,99,' ',1,NN,NT)
C-- DO THE PLOT
      DO 200 I=1,NPTS
      R1=T1+FLOAT(I-1)*DT
      R1=(R1-T1)/DX                    ! NUMBER OF CM
      IF(ITYPE.EQ.1) THEN
      R2=FLOAT(IBUF(I))
      ELSE
      R2=RBUF(I)
      ENDIF
C--
      R2=(R2-RMIN)/DZ            ! NUMBER OF Z CM
      IF(I.EQ.1) CALL LPOINT(R1,R2,3)          ! MOVE THE CURSOR (NO DRAW)
200   CALL LPOINT(R1,R2,2)                     ! JOIN UP
C--
      RETURN
      END
```

PHACOR.FTN

Spooling File: SWE.TNT From UIC=[304,1] 17:02:51 21-OCT-88

```
:FREQ SCAN FOR BOITE D'ACCORD IMPEDANCE:COMPARE PHAMAG.FTN
CALL DEBUG(1)
CALL SHOT(33903)
CALL PAGE(3,'SWEEP')
CALL AXIS(206,1.5E6,2.5E6,'X')
CALL BOX(1,1221,206,201)
CALL BOX(2.2221,206,202)
CALL BOX(3.3221,206,203)
CALL BOX(4.4221,206,204)
F=FUN(-240)
CALL CLOCK (.3/450.E-6,450.E-6,.3)
F=1.5E6+1.E6*F/5
CALL AXIS(201,-150,300,'ZANT')
CALL AXIS(202,-90,90,'PHASE')
CALL AXIS(203,0,3,'AMPS')
CALL AXIS(204,0,225,'VOLTS')
IC=1.9444*FUN(-250)*2.03E6/F
IS=1.9444*FUN(-249)*2.03E6/F
THI=ATAN2(IS,IC)
I2=IC*IC+IS*IS
CALL PLOT(F,I2*.5,3)
VC=35.*(FUN(-242)#FUN(-246))*2.03E6/F
VS=35.*(FUN(-241)#FUN(-245))*2.03E6/F
V2=VC*VC+VS*VS
CALL PLOT(F,V2*.5,4)
THV=ATAN2(VS,VC)
POW=(VC*IC+VS*IS)
REZ=POW/I2
CALL PLOT(F,REZ,1)
IMZ=(VS*IC#VC*IS)/I2
CALL PLOT(F,IMZ,1)
MAGZ=(V2/I2)**.5
CALL PLOT(F,MAGZ,1)
S=SIN(THV#THI)
C=COS(THV#THI)
CALL PLOT(F,57.3*ATAN2(S,C),2)
CALL PAGE(3,'SWEEP2')
CALL AXIS(201,-0.02,0.02,'ZANT')
CALL AXIS(202,2.5,'ZMAGIC')
CALL AXIS(203,0.250E-3,'RANT-BRUT')
CALL AXIS(204,0.250E-3,'RANT-CORR')
CALL BOX(5.1221,206,201)
CALL BOX(6.2221,206,202)
CALL BOX(7.3221,206,203)
CALL BOX(8.4221,206,204)
YMAG=1/MAGZ
CALL PLOT(F,YMAG,5)
YRE=REZ/MAGZ**2
CALL PLOT(F,YRE,5)
CALL PLOT(F,0,5)
YIM=0#IMZ/MAGZ**2
CALL PLOT(F,YIM,5)
ZMAGIC=SIN(F*1.5465E-7)/COS(F*1.5465E-7)
ZMAGIC=((F*6.283*160E-9)+ZMAGIC*5.556)/(1+ZMAGIC**2)**.5
CALL PLOT(F,ZMAGIC,6)
RANT=YRE*ZMAGIC**2
CALL PLOT(F,RANT,7)
LSER=158E-9
RANT=RANT/(1+F*YIM*6.2832*LSER)**2
CALL PLOT(F,RANT,8)
CALL PAGE(3,'COMPARE')
CALL AXIS(206,1.92E6,2.13E6,'COMPARE')
CALL AXIS(205,0,0.225,'CHARGE')
CALL BOX(9.1111,206,205)
CALL PLOT(F,RANT,9)
```

CABLES.FTN and SWE.THT

Spooling File: CABLES.FTN From UIC=[304,1] 11:03:39 10-OCT-88

```
      PROGRAM CABLES
C Calculates Zmagic with and without ideal cables
C  and phase at input to ringing circuit.
      DIMENSION W(51),ZMAGIC(51),REQ(51),WLEQ(51),ZMAG(51),RA(51)
      COMPLEX ZANT,ZO,GAMMA,ZEQ,ZI
      RANT=30.E-3
      CALL GETR('R-ANTENNA    ',5,5,RANT)
      CABLE=5.25
      CALL GETR('CABLE LEN    ',5,5,CABLE)
      ZOREAL=5.556
      CALL GETR('CHAR IMP ZOREAL ',5,5,ZOREAL)
      AI=160.E-9
      CALL GETR('ANT INDUCT L',5,5,AI)
      FRAC=.711
      CALL GETR('FRAC LIGHT V',5,5,FRAC)
      R=50.E-3
      CALL GETR('CAB RES 2MHZ',5,5,R)
      CI=140.E-9
      CALL GETR('CABLE IND    ',5,5,CI)
      PI=3.14159
      C=3.E8
      ZI=CMPLX(0,1)
      CALL LGRGO(-1)
      DO 1 I=1,51
      F=1.5+FLOAT(I-1)/50.
      FREQ=F**1.E6
      W(I)=2.*PI*FREQ
C  ACCOUNT FOR SKIN EFFECT ON CABLE RESISTANCE:
C   (USING G. COLLINS MEASUREMENTS)
      RCORR=R*(FREQ/2.E6)**.552
      CORR=RCORR/(2*W(I)*CI)
C     TYPE *,'CORR',CORR
      VEL=FRAC*C
      ZANT=CMPLX(RANT,W(I)*AI)
C     TYPE *,'RANT, WLANT',REAL(ZANT),AIMAG(ZANT)
      ZO=ZOREAL*CMPLX(1.,-CORR)
C     TYPE *,'ZO,ZOIMAG',REAL(ZO),AIMAG(ZO)
      DUM=W(I)*CABLE/VEL
      D=TAN(DUM)
      GAMMA=DUM*CMPLX(1.,-CORR)
C     TYPE *,'REAL GAMMA,IM GAMMA:',REAL(GAMMA),AIMAG(GAMMA)
      GAMMA=ZI*CSIN(GAMMA)/CCOS(GAMMA)
C     TYPE *,'DELTA, REAL DELTA',AIMAG(GAMMA),REAL(GAMMA)
      ZEQ=(ZANT+ZO*GAMMA)/(1+ZANT*GAMMA/ZO)
      REQ(I)=REAL(ZEQ)
C     TYPE *,'REQ',REQ
      WLEQ(I)=AIMAG(ZEQ)
C     TYPE *,'WLEQ',WLEQ
C     ZMAGIC(I)=RANT*WLEQ(I)**2/REQ(I)
C     TYPE *,'ZMAG $QO',ZMAGIC(I)
      ZMAGIC(I)=ZMAGIC(I)**0.5
C     TYPE *,'ZMAGIC',ZMAGIC(I)
      ZMAG(I)=(W(I)*AI+D*ZO)/(1+D*D)**.5
      RA(I)=ZMAG(I)**2*REQ(I)/WLEQ(I)**2
C  RATIO RANT(CORR):RANT(80MOHMS):
      RA(I)=RA(I)/(RANT+R)
1     CONTINUE

      CALL APLOT(IBUF,ZMAG,51.1.5E6,.02E6,22.1,2,.5,)
      CALL APLOT(IBUF,RA,51.1.5E6,.02E6,22,2,.5,1.25)
      DO 3, I=1,51
3     RA(I)=1.
      CALL APLOT(IBUF,RA,51.1.5E6,.02E6,22,2,.5,1.25)
      CALL APLOT(IBUF,WLEQ,51.1.5E6,.02E6,22,3.0,.6,)
      CALL LORIG(0,.0,)
      CALL LTYPE(20,.4.3,.2,'RANT   =',0,.8)
      CALL LTYPE(20,.4.9,.2,'CABLE R ',0,.8)
      CALL LTYPE(20,.5.5,.2,'CAB LEN=',0,.8)
      CALL LTYPE(20,.6.1,.2,'IMP ZO =',0,.8)
      CALL LTYPE(20,.6.7,.2,'ANT IND=',0,.8)
      CALL LTYPE(20,.7.3,.2,'CAB IND=',0,.8)
      CALL LNUMB(22,.4.3,.2,RANT,0,.3)
      CALL LNUMB(22,.4.9,.2,R,0,.4)
      CALL LNUMB(22,.5.5,.2,CABLE,0,.3)
      CALL LNUMB(22,.6.1,.2,ZO,0,.3)
      CALL LNUMB(22,.6.7,.2,AI*1.E9,0,.1)
      CALL LNUMB(22,.7.3,.2,CI*1.E9,0,.3)
      CALL LTYPE(23.4.4.9,.3,'MAW-H',0,.5)
      CALL LTYPE(23.4.4.9,.2,'OHMS',0,.5)
      CALL LGREND
      STOP
      END
      SUBROUTINE APLOT(IBUF,RBUF,NPTS,T1,DT,NTOT,NUM,AMIN,AMAX)
C-- IBUF IS AN INTEGER*2 ARRAY OF NPTS    T1-START TIME DT-DELTA TIME
      INTEGER IBUF(1)                     ! DUMMY LENGTH
      REAL RBUF(1)                        ! DUMMY LENGTH FOR REAL ARRAY
      REAL T1,DT                          ! REAL VARIABLES
      REAL AMIN,AMAX
C--     .
C--   CALL PARTSC(NTOT,NUM,XL,ZL,HN,HT)       ! SELECT PAGE 11 FIGURE 1
C--
      IF(ITYPE.EQ.1) THEN
      RMAX=FLOAT(IBUF(1))
      RMIN=RMAX
      ELSE
      RMIN=RBUF(1)
      RMAX=RMIN
      ENDIF
C--
      DO 100 I=2,NPTS
      IF(ITYPE.EQ.1) THEN
      RDUM=FLOAT(IBUF(I))
      ELSE
      RDUM=RBUF(I)
      ENDIF
C-- FIND THE MAX/MIN
      IF(RDUM.GT.RMAX) RMAX=RDUM
```

```
Spooling File:  AMPAL2.FTN  From  UIC=[304,1]  10:33:35 16-NOV-88

      PROGRAM AMPAL2
C  copy of PhM's AMPERE, adapted for rf antenna
      PARAMETER ND=21,PI2=6.2831853
      INTEGER FLAG1,E,F
      DIMENSION A(ND,ND),B(ND,ND),P(ND,ND),Q(ND,ND),R(ND,ND)
      DIMENSION FREQ(256),ZANT(256),RANT(256),RANT1(256)
      CALL LGRGO(-1)
      CALL LORIG(2.,2.)
      WRITE(5,*)'NO UNITES INPUT,OUTPUT? MUST BE 3 OR 5 IF GRAPHIC =2 OR 3'
      READ(5,*)IN,NOUT
6     IF(IN.EQ.5)WRITE(5,*)'CHOIX: R,L,C,ZMAGIC,EXECUTE'
      IF(IN.EQ.5)READ(IN,800)Z
      IF(IN.NE.5)READ(IN,799)Z
      IF(Z.EQ.'R')GOTO 14
      IF(Z.EQ.'L')GOTO 17
      IF(Z.EQ.'C')GOTO 19
      IF(Z.EQ.'E')GOTO 42
      IF(Z.EQ.'Z')THEN
        IF(IN.EQ.5)WRITE(5,*)'INPUT AI,CABLE,VEL,ZO'
        READ(IN,*)AI,CABLE,VEL,ZO
        WRITE(NOUT,799)Z
      ENDIF
      GOTO 6
C ******************************
14    IF(IN.EQ.5)WRITE(5,*)'NOEUDS A,B,RES[OHM]'
      READ(IN,*)I,J,V
      WRITE(NOUT,799)Z
      WRITE(NOUT,801)I,J,V
      V=1./V
      A(I,I)=A(I,I)+V
      A(J,J)=A(J,J)+V
      A(I,J)=A(I,J)-V
      A(J,I)=A(J,I)-V
      IF(I.GT.N)N=I
      IF(J.GT.N)N=J
      GOTO 6
C ************************
17    IF(IN.EQ.5)WRITE(5,*)'NOEUDS A,B,IND[HY]'
      READ(IN,*)I,J,V
      WRITE(NOUT,799)Z
      WRITE(NOUT,801)I,J,V
      V=1./V
      R(I,I)=R(I,I)+V
      R(J,J)=R(J,J)+V
      R(I,J)=R(I,J)-V
      R(J,I)=R(J,I)-V
      IF(I.GT.N)N=I
      IF(J.GT.N)N=J
      GOTO 6
C ********************************
19    IF(IN.EQ.5)WRITE(5,*)'NOEUDS A,B,CAP[F]'
      READ(IN,*)I,J,V
      WRITE(NOUT,799)Z
      WRITE(NOUT,801)I,J,V
      B(I,I)=B(I,I)+V
      B(J,J)=B(J,J)+V
      B(I,J)=B(I,J)-V
      B(J,I)=B(J,I)-V
      IF(I.GT.N)N=I
      IF(J.GT.N)N=J
      GOTO 6
C ************************
42    WRITE(NOUT,799)Z
      DO 43 I=1,ND
      DO 43 J=1,ND
      P(I,J)=A(I,J)
43    Q(I,J)=B(I,J)
      WRITE(5,*)'NODES=',N
      N=N-1
      WRITE(5,*)'I/O NODES ?'
      READ(IN,*)E,F
      WRITE(NOUT,*)E,F
      WRITE(5,*)E,F
C ****************************
200   CALL LSYNC(1)
220   WRITE(5,*)'Cadrage:     Fmin,Fmax,Amin,Amax'
C     READ(5,*)FMIN,FMAX,YMIN,YMAX
      FMIN=1.5E6
      FMAX=3.E6
      YMIN=0
      YMAX=200
           NPAS=256
      HN=.6
      HT=.8
C XLIN
      DUF=(FMAX-FMIN)/21.
      CALL LAXIS(0.,0.,21.,0.,FMIN,DUF,99.'FREQ',-4,HN,HT)
C YLIN
202   DUF=(YMAX-YMIN)/15.
      CALL LAXIS(0.,0.,15.,90.,YMIN,DUF,0.'ZANT',4,HN,HT)
      CALL LAXIS(0.,0.,15.,90.,0.,2/15.,0.'RANT',-4,HN,HT)
260   FREQ(1)=FMIN
            STEP=(FMAX-FMIN)/(NPAS-1)
            DO 263 IPAS=2,NPAS
263         FREQ(IPAS)=FREQ(IPAS-1)+STEP
      WRITE(NOUT,807)
      DO 262 IPAS=1,NPAS
      W=FREQ(IPAS)
      W=PI2*FREQ(IPAS)
      GOTO 50
261   ZANT(IPAS)=.01/ABS(V)
      Y2=1./ZANT(IPAS)**2
C  CALCULATE ZMAGIC:
      D=TAN(W*CABLE/VEL)
      ZMAG2=(W*AI+D*ZO)**2/(1+D*D)
      RANT(IPAS)=100.*COS(U*PI2/360.)*ZMAG2*ABS(V)
      RANT(IPAS)=ABS(RANT(IPAS))
      COR=(1.+W*158.E-9*SIN(U*PI2/360.)/ZANT(IPAS))**2
C     RANT1(IPAS)=RANT(IPAS)/COR
      RANT1(IPAS)=(ABS(COS(U*PI2/360.)/ZANT(IPAS))-.01*Y2)/(COR+1E-4*Y2)
      RANT1(IPAS)=RANT1(IPAS)*ZMAG2
262   WRITE(NOUT,806)W/PI2,ZANT(IPAS),U,RANT1(IPAS)
          CALL LJOIN(FREQ,ZANT,NPAS,0.0,FMIN,DUF,YMIN,DUY)
          CALL LJOIN(FREQ,RANT,NPAS,0.0,FMIN,DUF,0...2/15.)
          CALL LJOIN(FREQ,RANT1,NPAS,0.0,FMIN,DUF,0...2/15.)
C ********************************
270   CALL LGREND
      STOP 'AMPAL'
C ****************************************
C ENTREE POUR NOUV FREQ
50    D1=E
      D2=F
      ASSIGN 59 TO FLAG1
      GOTO 157
59    V=B1
      U=D2
      IF(-1**(E+F).LT.0)GOTO 63
      U=U+180.
63    D1=E
      D2=E
      ASSIGN 65 TO FLAG1
      GOTO 157
65    V=V/B1
      U=U-D2-180
66    IF(U.LE.180.)GOTO 67
      U=U-360.
      GOTO 66
67    IF(U.GE.-180)GOTO 68
      U=U+360.
68    GOTO 261
C ******
C ***CALCUL DU DETERMINANT***
C
94    IF(N.GT.1)GOTO 98
      D1=A(N,N)
      D2=B(N,N)
      GOTO 172
98    D1=1.
      D2=0.
      K=1
101   L=K
      S=ABS(A(K,K))+ABS(B(K,K))
      DO 108 I=K,N
      T=ABS(A(I,K))+ABS(B(I,K))
      IF(S.GE.T)GOTO108
      L=I
108   S=T
      IF(L.EQ.K)GOTO 118
      DO 117 J=1,N
      S=-A(K,J)
      A(K,J)=A(L,J)
      A(L,J)=S
      S1=-B(K,J)
      B(K,J)=B(L,J)
117   B(L,J)=S1
118   L=K+1
      DO 124 I=L,N
      S1=A(K,K)**2+B(K,K)**2
      S=(A(I,K)*A(K,K)+B(I,K)*B(K,K))/S1
      B(I,K)=(A(K,K)*B(I,K)-A(I,K)*B(K,K))/S1
124   A(I,K)=S
      J2=K-1
      IF(J2.EQ.0)GOTO 133
      DO 132 J=L,N
      DO 132 I=1,J2
      A(K,J)=A(K,J)-A(K,I)*A(I,J)+B(K,I)*B(I,J)
132   B(K,J)=B(K,J)-B(K,I)*A(I,J)-A(K,I)*B(I,J)
133   J2=K
      K=K+1
      DO 140 I=K,N
      DO 140 J=1,J2
      A(I,K)=A(I,K)-A(I,J)*A(J,K)+B(I,J)*B(J,K)
140   B(I,K)=B(I,K)-B(I,J)*A(J,K)-A(I,J)*B(J,K)
      IF(K.NE.N)GOTO 101
      L=1
      J2=INT(FLOAT(N)/2.)
      IF(N.EQ.2*J2)GOTO 148
      L=0
      D1=A(N,N)
      D2=B(N,N)
148   DO 155 I=1,J2
      J=N-I+L
      S=A(I,I)*A(J,J)-B(I,I)*B(J,J)
      S1=A(I,I)*B(J,J)+A(J,J)*B(I,I)
      T=D1*S-D2*S1
      D2=D2*S+D1*S1
      D1=T
155   GOTO 172
C ******
C
157   N1=N
      N=N-1
      I=0
      DO 170 K=1,N
      IF(K.NE.INT(D1))GOTO 163
      I=1
163   J=0
      DO 170 L=1,N
      IF(L.NE.INT(D2))GOTO 167
      J=1
167   A(K,L)=P(K+I,L+J)
170   B(K,L)=W*Q(K+I,L+J)-R(K+I,L+J)/W
      GOTO 94
172   N=N1
      IF(D1.NE.0.)B1=D1*SQRT(1.+(D2/D1)**2)
      IF(D1.EQ.0.)B1=D2
      D2=360.*ATAN2(D2,D1)/PI2
```

CORRECTION FOR LSER

CORRECTION FOR LSER AND RSER

AMPAL.FTN